THE EFFECT OF ALCOHOL ON CRANIAL NEURAL CREST CELLS: IMPLICATIONS FOR CRANIOFACIAL DEVELOPMENT

Olusegun Olufemi Oyedele

A thesis submitted to the Faculty of Health Sciences, University of the Witwatersrand, Johannesburg, in fulfilment of the requirements for the degree of Doctor of Philosophy.

Johannesburg, 2010

DECLARATION

I, Olusegun Olufemi Oyedele declare that this thesis is my own work. It is being submitted for the degree of Doctor of Philosophy in the University of the Witwatersrand, Johannesburg. It has not been submitted before for any degree or examination at this or any other University.

…… (Signature of Candidate)

……18th……..day of……June……..2010….

To my dad
James Oladiti Oyedele
1927-1992

You thirsted, and knowledge
She nourished you
You opened this door
Wide-eyed, I walked through
I, too keep the faith, I light the way
Wish you were here…..

PUBLICATION ARISING FROM THIS STUDY

Oyedele OO, Kramer B (2008) Acute ethanol administration causes malformations but does not affect cranial morphometry in neonatal mice. Alcohol 42:21-27.

PRESENTATIONS ARISING FROM THIS STUDY

O Oyedele and B Kramer. 36th Can the effects of ethanol on developing embryos be explained by abnormal migration of cranial neural crest cells? Annual Congress of the Anatomical Society for Southern Africa, Golden Gate, South Africa, 23-26 April 2006.

O Oyedele and B Kramer. Acute ethanol administration causes craniofacial malformations and affects cranial neural crest cells. Faculty of Health Sciences Research Day, University of the Witwatersrand, August 2006.

O Oyedele and B Kramer. Effects of acute administration of ethanol on mouse embryos. 1st Conjoint Conference on Anatomy, Morphological Sciences and Fertility, Lagos, Nigeria. September 18-22, 2007.

O Oyedele and B Kramer. The Effect of Ethanol Exposure on Developing Embryos May Not Depend on Cranial Neural Crest Cell Migration: Evidence from Avian Morphologic and Morphometric Observations. XVII Congress of the International Federation of Associations of Anatomists (IFAA), Cape Town South Africa, August 16-19, 2009.

ABSTRACT

While ethanol is recognised beyond doubt as a teratogen to the unborn fetus, research nevertheless continues in order to understand its mode of action and its effects at the cellular level. The present study aimed to investigate the effect of an acute dose of ethanol on cranial morphology and morphometry in mouse fetuses, as well as on the morphology, migration and the expression of cell migration related genes in cultured chick cranial neural crest cells (cNCCs). Thirteen pregnant C57/BL mice were orally administered with 0.03ml/g of 25% (v/v) ethanol daily on gestational days (GD) 6, 7 and 8. Ten control animals received an identical dose of saline. On GD 18, all mice dams were killed and their fetuses were removed. Fetal morphological observations and crown-rump lengths were evaluated as were mean litter size, survival rate, birth weight and cranial dimensions. Cranial neural crest cells (cNCCs) were cultured from *Potchefstroom koek koek* stages 8-10 (HH) chick embryo neural tubes either in culture medium (DMEM) to which 0.2%, 0.3% and 0.4% ethanol (v/v) respectively, was added (treated) or in DMEM only (controls). Whole-mount HNK-1 immunocytochemistry was performed on treated and control chick embryos, as was an assay for caspase-dependent apoptosis. Photographs were taken of the cultures and the distance which the neural crest cells migrated from the neural tube at 24 and 48 hrs post-culture was measured. 24-hr time-lapse video microscopy recordings were also made to analyse the migration of the neural crest cells. Rhodamine-phalloidin immunocytochemistry for the actin cytoskeleton and scanning electron microscopy of surface ultrastructure were performed on migrating treated and non-treated cNCCs, as were proliferation assays and quantitative PCR of cNCCs' *β-actin*, *Rac 1*, *Rho B* and *slug* genes. There was a statistically significant increase in fetal reabsorption as well as a significantly reduced fetal survival rate observed in newborn mice fetuses that had been exposed to ethanol *in utero* compared to control fetuses. Ethanol-exposed mice showed a number of abnormalities, which were not significantly increased over

controls ($p>0.5$). Birth weight, crown-rump length and mandibular length were also not significantly different in treated fetuses compared to controls ($p>0.5$). Treated (0.3%) chick cNCCs migrated over a significantly increased distance at both 24hrs and 48hrs compared to controls ($p<0.05$) in the axes of migration that were studied. The migratory distances of cNCCs derived from embryonic stage 9 (HH) were markedly affected by treatment with alcohol. The actin cytoskeleton of treated cNCCs showed disorganisation and loss of focal adhesion contacts while *Rac 1*, *Rho B* and *slug* genes were either up-regulated or down-regulated depending on the ethanol dose and duration of treatment. Ethanol promotes significant proliferation in cNCCs and may affect their migration by altering the expression of migration-linked genes and the arrangement of the actin cytoskeleton.

ACKNOWLEDGEMENTS

My supervisor, Professor Beverley Kramer has played a major role in my life since this journey began. She invited me to apply to Wits in the first place, and since that winter morning when she picked me up at the Johannesburg International Airport, has been an insightful mentor, tireless teacher and kind friend to me. We have worked, laughed, "fought", played, drank coffee and "chilled" together over the process of time that it took this work to be completed. Through your friendly but firm supervision, I have truly grown as a researcher and learner. Thank you Prof.

Next, my thanks go to the Anatomy Ladies – past and present technical and support staff in the School of Anatomical Sciences. I could not have done this without your patient and kind assistance – especially when I arrived at 5pm in the evening looking for this or that lab key or reagent! Gwen, Leslie, Alison, Sherrie, Hasina, Monica, Jill, Alice and Donna, you have my heartfelt appreciation.

Dr. Raquel Douarte-Lightfoot was of great assistance to me in the molecular aspects of this thesis. Her expertise provided a wealth of references and her quiet but determined attitude lent precision and accuracy to my PCR bench work. I hope that we can collaborate on future studies.

To my colleagues in the School of Anatomical Sciences, too numerous to mention individually, I thank you all. We endured (and enjoyed) those many teaching hours together and helped each other to pull through. I thank the immediate past and present Heads of the School, Professors JN Maina and TJM Daly respectively; in your unique ways you provided support to me and kept the School running from day to day. I needed the stability that you provided.

Special thanks go to Dr. Nalini Pather and Dr. Mubarak Bidmos, my dear friends and collaborators. Your encouraging words, knowing smiles and silent prayers boosted my resolve when the going was tough.

Professor JC Allan, great teacher, exemplary scholar and next door (office) neighbour, thank you for your wise words of support and encouragement.

Professor Trefor Jenkins was brought in by the Faculty of Health Sciences to provide the "tipping point" oversight and mentorship needed to complete the final stages of this thesis. I enjoyed those 30-minute sessions when we chatted about Scotland, Darwin, the early years of genetics research at Wits, and my thesis – in that order. Thank you Professor Jenkins.

My current boss, Professor Det Prozesky, is especially acknowledged. He supported my application for a Faculty of Health Sciences-funded time off grant, which allowed me to take a break from my duties at the Centre for Health Science Education (CHSE) for three months, in order to write this thesis. In addition, he always had words of encouragement and support for me every time he enquired after the progress of the work. I am truly grateful.

To Dorian and the boys in my men's Connect Group, thank you for cheering me on. I am carrying each one of you in my heart as I cross the "finish line". Your prayers and support have proved invaluable.

Finally to the love of my life - my wife and partner of 18 years this spring – Iyadunni; to our sons Ilerioluwa and Babaloluwa, and my princess, Ifeloluwa, I thank you for being the best family I could have ever wished for. I now hope to spend more time at home and who knows, take you on that holiday that I've been promising for years. I love you.

TABLE OF CONTENTS Page

LIST OF FIGURES Page

LIST OF TABLES Page

1.0 INTRODUCTION

1.1 History and epidemiology of the teratogenicity of alcohol

Ethanol has been recognized as a teratogen from medieval times. As Calhoun and Warren (2007) point out, references to the association between the ill-effects of ethanol and the unborn fetus are to be found in ancient Greek and Roman belief systems. Although, some authors have postulated that the interpretation of these early observations was somewhat misplaced and premature, since paternal rather than maternal drinking was often castigated, they nevertheless acknowledge that observers in classical times recognized the link between alcohol consumption and reproduction (Warner and Rosett, 1975; Sanders, 2009). The modern era of the systematic identification of the harmful effects of prenatal ethanol exposure on unborn fetuses arrived with the works of Lemoine *et al*. (2003) and Jones and Smith (1973). Following these landmark publications, there has been a flurry of scientific activity aimed at fully characterizing the social, clinical, epidemiological and molecular aspects of the fetal alcohol syndrome (FAS) (Jones *et al*., 1976; Sulik *et al*., 1981; Colangelo and Jones, 1982; Wynter *et al*., 1983; Streissguth *et al*., 1985; Webster and Ritchie, 1991; Werler *et al*., 1991; Blader and Strahle, 1998; Goodlett *et al*., 2005; Sulik, 2005; Yamada *et al*., 2005; Yoshinaga *et al*., 2007; Agrawal and Lynskey, 2008; Tanguay and Reimers, 2008; Loucks and Ahlgren, 2009).

It is now recognized that clinical FAS represents only one extreme of what has been termed the fetal alcohol spectrum disorders (FASD). This is because researchers realized early that the neurological and morphological effects of ethanol on unborn babies whose mothers were alcohol abusers were by no means homogenous. Hence terminologies such as fetal alcohol effects (FAE) (Clarren and Smith, 1978), partial FAS, alcohol-related birth defects (ARBD) and alcohol-related neurodevelopmental disorders (ARND) have been used to describe variations in the phenotypic outcome of alcohol-exposed children (Calhoun and Warren,

2007). Phenotypically, fully-developed FAS is said to be characterized by prenatal and postnatal growth retardation, mental retardation, motor incoordination, altered craniofacial features including microcephaly, micrognathia, maxillary hypoplasia, depressed nasal bridge, narrow palpebral fissure and epicanthal folds among others (Jones and Smith, 1973; Jones, 1986; Jones and Bass, 2003; May *et al*., 2007; Jones *et al*., 2009). However, not all affected patients exhibit these features. Indeed, there may not be any visible effects of the effect of ethanol on babies born to alcoholic mothers (Mattson *et al*., 1997; Mattson *et al*., 1998). Because the data on the prevalence of the various forms of FASD have been gathered from several sources, including population, prospective, retrospective and clinical studies, the numbers of affected individuals quoted in the literature vary. However in 1996, the Institute of Medicine in the United States of America estimated the occurrence of FAS to range from 0.6 to 3 births per 1000 in most populations (The Institute of Medicine, 1996). Abel (1995) estimated an overall international prevalence of FAS as 0.97 per 1000 live births. The prevalence of FAS in a South African cohort was found by (May *et al*., 2000) to be 18 to 141 times greater than these international rates. These high rates of FAS occurrence in South Africa, judged to be the highest in the world, coupled with the high amount of alcohol consumption by pregnant women in affected communities render the scientific understanding of the factors which influence the teratogenicity of ethanol a priority, among other interventions aimed at containing the devastating effects of FAS on the population (Croxford and Viljoen, 1999; Viljoen *et al*., 2002; May *et al*., 2005).

One confounding factor in the search for the biological triggers that render ethanol consumption in pregnancy fetotoxic is the fact that full blown FAS does not occur in all cases of prenatal ethanol abuse. Even in affected offspring, the severity of dysmorphic features or neurological deficit is highly variable (The Institute of Medicine, 1996; Goodlett *et al*., 2005). Sulik (2005) observed that "as with other teratogenic agents, the amount and

frequency of alcohol consumed by the pregnant mother, as well as the stage(s) of pregnancy during which an unborn child is exposed to alcohol, are critical in determining the pattern of abnormal development". These complexities of ethanol's teratogenicity require a careful and multi-level approach in the search for candidate mechanisms that underlie how ethanol damages the unborn fetus (Goodlett *et al*., 2005).

1.2 The role of neural crest cells in ethanol's teratogenicity

The study of neural crest cells (NCCs) represents one such effort to discover the mode of action by which ethanol produces its toxic effects on fetuses *in utero.* NCCs are the principal source of the majority of the embryonic head in vertebrates, forming cranial skeletal and soft tissues (Horstadius, 1950; Gans and Northcutt, 1983; Couly *et al*., 1993; Le Douarin and Kalchiem, 1999). These cells are formed at the crests of the developing neural folds. In amphibian and avian embryos, NCCs emerge from the neural tube at the time of neural tube closure, while in mammals, emigration takes place, particularly in the cranial region, while the neural folds are still widely open (Morris-Kay and Tan, 1987; Le Douarin and Kalchiem, 1999). In particular, a distinct population of NCCs termed cranial neural crest cells (cNCCs), which originate from the level of the mid-diencephalic, mesencephalic and rhombencephalic segments of the neural folds up to the level of the 5^{th} somite, migrate into the developing nasofrontal and periocular masses as well as pharyngeal arches 1 – 4 (Graham *et al*., 1996; Le Douarin and Kalchiem, 1999; Smith and Debelak-Kragtorp, 2005). An origin in the prosencephalon for cNCCs has been proposed in avian (Le Douarin and Kalchiem, 1999), murine (Serbedzija *et al*., 1992) and rat (Matsuo *et al*., 1993) embryos.

The mechanisms by which NCCs segregate from the neuroepithelium have been extensively studied, especially in the amphibian and avian models (Dickinson *et al*., 1995; Liem *et al*., 1995; Mancilla and Mayor, 1996a; Baker and Bronner-Fraser, 1997; LaBonne and Bronner-Fraser, 1998; Mayor and Aybar, 2001a; Garcia-Castro *et al*., 2002; Luo *et al*., 2003; Basch

and Bronner-Fraser, 2006; Bronner-Fraser and Sauka-Spengler, 2009). These mechanisms, described by Le Douarin and Kalchiem (1999) include the temporal and spatial molecular interactions between the mesoderm and competent non-neural ectoderm, the stimulation of crest cell epithelial-to-mesenchymal transformation, modification of cell-to-cell interactions, permissive breakdown of the basement membrane adjacent to NCC exit regions, dissolution of N-cadherin junctions, and the promotion of cell motility. The latter mechanism is dependent on a host of molecular factors including members of the transforming growth factor β family of factors, hepatocyte growth factor/scatter factor (SF/HGF) and the transcription factor PAX-3 (Le Douarin and Kalchiem, 1999). After delaminating from the neural ectoderm, NCCs undergo a transformation from epithelial to mesenchymal morphology and migrate over long distances in the vertebrate embryo to contribute to a wide variety of definitive structures (described further in section 1.4) ranging from the skeleton of the head to ganglion cells of the peripheral nervous system (Le Douarin and Kalchiem, 1999)

1.3 Actin cytoskeleton and cell migration

The role of the actin cytoskeleton in cell migration continues to enjoy intellectual scrutiny (Sun *et al*., 1995; Evangelista *et al*., 1997; Tapon and Hall, 1997; Welch *et al*., 1997; Hall, 1998; Edwards *et al*., 1999; Maekawa *et al*., 1999; Gurniak *et al*., 2005; Maloney *et al*., 2008). Two forms of actin exist in eukaryotic cells: the globular monomeric G-actin and the polymeric F-actin. G-actin is nucleotide-binding and is either coupled to ATP (ATP-G actin) or ADP (ADP-G-actin) (Maloney *et al*., 2008). Under physiologic ionic conditions, G-actin spontaneously assembles into F-actin *in vitro*. This spontaneous polymerization is prevented *in vivo* by G-actin sequestering proteins (Sun *et al*., 1995; Maloney *et al*., 2008), which however present G-actin to intracellular sites where it is needed to form F-actin. Examples of such sites include the cortical regions in yeast cells, neuronal growth cones, and the leading edge and ruffling membranes of motile cells (Palmgren *et al*., 2002; Vartiainen *et al*., 2002).

These leading edges or cell protrusions (e.g. filopodia, lamellipodia and stress fibres) in migrating cells consist of a core of actin cytoskeleton filaments that are continuously being polymerised, while their proximal ends are being depolymerised (Welch *et al*., 1997; Maloney *et al*., 2008). This energy-dependent "treadmilling", coupled with the activity of the actin-binding proteins, is central to the motility of migrating cells, including neural crest cells (Carlier *et al*., 1997; Gurniak *et al*., 2005; Maloney *et al*., 2008). The expression of intracellular actin is encoded by the actin genes. The number of actin genes in higher organisms varies widely, with humans having between 20-30, the mouse more than 20 and the chick between four and seven actin genes (Kost *et al*., 1983). There are at least six known isoforms of actin in vertebrates, namely four different types of α-actin, β- and γ-actin. These are encoded by the genes ACTA1, ACTA2, ACTC, ACTG2, ACTB and ACTG1 respectively (Sparrow and Laing, 2008). While ACTC, ACTG2, ACTA1, ACTA2 are expressed in different forms of muscle (cardiac, enteric, skeletal and smooth), ACTB and ACTG1 are cytoplasmic actin genes and are expressed almost uniformly in non-muscle cells of several species (Kost *et al*., 1983; Nakajima-Iijima *et al*., 1985; Sparrow and Laing, 2008). Since it is known that actin gene expression is tissue-specific and developmentally regulated (Vandekerckhove and Weber, 1978; Kost *et al*., 1983) and that abnormalities in actin gene expression have been associated with abnormalities of fibroblast cell division and motility (Nakajima-Iijima *et al*., 1985), it would appear to be of some value to examine how ethanol may affect actin gene expression in the highly motile and dividing cNCCs.

1.4 Cranial neural crest cell migration and fate

For decades, the migration of neural crest cells has been observed by scientists in search of clues that may explain the behaviour of these cells *in vivo.* NCC migratory pathways have been previously mapped using immunocytochemistry methods that identify a 140 kD surface antigen expressed by migrating NCCs in several vertebrate species. This antigen is

recognised by the monoclonal antibody, HNK-1. The ability of workers to thus track neural crest cell migration has contributed a great deal to our current knowledge about the origin, migration and fate of these cells (Tucker *et al*., 1984; Bronner-Fraser, 1985; Rickmann *et al*., 1985; Bronner-Fraser, 1986; Bronner-Fraser, 1987; Erickson *et al*., 1989; Sadaghiani and Vielkind, 1990; Lee and Lwigale, 2008).

In the avian head, the pathways through which cNCCs migrate are related to their eventual fate. Thus, maxillary and mandibular arch-yielding mesencephalic cNCCs migrate rostrally towards the nose, then laterally into the first and second pharyngeal arches (Le Douarin and Kalchiem, 1999). On the other hand, migration of rhombencephalic crest cells occurs in segmental "waves" to ultimately yield pharyngeal arch components and cranial ganglia (Lumsden *et al*., 1991; Bronner-Fraser, 1994; Graham *et al*., 1996; Le Douarin and Kalchiem, 1999). More specifically, the structures derived from NCCs include the skeleton and dermis of the head, melanocytes, Schwann cells, ganglion cells of certain cranial nerves and those of the peripheral and enteric nervous systems, chromaffin cells of the suprarenal medulla as well as components of the outflow tract of the heart (Bolande, 1974; Dupin *et al*., 1993; Le Douarin and Kalchiem, 1999; Trentin *et al*., 2004; Smith and Debelak-Kragtorp, 2005). It is noteworthy that cNCCs give rise to the entire skeleton of the face (viscerocranium), including the loose connective tissue thereof (Trainor and Tam, 1995; Le Douarin and Kalchiem, 1999). The foregoing observation is of critical importance, given that ethanol appears to target the structures of the face leading to abnormalities such as absent philtrum, depressed nasal bridge, narrow palpebral fissure, hypognathia, agnathia, microcephaly and midline clefts to the lip, palate or cranium (Jones and Smith, 1973; Cook *et al*., 1987; Sulik *et al*., 1988; Jones and Bass, 2003; Jones *et al*., 2009). Sulik (2005) restated the pertinent fact that modern tools that are being developed to assist clinicians to

accurately diagnose FAS rely on the facial phenotype as a key component of their toolkit (Sulik, 2005; Hoyme *et al*., 2005).

1.5 Proposed mechanisms by which ethanol exerts its teratogenic effects

In general, research scientists have relied on animal models in their effort to elucidate the underlying cellular and molecular factors, which determine fetal outcome after prenatal alcohol exposure, using mouse and rat animal models. To a lesser extent, pig, sheep and non-human primates have also been employed for this purpose (Becker *et al*., 1996; McBride and Li, 1998; Astley *et al*., 1999; Cudd, 2005). However, specifically regarding cNCCs and their role in ethanol's effect on craniofacial appearance, amphibian (Nakatsuji, 1983; Peng *et al*., 2004a; Peng *et al*., 2004b; Yelin *et al*., 2007), avian (Cartwright and Smith, 1995b; Debelak and Smith, 2000; Su *et al*., 2001; Giles *et al*., 2008; Smith, 2008) and murine (Sulik *et al*., 1981; Van Maele-Fabry *et al*., 1995; Dunty *et al*., 2002) models have been found most suitable. Each model has its own distinct advantages and disadvantages in terms of how well it replicates the FAS phenotype, permits access to developmental pathways and simulates human FAS (Becker *et al*., 1996; McBride and Li, 1998; Cudd, 2005). It is accepted that no single animal model will resolve the many questions of ethanol's teratogenicity. The optimum approach will utilise multiple animal models to engage different questions about the effects of ethanol on developing fetuses (Driscoll *et al*., 1990; Cudd, 2005).

Several molecular mechanisms have been proposed to explain how ethanol exerts its effects on the developing embryo. (Goodlett *et al*., 2005) categorised these mechanisms into seven broad groups as follows:

1. Disrupted cellular events (e.g. altered glucose utilization/transport; suppression of protein and DNA synthesis and oxidative stress).
2. Impaired cell acquisition or altered developmental timing (e.g. altered cell cycle, mistimed events of cell generation, migration or neurite outgrowth).

3. Altered regulation of gene expression (e.g. reduced retinoid acid signalling or effects on other transcription factors).
4. Disrupted cell-cell interactions (e.g. inhibition of L1 cell adhesion molecule function).
5. Interference with growth-factor signalling or other cell-signaling pathways.
6. Cell damage/cell death (e.g. apoptosis or oxidative stress).
7. "Secondary" sources of damage (e.g. altered placental function, hypoxia/ischemia or acetaldehyde formation).

1.6 A possible role for cranial measurements in the study of the aetiology of FAS

Sulik (2005) in her review enumerated the most likely mechanistic routes by which ethanol damages fetuses, including excessive death of sensitive cells, particularly those of the telencephalic midline structures that constitute the "anterior neural ridge", and neural crest cells. Other mechanisms explored by the latter author also included free radical damage, perturbations to calcium ion signalling cascades and alterations to the expression of genes such as sonic hedgehog (*Shh*), *Fgf-8, Pax6,* and the genes that code for bone morphogenetic proteins, (BMP) (Sulik, 2005). Virtually all authors who have reviewed the wide-ranging mechanisms by which ethanol exerts its effects have agreed however that more work needs to be done to define these effects more accurately (Goodlett *et al*., 2005; Smith and Debelak-Kragtorp, 2005; Sulik, 2005). One such area of enquiry is the detailed definition of how ethanol affects both hard and soft tissues of the face. Earlier workers have tended to quantify fetal craniofacial changes attributed to ethanol by examining either skulls denuded of soft tissue (Edwards and Dow-Edwards, 1991; Su *et al*., 2001) or radiographs (Giglio *et al*., 1987; Hernandez-Guerrero *et al*., 1998). Although it has been postulated that the underlying neural crest cell-derived visceral skeleton eventually determines the shape of the facial soft tissues

(Smith and Debelak-Kragtorp, 2005), it is still important to determine to what extent the soft tissues themselves are altered by *in utero* alcohol exposure. Hence, by measuring both the craniofacial skeletal elements and soft tissues following prenatal ethanol exposure, new information about the role played by alcohol in the generation of facial dysmorphologies may come to light. Another area where direct measurement could be beneficial is the assessment of actual distances that alcohol-treated cNCCs travel *in vitro*. Apart from the work of Rovasio and Battiato (2002), published work that details the distances over which these cells migrate *in situ* or under culture conditions after exposure to ethanol is limited. Measurement of such distances may elucidate the effect of ethanol on cNCCs migration.

1.7 The rationale for extending some previous studies of the effect of ethanol on cNCC cytoskeleton

There have been some attempts to visualize the morphology and actin cytoskeleton of cNCCs after exposure to ethanol. Work by authors such as Hassler and Moran (1986a; 1986b), Davis *et al*. (1990) and Rovasio and Battiato (2002), where a combination of light and scanning electron microscopic methods were used, were pioneering in this regard. There could be some value in reproducing the results of these earlier efforts and fine-tuning them by accurately determining the amount of ethanol to which cultures are exposed rather than approximating final concentrations (Davis *et al*., 1990) in systems where the ethanol concentrations were "estimates" (Rovasio and Battiato, 2002). Moreover since in humans, the mildest clinical effects of ethanol commence at blood alcohol concentrations (BAC) as low as 0.05% (v/v) or 110 mM, while marked uncoordination and stupor occur at BAC of just under 10% ethanol (v/v) or 870 mM (Bryson, 1996), it is conceivable that ethanol abusers will have blood ethanol concentrations that lie in the intoxicating, but sub-lethal range of these values. In contrast to the aforementioned authors, who exposed neural crest cell cultures to ethanol

concentrations in the range of 7mM – 150mM it is proposed in the present study that the simulation of human BAC require that *in vitro* cultures of cNCCs be exposed to ethanol concentrations nearer the range of 430 mM – 860 mM (0.2% - 0.4%, v/v).

1.8 Ethanol-induced changes to neural crest cell gene expression

Regarding investigations into the possible roles of altered cNCCs gene expression in the FAS phenotype, while current work has focused on assessing ethanol-induced changes in the expression of genes and signalling molecules that are implicated in establishing rostro-caudal identity or patterning in the embryo (e.g. BMP, *Fgf8, msx-2, Pax6, Shh, slug* and retinoic acid) (Duester, 1991; Graham *et al*., 1993; Deltour *et al*., 1996; Graham *et al*., 1996; Duester, 1998; Peng *et al*., 2004b; Yelin *et al*., 2005; Yelin *et al*., 2007), genes that code for the structure of cell cytoskeleton (e.g. β-*actin*) and those implicated in the function of the cytoskeleton (e.g. *Rac 1* or *Rho B*) are yet to be examined.

β-actin is the actin isoform, which, upon polymerization and subsequent assembly, forms the principal component of the cytoskeleton in non-muscle cells. It is encoded by the ACTB gene. (Chhabra and dos Remedios, 2008). Due to the central role played by actin in the cytoskeleton of migrating cells (pages 4 and 5), it is important to investigate how ethanol exposure to migrating cNCCs may modulate the expression of the ACTB gene.

Closely related to actin and its function in cytoskeleton assembly cell migration are the members of the Ras and Rho family of GTPases, including Rac1 and Rho B. Other Rho family members include Rac 2 and 3, Rho D and Rho G as well as Cdc42Hs and G25K. All these members share 50-55% identity to each other (Hall and Nobes, 2000). These molecules are of special interest because they "couple intracellular signal transduction pathways to changes in the external environment" of Eukaryotic cells (Bar-Sagi and Hall, 2000). In animal cells, Ras and Rho GTPases regulate an overlapping set of cellular responses,

including gene expression, cellular proliferation and actin-based cell motility (Bar-Sagi and Hall, 2000). For the latter function, Rho GTPases are thought to be pivotal. Specifically, while Rac is required at the front of the cell where it regulates actin polymerization and membrane protusion, Rho is thought to regulate the contraction and retraction of forces that occur in the cell body and at the rear (Raftopoulou and Hall, 2004). As the disruption of these cellular forces form one mechanism of ethanol's teratogenicity (Goodlett *et al*., 2005), an area of enquiry would be valuable to explore whether the genes that code for Rho GTPases are perturbed by *in vivo* ethanol exposure of cNCCs.

Another gene of interest with regard to cNCC function is *slug*. *Slug* is a member of the Snail zinc-finger transcription factors. The only other known member of this family in vertebrates is *zinc* (Sefton *et al*., 1998). In chick and amphibian animal models, *slug* is expressed in the primitive streak, ingressing mesodermal cells and premigratory neural crest cells (Mayor *et al*., 1995; Mancilla and Mayor, 1996b; Sefton *et al*., 1998; Mayor and Aybar, 2001b). When the expression of slug either NCC precursors are not formed at earlier stages or formed NCCs fail to migrate (LaBonne and Bronner-Fraser, 2000). Furthermore, when either *slug* or *snail* mRNA was used to reverse the downregulation of *slug*, NCC migration recovered dramatically (Carl *et al*., 1999). With such a strong link between gene expression of *slug* and NCC formation and migration, a formidable tool is provided to investigate whether ethanol regulates the induction of cNCCs at the level of gene expression.

The roles of β-actin, the Rho family of GTPases and the *slug* transcription factors delineated above provided the rationale for our efforts in the present study to investigate whether or not the expression of these genes in cultured cNCCs is perturbed by their exposure to ethanol concentrations similar to those that have been implicated in human FASD.

1.9 Aims of this study

Specifically, we set forth to accomplish the following aims:

1. To investigate the effect of acute administration of oral ethanol on some maternal and fetal growth indices in the mouse.
2. To describe the effect of *in vitro* ethanol exposure on the morphology, migration and cell death of cultured chick cNCCs.
3. To investigate the effect of *in vitro* ethanol exposure on the expression of the *β-actin*, *RhoB* and *slug* genes derived from chick cNCCs.
4. To determine whether ethanol exerts dose-dependent and embryonic stage-dependent effects on cultured cNCCs *in vitro.*

2.0 MATERIALS AND METHODS

Animal ethics clearance was obtained from the Animal Ethics Screening Committee of the University of the Witwatersrand for all aspects of this project that involved the use of mice (number 2001/65/3; 2004/89/1) and chick eggs (number 2005/55/1; 2007/2/1).

2.1 Mice fetuses and ethanol exposure

Twenty-three adult time-mated C57BL/6J female mice were sourced from the Central Animal Services of the University of the Witwatersrand, Johannesburg. The gestation period of the animals at the time at which they were acquired ranged between gestation days (GD) 0 and 3, GD 0 being recorded as the date that a vaginal plug was observed in an animal. The pregnant mice were maintained under standard laboratory conditions and fed on lab chow and water *ad libitum*. The animals were weighed daily to assess weight gain. They were then separated into two groups: Group 1 mice (n=13) were given 0.03 ml/g of an aqueous solution of 25% (vol/vol) ethanol (Spong *et al*., 2001) via an orogastric tube at 0900 h on GD 6, 7, and 8, coinciding with the period of primitive groove formation and neural-fold elevation and closure in the mice (Waterman, 1976; Kaufman, 1990). Group 2 mice (controls, n=10) received the same amount of water by the same route at the same times. In mammalian species, neural crest cells exit the neural tube before closure of the neural folds (Lumsden *et al*., 1991; Bronner-Fraser, 1994; Le Douarin and Kalchiem, 1999). The timing of the ethanol insult in this study was therefore aimed at neural crest cells at the time which they acquire migratory potential and start to migrate. Group 1 mice, due to the effects of alcohol intoxication were unable to eat for periods of time. Hence, Group 2 mice were kept without food and water for the duration that Group 1 mice were unable to feed. All the pregnant mice were kept without further treatment until GD 18 when they were killed by an intraperitoneal injection of 0.01 ml/g of Euthanase® (Kyron Laboratories, Johannesburg).

Fetuses were removed from the mice and the number of live, dead, or reabsorbed fetuses was noted. Mean litter size was determined and the percent reabsorptions calculated using the total number of fetuses (live, dead, and reabsorbed) as the denominator. Fetal survival rate was calculated as the percentage live fetuses divided by the total. The live fetuses were weighed and their crown-rump lengths were measured with a standard vernier caliper. The detailed morphological appearance of the mice fetuses was studied under a stereomicroscope. In particular, the fetuses were checked for the presence or absence of craniofacial abnormalities such as cleft lip or palate, hypognathia or agnathia, anophthalmia, absent philtrum, and other previously reported anomalies said to occur in the head of children suffering from FAS (Chernoff, 1977; Sulik *et al*., 1981). All animals were photographed in the left lateral position using a stereomicroscope with an attached image analyzer (Nikon SMZ 1500 Nikon, Japan). All photographs were taken at the same vertical height from the microscope objective using the same magnification.

From the digital photographs, the following measurements were taken after Giglio *et al*., (1987); Ward (1989); Brown (1990); Hernandez-Guerrero *et al*. (1998):

- Vertico-mental length (VML) - defined as the perpendicular distance between two parallel lines, each at 45° to the horizontal, with one line at the vertex of the fetus and the other at the mental protuberance (Fig. 1A).
- Maxillary length was defined as the horizontal distance between two vertical lines, with one line at the most anterior part of the maxilla and the other at the maxillary skin crease (Fig. 1B).
- Mandibular length (MANL) was defined as the horizontal distance between the most anterior part of the mandible and the junction between the mandible and the neck (Fig. 1B).

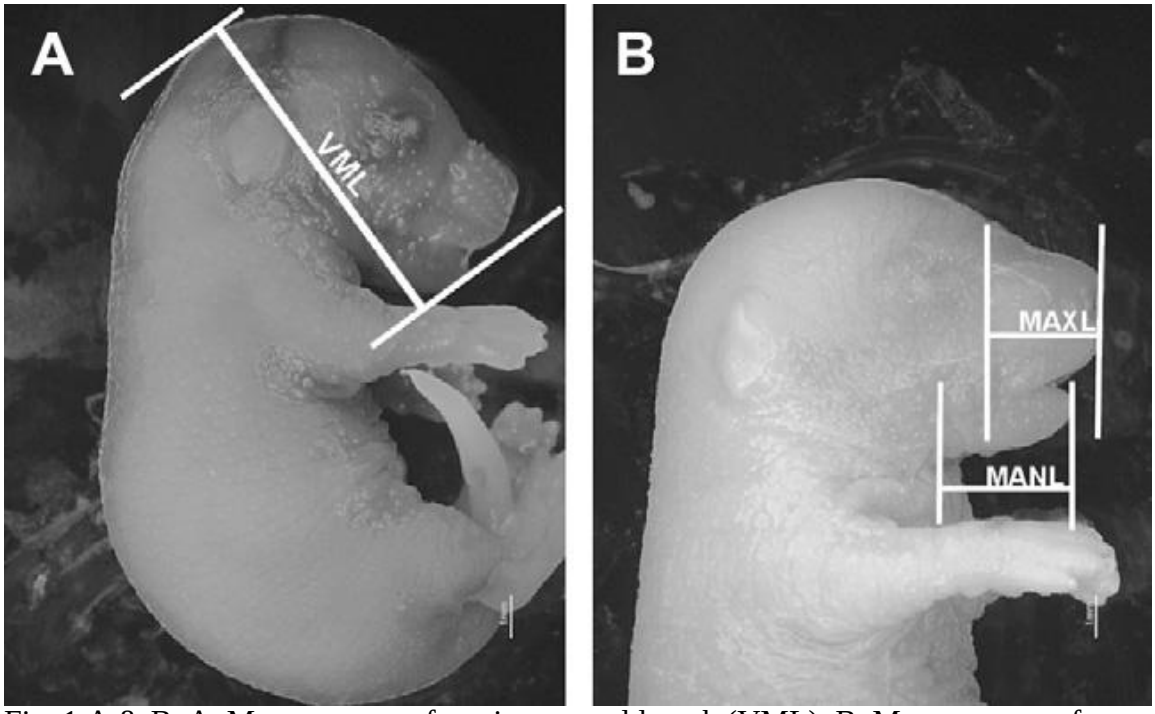

Fig. 1 A & B. A. Measurement of vertico-mental length (VML). B. Measurement of maxillary length (MAXL) and mandibular length (MANL).

Animals with gross head and face deformities, or those where the maxillary or cervical landmarks could not be ascertained with confidence, were not measured. Measurements were carried out using the Corel Draw® software program. This program has vector analysis capability and is designed to convert the measured digital distance into actual distances using the appropriate scale. All measurements were taken at two different times, 24 h apart and the obtained data verified using Lin's coefficient of concordance (Lin, 1989) to ensure repeatability (Appendix A). The measurements were then analyzed for statistical significance using the Microsoft Excel® computer program, where $P<0.05$ was considered as significant.

2.1.1 Determination of blood ethanol concentration

To address concerns about blood ethanol concentrations and the possible effect of this on feeding patterns and nutrition in maternal mice, an additional group of 11 pregnant

C57BL/J dams consisting of six ethanol-fed and five control animals were similarly treated in all respects to the initial 23 dams in the main study. Daily food intake was monitored in these 11 dams by subtracting the weight of the lab chow remaining in the feeding trough at 08h00 each morning from the weight of the food given the previous morning. Furthermore, blood samples were withdrawn from the tail veins of all mice at 30, 60, 90, and 120 min after an orogastric feed of either ethanol or water. The samples were collected in Modulohm Vitrex© plain micro hematocrit capillary tubes and immediately placed on ice. All samples were then frozen at -70 ºC until analyzed for ethanol concentration.

Blood ethanol concentration (BEC) was determined as follows: To 10-40µl of whole blood obtained from mice, 40-70 µl of distilled water in 0.5 ml Ultrafree-MC© Millipore centrifuge tubes (Amicon bioseparations) were added. This achieved an initial volume of 80 ml to which an additional 80 ml of 0.1% propanol solution in water was added, yielding a final volume of 160 ml. This was centrifuged for 30 min at 13,000 rotations per minute at a temperature of 10 ºC in Mikro 22R© centrifuge machines (Hettich/Zentrifugen). Five microlitres of the ultra-filtrate were then analyzed in a 5890A gas chromatograph (Hewlett Packard), which was attached to an SP4290 integrator (Spectra-Physics). BECs were determined from the areas that each sample produced in comparison to standard curves previously obtained by analyzing solutions of known ethanol/propanol mixtures. Samples were analysed in duplicates and mean values were recorded after correction for dilution.

2.1.2 Skeletal staining

A total of 14 fetuses from dams to which ethanol had been administered and 14 fetuses from control mice were used for skeletal staining by the Alizarin red S and Alcian Blue method modified from the method described by Menegola *et al*. (2001). Immediately after extraction from maternal deciduas, fetuses were left immersed in tap water overnight to macerate the

skin. They were then skinned, eviscerated, and placed in an acid staining solution for 24hrs at room temperature, after which they were dehydrated in 96% ethanol for at least 6hrs. The fetuses were then placed in a basic staining solution for 48hrs at room temperature to allow muscle maceration. Following this, the fetuses were cleared and hardened by placing them in a cleaning solution for 8hrs. Finally, they were preserved in a 1:1 mixture of glycerin and 70% ethanol solution. All the solutions used were prepared as described by Menegola *et al*. (2001) (Appendix C). Representative fetal samples were photographed as described earlier.

Results from the work undertaken in section 2.1 have been published in the journal *Alcohol* (Appendix B).

2.2 Chick embryos and ethanol exposure

The avian embryo is widely recognized as a good model for developmental studies, particularly for the experimental visualization and manipulation of neural crest cells (Le Douarin and Kalchiem, 1999; Le Douarin, 2004; Stern, 2005). This animal model has proved to be more accessible to *in vitro* culture of neural crest cells (NCCs) in our laboratory, and there exists a significant amount of experience in the successful use of the chick as a model animal for experimental manipulations. Furthermore, considerably more work in the vast area of neural crest biology has been published using avian rather than murine models. Therefore, since the neural crest is the focus of this study and for the foregoing reasons, the chick embryo was chosen as the animal model for the *in vitro* section of this work. Embryos aged between stages 8-10 Hamburger and Hamilton (Hamburger and Hamilton, 1992) (HH) were used throughout this study because at those embryonic stages, the chick neural folds begin to fuse and cranial neural crest cells emigrate from the neural tube (Lumsden *et al*., 1991; Le Douarin and Kalchiem, 1999).

2.2.1 Whole mount HNK-1 antibody labeling of chick embryos for visualizing neural crest cells

Fertile chick eggs of a South African strain (*Potchefstroom koekoek*) were obtained from the National Health Laboratory Service. They were incubated at 37ºC and 80% humidity for 36 hours. The eggs were then swabbed with 70% alcohol and broken into egg dishes containing previously sterilized chick Ringer solution (Appendix D), under aseptic conditions. The chick blastoderm was visualized, the embryo was staged and the blastoderm excised off the yolk and transferred into a 35mm Nunc culture dish (Nunclon, Denmark) containing either chick Ringer solution (control, n=6) or chick ringer containing 0.2% or 0.4% v/v ethanol (n=6 each) (Davis *et al*., 1990; Deltour *et al*., 1996; Peng *et al*., 2004b). The intact blastoderm of each embryo was incubated at 37°C and 5% CO_2 in air in a humidified incubator (Labcon, South Africa) for three hours, after which they were fixed overnight in 3% paraformaldehyde solution in PBS. Three hours was chosen as the duration of ethanol exposure in order to simulate the conditions in which embryos are exposed to maternal binge alcohol consumption (Bonthius and West, 1990).

Following fixation, the embryos were washed twice in PBS containing 0.5% bovine serum albumin (BSA), and then permeabilized with 0.1% Triton® X-100 in PBS for 20 minutes while rocking gently. Permeabilization was followed by incubation with the primary antibody HNK-1 (monoclonal antibody, Sigma), diluted 1:50 with 0.5% BSA and 0.5% Triton® X-100 in PBS. The primary antibody was substituted with PBS in the embryos which served as negative controls. Incubation took place overnight at 4°C. The following day, the embryos were washed in 0.5% BSA in PBS twice for 20 minutes each, after which they were incubated in secondary (goat-anti-mouse) antibody diluted 1:200 in 0.5% BSA at room temperature in a humidified chamber for one hour, while rocking the containers gently. The

antigen-antibody reaction was then visualized by incubation of the intact embryos in 3, 3'-diaminobenzidine solution (DAB, Sigma) for exactly 5 minutes each, timed exactly. All embryos were washed twice in 0.5% BSA in PBS for the duration of 20 minutes each, after which they were placed in PBS and observed with a Zeiss IM 35 phase contrast microscope using the X4 phase contrast objective. Representative embryos were digitally photographed (Olympus) and the photographs stored electronically.

2.2.2 Chick neural crest cell *in vitro* culture

Fertile *Potchefstroom koekoek* chick eggs were obtained, incubated and prepared as described previously (Section 2.2.1). From these embryos the neural tubes were excised from mid-diencephalon to the level of the fifth somite. These levels yield cranial neural crest cells that contribute to the facial skeleton and soft tissues of the head of vertebrates (Le Douarin and Kalchiem, 1999). The neural tubes were placed in a glass container to which a 0.04% collagenase (Sigma) solution was added. The explants were incubated for at least 30 minutes at 21ºC. After this, the collagenase was removed and the neural tube explants were placed in chick Ringer and dissected free of any somites, notochord, epithelium and other membranes that remained, to yield only neural tube explants. These explants were then placed either on to coverslips or within four-well Nunc culture dishes (Nunclon, Denmark) which had been previously coated with 2.5% fibronectin (Sigma) (Appendix D) and incubated at 37°C for one hour.

The neural tube explants were divided into four groups comprising three groups of ethanol-treated (experimental) explants and one group of control (untreated) explants. The ethanol-treated explants were cultured in Nunc culture dishes (Nunclon, Denmark) containing 0.2%, 0.3% or 0.4% v/v ethanol respectively (n=25 each) made up in Dulbecco's minimal essential medium (DMEM) (Gibco, South Africa), while the control group (n=25) was cultured in

Nunc dishes with DMEM only. The cultures were maintained at 37°C in a 5% Co_2 in air humidified incubator for six days of continuous culture, with medium changes (and fresh ethanol treatment for the treatment group) taking place at intervals of 48hrs. All cultures were observed on a phase contrast inverted microscope (Olympus) and digitally photographed daily (Olympus). Photographs were stored electronically for further analysis.

2.2.3 Determination of the ethanol concentration of the culture medium

To ensure that the ethanol concentration in the ethanol-treated groups remained constant, ethanol contents were determined at 24 hrs and at 48-hour intervals on selected cultures, using the K-620 Ethanol Assay Kit® (Biovision California, USA). Prior to the ethanol assay, a Reaction Mix® was prepared from reagents supplied in the Assay Kit as follows:

46 µl Ethanol Assay Buffer®
2 µl Ethanol Probe® (to which 220µl DMSO* was previously added)
2 µl Ethanol Enzyme Mix® (to which 220µl DMSO was previously added)
Total = 50µl Reaction Mix®

*DMSO = Dimethylsulphoxide

The Reaction Mix was prepared in multiples of the number of samples required, including those used to prepare the standard curve. All samples and standard curve preparations were made up to a volume of 50µl, bringing the total assay unit to 100 µl.

The standard curve was prepared by mixing 11.7µl (9.2 mg) of pure ethanol standard with 988.3µl of the Ethanol Assay Buffer® and mixed well. 10µl of the diluent was then added to 990µl of the Ethanol Assay Buffer® to generate 2 nmol/µl of ethanol standard. Known volumes of this diluted ethanol standard (0, 4, 8, 12, 16, and 20µl) were then placed into individual wells of a Falcon® 90-well micro plate and the volume adjusted to 50µl per well with Assay Buffer to generate the amount of 0, 8, 16, 24, 32, 40 nmol per well of ethanol standard . Samples of the medium from 0.2%, 0.3% and 0.4% ethanol-treated neural crest cultures were pipetted into designated wells in the 90-well micro plate in known dilutions, up

to a maximum of 50µl, to each of which was added 50 µl of the Reaction Mix. The reaction was then incubated in the dark for 60 minutes, after which the optical density (OD) was read at 570nm in a spectrophotometer. After correcting for the background reading by subtracting the OD of the zero ethanol standard preparation from all the readings, the ethanol concentration of the samples was calculated from their value on the standard curve, multiplied by the dilution factors in the following equation:

C = Sa/Sv nmol/ul (or mM)

Where

Sa = sample amount from the standard Curve (nmol).

Sv = sample volume added into the sample well (ul).

Ethanol determination of the samples was done in triplicates.

2.3. Measurement of chick cranial neural crest cell migratory distances

The distance migrated by chick cNCCs from the neural tube in both the control and treated cultures was measured using the Corel Draw® software programme. The method of measurement used was adapted from that previously described by Rovasio and Battiato (2002). While these aforementioned authors used advanced computer software to measure the area, perimeter, "compactness", "curvilinear distance" and velocity of neural crest cells, only the linear distance was measured in the present work. Furthermore, while Rovasio and Battiato (2002) used the centre of the neural tube as their reference to determine the linear distance migrated by cNCCs, the lateral edge of the neural tube was employed in this study, as we found that this edge was well-defined, clearly visualized and was a more reliable reference point than the centre of the neural tube. After accurately calibrating the software,

photographs of control and ethanol-treated cultures were subjected to image analysis as follows (Fig. 2): Two axes were defined, parallel (x) and perpendicular (y) to the long axis of

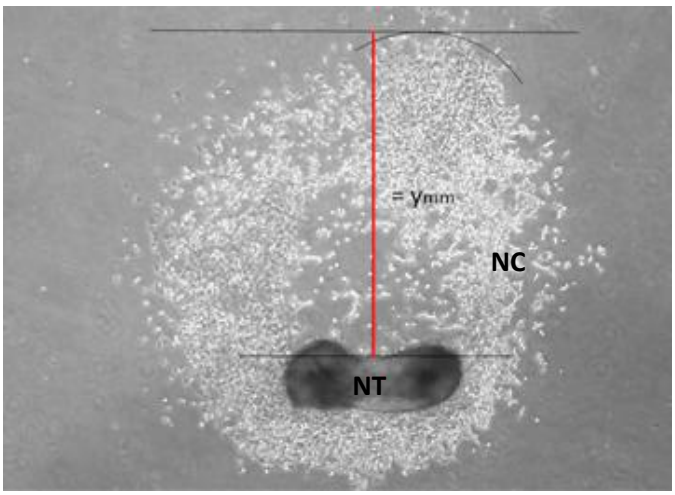

A

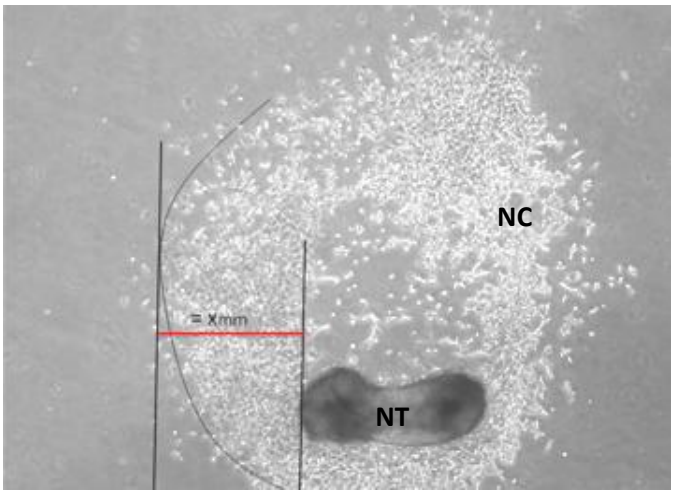

B

Fig. 2 A & B. Measurement of migratory distance in the y axis (A) and x axis (B). NT, neural tube; NC, neural crest cells (Olympus stereomicroscope X40).

an explanted neural tube. Cells that were farthest from a line drawn to coincide with the edge of the neural tube in these two axes were identified as being at the migratory front of migrating crest cells. An arc was drawn to mark this migratory front (Rovasio and Battiato, 2002). A line was then drawn from the edge of the neural tube to meet the centre of this arc. This was taken as the distance of migration in that particular axis. While the distance migrated by cells emerging from both sides of the neural tube was measured in this way, the greater value of the two sides was chosen as the distance of migration. In strict mathematical terms, the value obtained for 'distance' of migration as defined above is in fact rightly termed 'displacement', having both magnitude and direction in space. It is a vector quantity (Horan and Lavelle, 2004). A mathematical operation was therefore carried out to obtain a value, whose magnitude would be a sum of the displacements in the x- and y- axes and whose direction would be 45° to either axis (Spiegel, 1959; Matthews, 1998; Horan and Lavelle, 2004). This new value, which was defined as the "vector distance (vDistance)", gave an indication of the outer limit at 45° from the x and y axes of the explanted neural tube, at which migrating cNCCs could be located.

Two categories of measurements were made. First, the distance migrated by control and ethanol-treated neural crest cells was measured without regard to the Hamburger and Hamilton (1992) (HH) embryonic stage of the embryos from which they were derived. For this category, only the broad groups of control and the different concentrations of ethanol-treated cultures were taken into account. A second set of measurements was made by further separating control and ethanol-treated cNCCs cultures into the HH stage at which their source embryo (and neural tube) was obtained. This was done so as to take into account any possible effect on cNCCs migration, of developmental cues programmed into the cells at specific HH stages (Lumsden *et al*., 1991). The numbers of cultures measured for the first category are as follows: 24hr control cultures: n=26; ethanol-treated cultures: (0.2%, n=13, 0.3%, n=10 and

0.4%, n=24 respectively); 48hr control cultures: n=15; ethanol-treated cultures: (0.2%, n=9; 0.3%, n=6 and 0.4%, n=10 respectively). For the stage-specific cultures, the numbers were as follows: HH stage 8, 24hr cultures control: n=6; ethanol-treated cultures: (0.2%, n=6, 0.3%, n=6 and 0.4%, n=6 respectively). HH stage 9, 24hr cultures control: n=6; ethanol-treated cultures: (0.2%, n=6, 0.3%, n=6 and 0.4%, n=6 respectively). HH stage 10, 24hr cultures control: n=6; ethanol-treated cultures: (0.2%, n=6, 0.3%, n=6 and 0.4%, n=6 respectively). HH stage 8, 48hr control cultures: n=6; ethanol-treated cultures: (0.2%, n=6, 0.3%, n=6 and 0.4%, n=6 respectively). HH stage 9, 48hr cultures control: n=6; ethanol-treated cultures: (0.2%, n=6, 0.3%, n=6 and 0.4%, n=6 respectively). HH stage 10, 48hr cultures control: n=6; ethanol-treated cultures: (0.2%, n=6, 0.3%, n=6 and 0.4%, n=6 respectively).The measurements were repeated and validated using the Lin coefficient of concordance (Lin, 1989) as described earlier.

2.4 Cranial neural crest cell (cNCC) Proliferation Assay

Primary cultures of control and ethanol-treated cNCCs which had been cultured on cover slips were harvested at 24hrs (control n=4 cultures; ethanol-treated 0.2%, 0.3% and 0.4% v/v n= 4 cultures each) and at 48hrs (control n=4 cultures; ethanol-treated 0.2%, 0.3% and 0.4% v/v n= 4 cultures each) respectively. Following fixation in 70% ethanol, all cultures of cNCCs were immunostained using the protocol for the Proliferating Cell Nuclear Antigen (PCNA) BioAssay™ Kit (US Biologicals, Massachusetts) (Appendix E). The PCNA is a nuclear antigen that is widely used to identify replicating cells (Connolly and Bogdanffy, 1993; Dietrich, 1993; Kubben *et al*., 1994; Kurki *et al*., 1988; Leung *et al*., 2005; Ahlgren, 2008). After immunostaining, all cultures (on cover slips) were covered with Histomount® (US Biologicals, Massachusetts) and inverted on to slides, preparatory to microscopy. Control and ethanol-treated cultures were visualized at high-power magnification using the

Zeiss Axioscope® microscope (Zeiss, Germany) attached to a Nikon image analysis system (Nikon, Japan). Six representative images were captured for each culture by advancing the mounting stage of the microscope systematically (vertically or horizontally) through six consecutive fields of view. The images were then analysed using the Image J software (National Institutes of Health, USA). For each (control or ethanol-treated) sample, the number of PCNA-positive cells was counted as was the number of PCNA-negative cells. The number of PCNA-positive cNCCs was then expressed as a percentage of the total number of cells. This was regarded as the mitotic index (MI). The average MI was then calculated for control and 0.2%, 0.3% and 0.4% v/v ethanol-treated cells respectively. Cell counts were validated using the Lin's coefficient of correlation (Lin, 1989) as described earlier. Statistical analysis was performed using the MS Excel® software, with statistical significance being set at $p<0.05$.

2.5 Time-lapse video microscopy of migrating chick cranial neural crest cells

Time-lapse video microscopic recordings of the migration of control and ethanol-treated cranial neural crest cells were made using the Zeiss Axiovision® 4.5, 2005 software, to visualize dynamic aspects of cNCC migration, not available from still photographs (Rovasio and Battiato, 2002). Three control and six ethanol-treated cultures of HH stage 8-10 cNCCs (0.2% v/v ethanol-treated, n=3; 0.4% v/v ethanol-treated, n=3) were recorded. After culturing the chick neural crest cells as described previously, selected cultures were placed in an incubator mounted over a Zeiss Axioscope® inverted phase contrast microscope. The humidified incubator is constructed in such a way that temperature was maintained at 37°C and CO_2 concentration was maintained at 5% in air. Digital images of cultures were captured continuously at 30 minute intervals, and recordings were made over 24 hours using the

multichannel camera settings of the video microscope. The images were fed to a computer connected to the video microscope and stored for further analysis (See Appendix H).

2.6 Observation of the actin cytoskeleton of chick cranial neural crest cells

Morphology of the actin cytoskeleton of the control (n=10) and ethanol-treated (n=10 each for 0.2%, 0.3% and 0.4% v/v concentration) cNCCs of stages 8 – 10 HH was studied by Rhodamine-Phalloidin® immunofluorescence (Molecular Probes). Control and ethanol-treated cells were fixed in 3.7% formaldehyde solution made up in phosphate buffered saline, pH 7.4 (PBS) (Appendix D) for 30 minutes at room temperature. The fixed cells were then washed twice for 20 minutes each with PBS, and then permeabilized with 0.1% Triton® X-100 in PBS for 20 minutes while rocking the cultures gently. Permeabilization was followed by incubation with primary antibody (HNK-1 monoclonal antibody, Sigma), diluted 1:50 with 0.5% BSA and 0.5% Triton® X-100 in PBS for one hour at room temperature in a humidified chamber. The cultures were then washed in 0.5% BSA in PBS twice for 20 minutes each. After this, the cultures were incubated in secondary (goat-anti-mouse) antibody diluted 1:200 in 0.5% BSA at room temperature in a humidified chamber for one hour, while rocking the cultures gently. This was immediately followed by incubation of individual cultures with 3, 3'-diaminobenzidine solution (DAB, Sigma) for 5 minutes each. Following incubation with DAB, the cultures were washed twice in 0.5% BSA, diluted in PBS for 20 minutes each. They were then incubated in 5µl Rhodamine -Phalloidin® antibody (Molecular Probes) diluted 1:200 in PBS for 20 minutes at room temperature in a damp chamber. Finally, the cultures were washed twice in PBS for five minutes and preserved in PBS for subsequent observation on a Zeiss Axioscope® fluorescence microscope. Representative cultures were photographed.

2.7 Scanning electron microscopy of chick cranial neural crest cells

High-resolution ultrastructure of the surface features of migrating cells or cells in culture have been shown to illuminate functional changes occurring within those cells (Gray and Whittaker, 1962; Bowman *et al*., 1983; Rovasio and Battiato, 2002; Thapa *et al*., 2003). To investigate the ultrastructural features of cNCCs which have been exposed to ethanol *in vitro*, cranial neural crest cells from chick embryos at stages 8 – 10 (HH) were cultured as described in Section 2.2.2. After removing the culture medium, the cultured neural crest cells were fixed for four hours in 2.5% glutaraldehyde made up in phosphate buffer. Cultures were then rinsed in PBS for 10 minutes, after which they were post-fixed in 1% osmium tetroxide in PBS for 1 hour. Cultures were rinsed in two changes of PBS for 10 minutes each. This was followed by dehydration in a graded alcohol series, for 15 minutes each after which the cells were critical-point dried with liquid CO_2 in an HPC-2 critical point dryer (Hitachi, Japan). Samples were mounted on to stubs, then sputter coated with gold and palladium, and examined at 20 kV in a JSM 840 scanning electron microscope (JEOL, Tokyo, Japan). The surface ultrastructure of ethanol-treated and untreated neural crest cells were then observed under a scanning electron microscope (JEOL 840, Japan). The numbers of control and ethanol-treated neural crest cell cultures processed for scanning electron microscopy are summarized in Table 1.

Table 1. Neural crest cultures utilised for scanning electron microscopy

Cultures*	**8 HH (n)**	**9 HH (n)**	**10 HH (n)**	**Total (n)**
Control	18	18	18	54
0.2%	18	18	18	54
0.3%	18	18	18	54
0.4%	18	18	18	54
Total	72	72	72	216

*HH number refers to the Hamburger and Hamilton (1992) stage of the embryo from which the neural tube (and neural crest cells) was derived.

2.8 Determination of apoptosis

Apoptosis was determined in cultured neural crest cells using the K-180 CaspGLOW™ Fluorescein Caspase Staining Kit (Biovision California, USA). The assay utilizes the caspase family inhibitor VAD-FMK® conjugated to FITC (FITC-VAD-FMK®) as a marker. FITC-VAD-FMK® is cell permeable, non-toxic, and irreversibly binds to activated caspases in apoptotic cells. The FITC label allows for direct detection of the activated caspases in apoptotic cells by fluorescence microscopy.

Insect pins were used to remove neural tubes from control (n=6) and experimental (n= 6 for each of 0.2%, 0.3% and 0.4% v/v ethanol-treated) cultures, following which the remaining neural crest cells were trypsinised in 300µl of 0.25% trypsin per culture well for 5 minutes. The trypsin was then neutralised with an equal volume of 5% horse serum. The contents of each well were aliquoted into 1.5ml eppendorf tubes and 1µl of FITC-VAD-FMK® was added into each tube. A negative control was instituted by adding 1µl of horse serum to a tube containing untreated cells to allow for determination of background fluorescence. All the eppendorf tubes containing treated, untreated and negative control cells were then incubated at 37°C for 1 hour in a 5% CO_2 in air incubator. After incubation, the tubes were centrifuged at 3000rpm for 5 minutes. The supernatant was carefully pipetted off and the cells were

resuspended in 500µl of wash buffer and again centrifuged for 5 minutes at 3000rpm. After removing the supernatant, each sample was resuspended in 100µl of wash buffer. One drop (≈20µl) of this sample was placed on to a glass slide and covered with a coverslip. The samples were then observed for fluorescence using a Zeiss Axioscope® epi-fluorescence microscope using an FITC filter. Caspase positive cells were expected to have brighter green signals, whereas caspase negative control cells should show much weaker signals. Photographs of control and treated samples were digitally captured. These photographs were then used to quantify and compare apoptosis between control and ethanol-exposed samples. Phase-contrast and fluorescent images of the same microscopic fields were compared with each other and the number of cNCCs that were fluorescent (apoptotic) was expressed as a percentage of the total number of cNCCs for control cells (n = 6 fields of view) and cells exposed to 0.2% ethanol (v/v) (n = 6 fields of view) and 0.4% ethanol (v/v) (n = 6 fields of view).

2.9 RNA extraction

RNA was extracted from 48 control and experimental cultures of neural crest cells, using the RNeasy® Micro kit (Qiagen, South Africa), as follows: Control (n=6) and ethanol-treated (n=6 for each of 0.2%, 0.3% and 0.4% v/v ethanol solution) cultures were harvested at 24hrs (Total n=24) and 48hrs (Total n=24). The ethanol-treated samples had been cultured in 0.2%, 0.3% and 0.4% v/v ethanol solutions in DMEM, while the controls were cultured in DMEM alone. Each culture was trypsinized with 200µl of 0.25% trypsin solution in PBS for 20 minutes at 37°C. The trypsinization was stopped with an equal volume of DMEM. The cell suspension was pipetted into a 1.5µl Nunc® tube and centrifuged at 2000 rpm for 10 minutes in Mikro 22R© centrifuge machines (Hettich/Zentrifugen). The supernatant was decanted and the cell pellet re-suspended in 750 µl of RNA extraction buffer.

Total RNA was extracted from the harvested and washed neural crest cells (described above) using the RNeasy® Micro kit (Qiagen, South Africa), as follows:

The neural crest suspension (above) was centrifuged at 2000rpm for 10 minutes in a Mikro 22R© centrifuge machine (Hettich/Zentrifugen), and then resuspended in 750µl of buffer RLT® (Qiagen, South Africa) to which 2µl β-mercaptaethanol had been added. Lysis and homogenization of the suspended cells was accomplished by transferring each sample into a QIA shredder Spin Column™ (Qiagen, South Africa), which was micro-centrifuged at maximum speed (Hermle Z 229, Zeiss West Germany) for 2 minutes. The homogenate was then transferred into a new 2ml collection tube, to which 750µl of 70% ethanol was added to precipitate any remaining DNA or proteins. The homogenate was now placed into an RNeasy® MiniElute Spin Column (Qiagen, South Africa) and centrifuged at maximum speed (Hermle Z 229, Zeiss West Germany) for 15 seconds. The flow-through was discarded and 700 µl of buffer RW1® (Qiagen, South Africa) was added. The lysate was micro-centrifuged (Hermle Z 229, Zeiss West Germany) for 15 seconds, poured into a new 2ml collection tube and 500 µl of buffer RPE® (Qiagen, South Africa) was added to the spin column for washing. The spin column was micro-centrifuged for 15 seconds at maximal speed (Hermle Z 229, Zeiss West Germany) and 500 µl of 80% ethanol was added. This was centrifuged for 2 minutes to dry the column, following which both the outflow and 2ml collection tube were discarded. Finally, the RNEasy® MiniElute Spin Column (Qiagen, South Africa) was transferred into a new 1.5ml previously autoclaved eppendorf tube, and the RNA eluted from the Spin Column by adding 50µl of RNAse-free water to the column and micro-centrifuging for 2 minutes. The yield and purity of the total RNA was determined using the Nano-Drop® spectrophotometer, Series ND-100 (Appendix F). The RNA samples were then stored at -70°C, preparatory to reverse transcription.

2.10 Reverse Transcription

RNA was reverse-transcribed using the Transcriptor High Fidelity cDNA Synthesis Kit (Roche, Germany). Standard sterile and RNAse-free protocols, according to the Minimum Information for Publication of Quantitative Real-Time PCR Experiments (MIQE) (Bustin, 2002; Fleige and Pfaffl, 2006; Bustin *et al*., 2009), were maintained at all times and all reagents were thawed before use and kept on ice during the procedure. Previously autoclaved, thin-walled PCR tubes were used to mix the reagents.

Reactions were set up as follows (Table 2):

Table 2. Set-up of template-primer mixture for reverse transcription

Component	**Volume**	**Final Concentration**
Total RNA	variable	50ng
Random Hexamer	2ul	60uM
Water	variable	To make up volume=11.4ul
Total	11.4ul	

The resulting template-primer mixture was denatured by heating at 65°C for 10min in a block cycler with a heated lid (to minimize evaporation). This step ensures denaturation of RNA secondary structures. After denaturation, the mixture was immediately cooled on ice, followed by the addition of the following reagents in the order listed below (Table 3):

Table 3. Reagents used to synthesize cDNA (Reverse Transcription)

Component	**Volume**	**Final Concentration**
Reverse transcriptase reaction buffer, 5X	4ul	1X
RNase Inhibitor	0.5ul	20U
Deoxynucleotide (dNTP) mix	2ul	1mM each
DTT	1ul	5mM
Reverse Transcriptase	1.1ul	10U
Final Volume	20ul	

The reagents were mixed carefully in the PCR tube and placed in a block cycler with a heated lid. The reaction was then incubated at 55°C for 40min, following which the Reverse

Transcriptase was inactivated at 85°C for 5min. The cDNA was stored at 4°C until required for quantitative PCR.

2.11 Quantitative PCR (qPCR)

2.11.1 Primer design

Sequences of avian genes of interest were obtained online (www.pubmed.com). Specifically, the β-actin mRNA sequence was found at the following National Centre for Biotechnology Information (NCBI) web address:

http://www.ncbi.nlm.nih.gov/nuccore/45382926?ordinalpos=1&itool=EntrezSystem2.PEntrez.Sequence.Sequence_ResultsPanel.Sequence_RVDocSum#sequence_45382926

Similarly, the mRNA sequences for RhoB, Rac 1 and Slug were found at these addresses respectively:

RhoB: http://www.ncbi.nlm.nih.gov/nuccore/118090145?log$=seqview_refseq_mRNA

Rac 1: http://www.ncbi.nlm.nih.gov/nuccore/NM_205017.1

Slug:

http://www.ncbi.nlm.nih.gov/nuccore/XM_001236568.1?ordinalpos=2&itool=EntrezSystem2.PEntrez.Sequence.Sequence_ResultsPanel.Sequence_RVDocSum

Forward and reverse primers were then designed using the Integrated DNA technologies (IDT) SciTools Oligo Analyzer 3.1™ primer design software. Care was taken to find primers with optimum annealing temperatures and a G:C ratio of about 50%. The primers and the sequences are listed in Table 4. (See also Appendix G). All primers were synthesized by IDT (Whitehead Scientific, South Africa) and all primer pairs were used at an annealing temperature of 60^0C.

Table 4. Oligonucleotide primers and sequences used for qPCR

Primer name and direction	**Primer sequence**
Gallus β-Actin Forward	5'- ACCCCAAAGCCAACAGA- 3'
Gallus β-Actin Reverse	5'- CCAGAGTCCATCACAATACC- 3'
Gallus GAPDH Forward	5'-GTTCTGTTCCCTTCTGTCTC- 3'
Gallus GAPDH Reverse	5'-GTTTCTATCAGCCTCTCCCA-3'
Gallus Rac 1Forward	5'- ACGAAGCTATCCGAGCAGTTCTGT-3'
Gallus Rac 1Reverse	5'- TTCTGAGCAAAGCACAGGGTTTGG-3'
Gallus Rho B Forward	5'-TCTTTGAGAACTACGTGGCCGACA-3'
Gallus Rho B Reverse	5-'TGTCCACTGAGAAGCACATGAGGA-3'
Gallus *slug* Forward	5'-TCCTCCAAAGATCACAGCGGTTCA-3'
Gallus *slug* Reverse	5'-TGTGTTTGGCCAACCCAGAGAAAG-3'

2.11.2 qPCR protocol

The Brilliant II SYBR Green® QPCR protocol (Stratagene, California USA) was followed for the quantitative PCR procedure. The PCR reaction was set up in strip tubes (Applied Biosystems) as follows (Table 5):

Table 5. PCR reaction set-up (Applied Biosystems)

Reagent	Volume	Final Concentration
Brilliant II SYBR Green® qPCR Master Mix with ROX	12.5µl	30 nM
cDNA	2 µl	
Forward primer	1 µl	200 nM
Reverse primer	1 µl	200 nM
Nuclease-free PCR grade water	variable, adjusted to total volume = 25 µl	

The reaction was mixed gently, taking care not to create bubbles, as these interfere with fluorescence detection. The reaction was centrifuged and then placed in the PCR machine (Applied Biosystems, South Africa). The Three-Step Cycling qPCR program (as recommended by Stratagene, California USA) was adopted as shown in Table 6 (below):

Table 6: The Three-Step Cycling qPCR protocol (Stratagene, California USA)

Cycles	**Duration of cycle**	**Temperature**
1	10 minutes	95°C
40	30 seconds	95°C
	60 seconds	60°C
	30 seconds	72°C

The threshold amplifications were determined using the AB7500 real time PCR machine (Fig. 3). The glyceraldehyde 3-phosphate dehydrogenase (GAPDH) gene was used for normalization. This was because when GAPDH, Actin and 18S ribosomal RNA genes were run as controls, GAPDH had the most stable expression between the different samples. As a negative control, in order to check for reagent contamination, cDNA was excluded from the reactions and replaced with water. All reactions were carried out in duplicate.

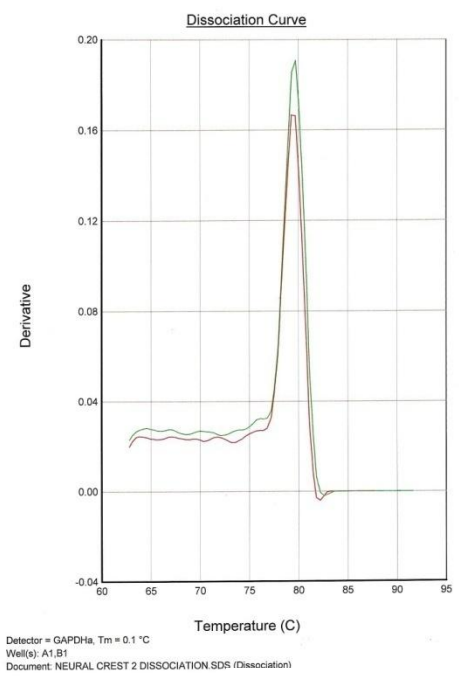

A

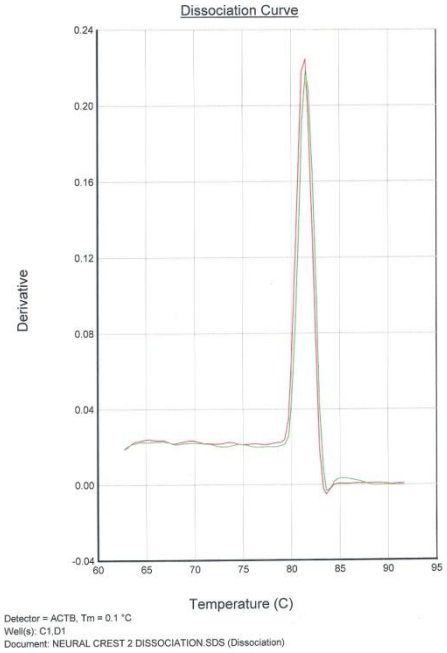

B

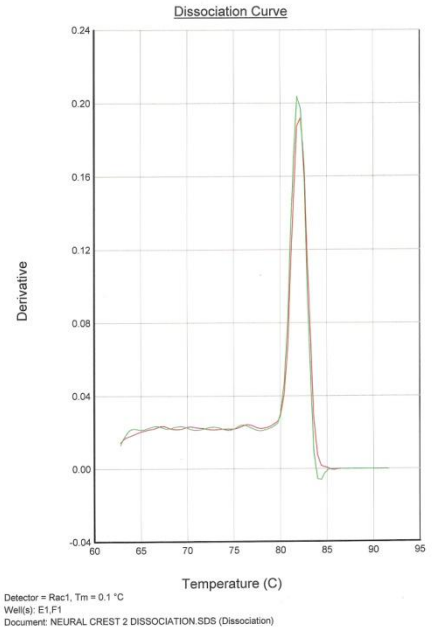

C

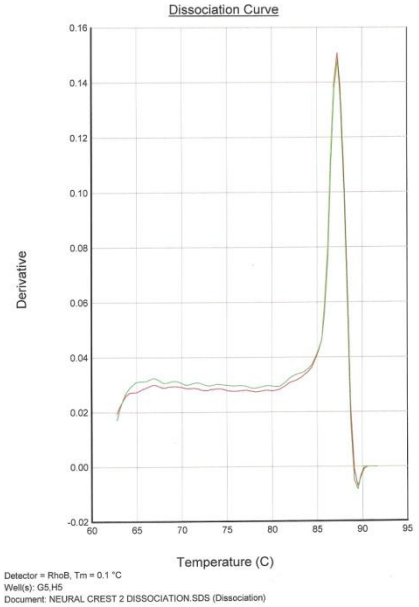

D

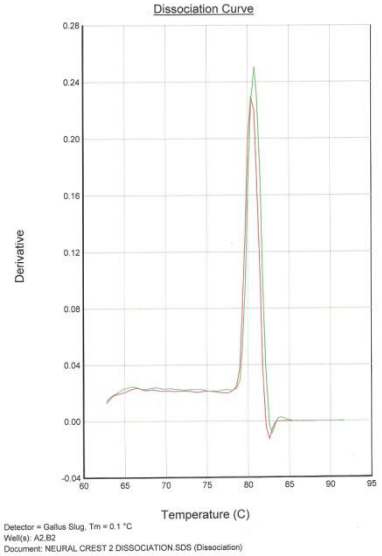

E

Fig. 3. See Legend on the next page.

Legend for Fig. 3

Fig. 3 A, B, C, D, E & F. Melt curve analysis of oligonucleotide primers showing the temperatures at which maximum amplification of GAPDH, β-Actin, Rac 1, Rho B and Slug genes occurred using the AB7500 real time PCR machine (Applied Biosystems, South Africa). A. GAPDH; B. β-Actin ; C. Rac 1; D. Rho B; E. Slug

2.11.3 qPCR data analysis

Data from the qPCR was stored electronically and analysed with the Applied Biosystems Software 7500 version 1.2.3. The relative quantity of the gene of interest was determined from the threshold cycle (Ct) using the formula:

1. $\Delta C_t = C_{t(sample)} - C_{t(endogenous\ control)}$
2. $\Delta\Delta C_t = \Delta C_t - C_{t\ (calibrator)}$
3. $2^{-\Delta\Delta Ct}$ = relative quantity

Where

Endogenous control = GAPDH

Calibrator = Control (untreated) sample

To determine whether the expression of the genes of interest from untreated neural crest samples differed significantly from those from ethanol-treated samples, a paired Student's "t"-test was performed using the MS Excel® software (Office 2007, Microsoft Corp, USA) and the Strata11 software (1984-2009, Strata Corp, USA). Significance was set at $p<0.05$.

3.0 RESULTS

The part of this study which was based on the murine model (Section 2.1) has been published in the journal *Alcohol* (Oyedele and Kramer, 2008) (see Appendix B).

3.1 Blood ethanol concentration

Mean blood alcohol concentration (BAC) peaked after 60 minutes, after which it gradually declined toward the zero mark (Fig. 4). The maximum BAC recorded in the treated animals was in the region of 260 mg/dl.

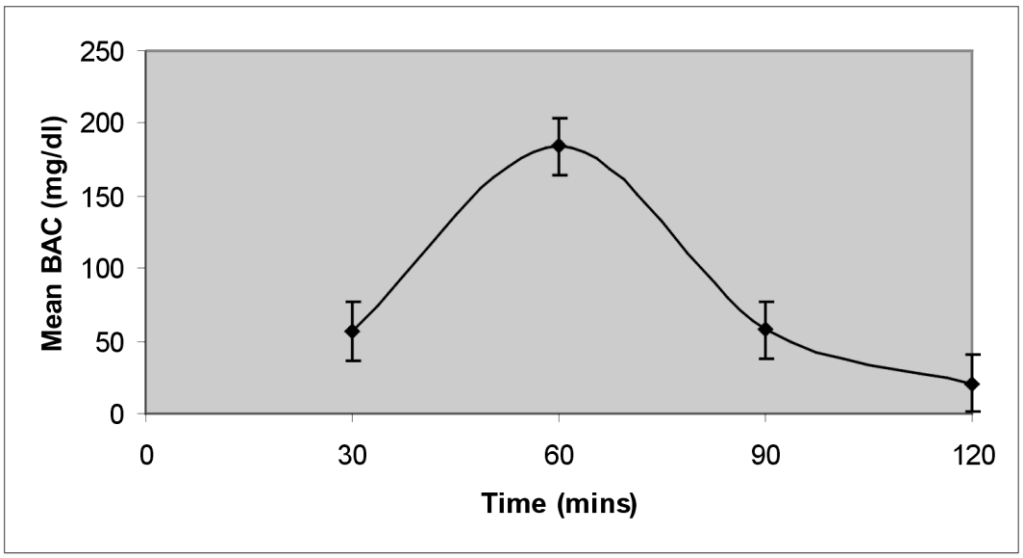

Fig. 4. Mean blood alcohol concentration (BAC) profiles of maternal mice (n=6) after ingestion of 25% v/v ethanol at time 0 minutes (mins).

3.2 Food consumption and weight gain in maternal mice

Weight gain in ethanol-treated and control maternal mice was comparable ($p=0.12$), (Fig. 5A). While the amount of food consumed by treated mice decreased on GD 11 and increased again on GD 15, food consumed by control and ethanol-fed animals increased steadily until they were killed on day 18. The differences in food consumption between control and experimental animals were not significant ($p=0.21$) (Fig. 5B).

3.3 Fetal survival following ethanol exposure *in utero*

The 13 ethanol-fed mice yielded a total of 82 live fetuses, 15 absorbed fetuses, and 1 fetal death *in utero*. The average litter size among this group was 7.5 and the reabsorption rate was 15.3% of all conceptions that took place (Table 7). The average litter size among the 10 control mice was also 7.5. There was no fetal death or reabsorbed fetuses in this group of mice. When the average litter sizes, number of live and dead fetuses were compared between the two groups, the results were statistically significant ($p<0.05$) (Table 7). A total of seven birth defects were observed in the entire series, including controls. 86% of defects occurred in the ethanol-fed group (Table 8). Only one case of anophthalmia was observed in the control group compared with four cases in the ethanol group, one of which occurred bilaterally. Both cases of agnathia that were observed occurred in the ethanol-fed group. When compared to the control group, these differences were however not significant ($p=0.5$) (Table 8).

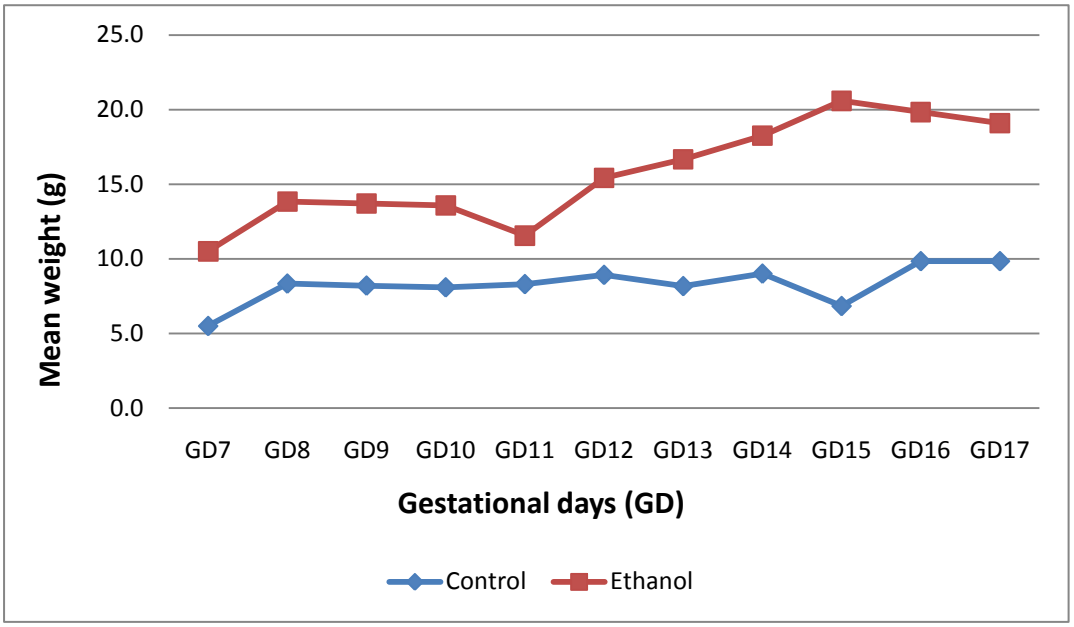

A

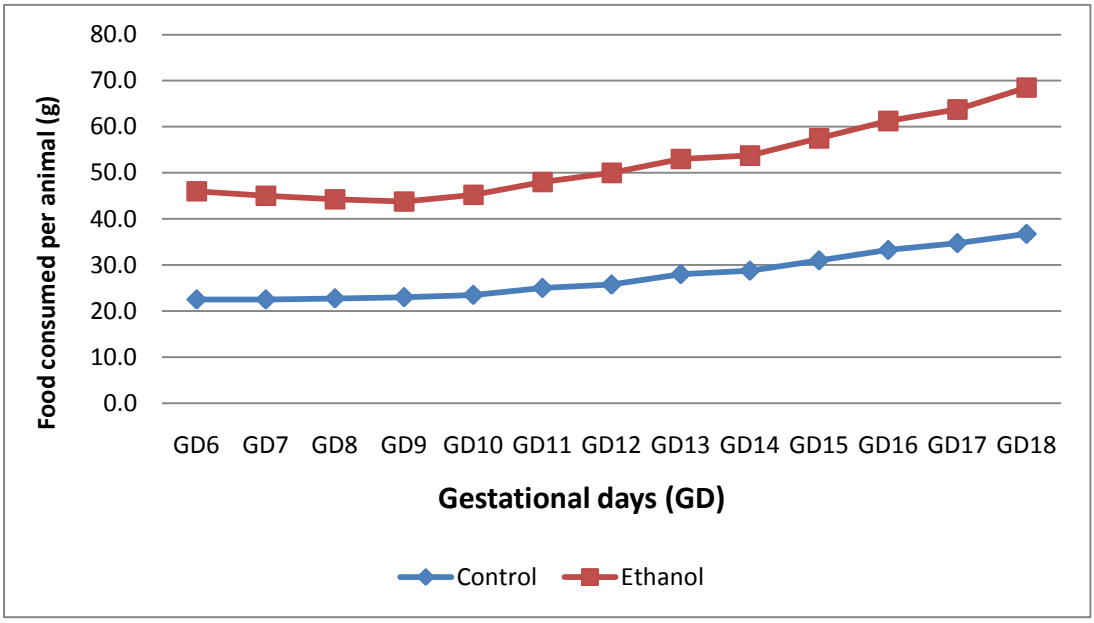

B

Fig.5 A & B. A. Pattern of weight gain of ethanol-fed (n=13) and control (n=10) pregnant mice. Differences in weight gain were not statistically significant. (p=0.12; Student's t-test). B. Food consumption pattern in ethanol-fed and control pregnant mice. No statistical significance was observed in food consumption between the two groups. (p=0.21; Student's t-test).

Table 7. Comparison of fetuses between ethanol-fed and control mice

	Ethanol (n)	**Control (n)**
Maternal mice	13	10
Live fetuses	82	75
Dead fetuses	1	0
Reabsorptions (% of total conceptions)	15 (15.3)	0 (0)
Total conceptions/gravid deciduas	98	75
Average litter size	7.5	7.5
Fetal survival rate (%)	83.7	100*

*$p = 0.004$ (χ^2, 3 degrees of freedom).

Table 8. Anomalies observed in ethanol-fed and control mice*

Type of anomaly	**Ethanol n (%)**	**Control n (%)**	**Total n (%)**
Anopthalmia	4[a] (80)	1 (20)	5 (100)
Agnathia	2 (100)	0 (0)	2 (100)
Total	6 (85.7)	1 (14.3)	7 (100)

*$p = 0.494$ (χ^2, 1 degree of freedom).
[a]One case had bilateral anophthalmia.

3.4 Fetal body measurements and cephalometry

Birth weight, crown-rump length (Table 9), and head measurements (Table 10) all showed no statistically significant difference between the two groups. The mean VML was not significantly greater in control animals (p=0.13) (Table 10). As for the maxillary and mandibular lengths, the mean values hardly differed between treated and untreated groups and the maximum values for these two parameters were found among the ethanol-fed fetuses

(Table 9). Although the shortest maxilla occurred among the control animals, the shortest mandible was found in the ethanol-treated group.

Table 9. Birth weights and crown-rump lengths of 25% ethanol (v/v)-treated and untreated fetuses

	Birth weight (g)		**Crown-rump length (cm)**	
	Ethanol	**Control**	**Ethanol**	**Control**
n	70	39	17	13
Mean (±SD)	1.05 (±0.20)	1.07(±0.16)	2.3(±0.199)	2.3(±0.175)
Min	1.45	1.39	2.6	2.6
Max	0.72	0.63	1.8	2.0
p	0.51		0.75	

3.5 Skeletal staining

Skeletal staining revealed no significant differences in bone or skeletal morphology between ethanol administered and control fetuses, apart from some absent segments of cranial bones in the premaxilla and mandible of some treated animals. Also, some ethanol-exposed fetuses possessed only cartilage in their ribs where clearly ossified bone was already demonstrable in control fetuses of the same age (Fig. 6). These differences were not significant (p=0.14; Table 11).

Table 10. Cranial measurements in treated and untreated fetuses

	VML (cm)		MAXL (cm)		MANL (cm)	
	Ethanol	**Control**	**Ethanol**	**Control**	**Ethanol**	**Control**
n	67	43	66	43	64	43
Mean (±SD)	5.78(±0.31)	5.87(±0.31)	2.24(±0.39)	2.22(±0.34)	2.48(±0.57)	2.49(±0.46)
Max	6.43	6.70	2.89	2.75	3.82	3.27
Min	5.42	5.08	2.09	1.65	2.07	2.36
p	0.13		0.69		0.94	

VML, Vertico-mental length; MAXL, Maxillary length; MANL, Mandibular length.

Table 11. Number of skeletal defects in treated and untreated fetuses following skeletal staining

Observation	**Ethanol (n)**	**Control (n)**
With defects [a]	2	0
No defects	12	14
Total	14	14

$p=0.14$ (χ^2, 1 degree of freedom).

[a] Defects included absent segments of cranial bones and delayed rib ossification in ethanol-fed fetuses as compared to controls.

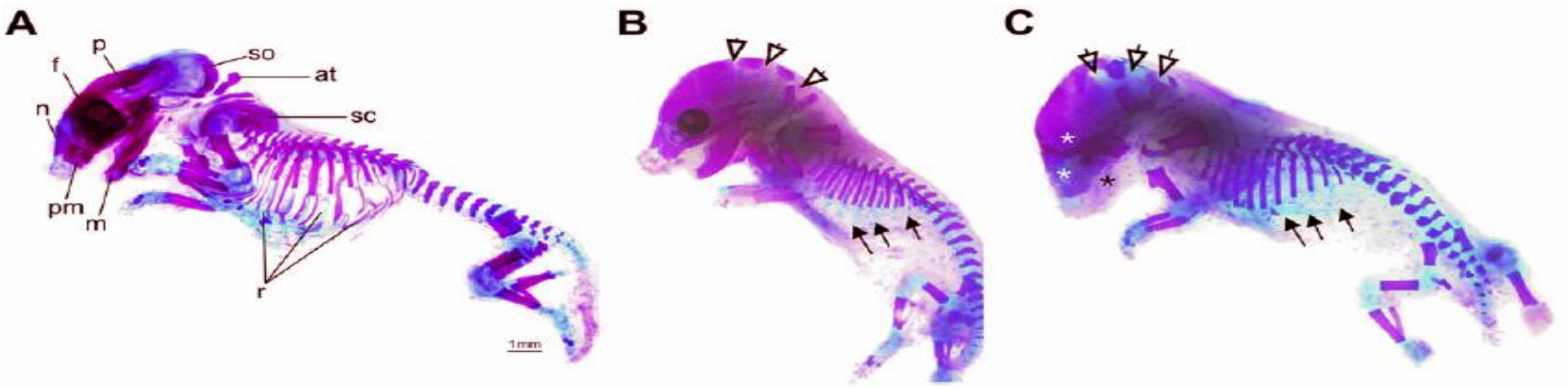

Fig. 6 A, B & C. Comparison of the skeletal preparation of day 18 mouse fetuses untreated (A) and treated with ethanol in utero (B and C). There are defects in the cranial bones (arrowheads). The ribs of ethanol-treated animals show a lag in the state of ossification relative to the control (arrows). The animal depicted in Fig. C shows anophthalmia, agnathia, and defects in the premaxilla (asterisks). Abbreviations: at, atlas; f, frontal bone; m, mandible; n, nasal bone; p, parietal bone; pm, premaxilla; r, ribs; sc, scapula; so, supraoccipital bone. 40X magnification.

Summary of the results of murine experiments

- Ethanol significantly increased fetal reabsorptions and reduced fetal survival rate of newborn mice fetuses, which had been exposed *in utero* to a peak blood ethanol concentration of about 200mg/dl, administered orally in binge-doses to their dams over a period of three days.
- Fetal birth weight and litter size were not affected by a daily oral administration of 25% ethanol (v/v) to maternal mice on days 6, 7 and 8 of pregnancy.
- Cranial birth defects such as agnathia and anophthalmia, as well as defects in the cranial skeleton, while exclusively observed among ethanol-exposed fetuses, were not significantly increased in them, compared to controls.
- There appeared to be delayed ossification in the thoracic skeleton in ethanol-exposed embryos, compared to controls.
- Cranial measurements (cephalometry) did not differ significantly between ethanol-treated and control embryos.

3.6 Whole mount HNK-1 antibody labelling of chick embryos for neural crest cells

HNK-1 antibody immunoreactivity was found in a cranio-caudal sequence relative to time in all chick embryos, such that crest cells appeared at progressively more caudal regions of the neural tube as the embryo advanced in age (Fig. 7). At higher magnification (100X) the column of HNK-1 positive neural crest was observed to be relatively thicker in treated chick embryos as ethanol concentration increased, and appeared maximal in the embryos treated with 0.3% ethanol (v/v) (Fig. 8C). The pattern of HNK-1 immunoreactivity in the embryos treated with 0.4% ethanol (v/v) resembled that of control embryos and the 0.2% ethanol-treated embryos (Fig. 8 A, B and D). Furthermore, HNK-1-positive cells were located within the surface ectoderm covering the neural tube of ethanol-treated and untreated samples,

particularly in stages 9 and 10 HH embryos (Figs. 7E and 7F). These presumptive neural crest cells were present in both control and ethanol-treated embryos at all developmental stages (Fig. 8). In addition, a column of HNK-1 immunoreactivity appeared between the surface ectoderm and the neural tube in stage 10- HH embryos that were treated with 0.4% ethanol (v/v) (Fig. 8F). This was neither observed in non-treated embryos nor in embryos treated with lower ethanol concentrations. Finally, closure of the anterior neuropore occurred in the 0.4% (v/v) ethanol-treated stage 8+ (HH) embryos while it was still open in same-stage control embryos (Fig. 8 A and D).

Summary of the results of whole-mount immunocytochemistry

- The cranio-caudal presence of cNCCs relative to time was observed in all chick embryos. Neural crest cells were found at progressively more caudal embryonic levels as the embryos progressed in age. This was the observation regardless of whether or not the embryo was exposed to ethanol.
- The column of cNCCs appeared to be thicker in embryos treated with 0.3% (v/v) ethanol than in either control embryos or embryos in other ethanol treatment groups.
- HNK-1 immunoreactive cells were present within the surface ectoderm of all control and ethanol-treated embryos, but more so in embryos at stages 9 and 10 HH.
- Treatment with 0.4% ethanol (v/v) appeared to accelerate closure of the anterior neuropore when same stage ethanol-treated and control embryos were compared.
- A column of cNCCs, not seen either in control embryos or in embryos in other ethanol treatment groups was observed between the dorsal neural tube and surface ectoderm of embryos treated with 0.4% ethanol (v/v).

Fig. 7. See legend on the next page

Fig. 7 A – F. Phase-contrast micrographs of whole mount chick embryos immunostained with HNK-1 monoclonal antibody specific for neural crest cells. A. Non-treated stage 8 HH embryo. HNK-1 immunoreactivity is visible at the edges of the closing diencephalon (open arrowheads) and mesencephalon (solid arrowheads), but not in the lower mesencephalon and spinal cord regions (dashed line on the left represents the position of the neural tube. Only one side highlighted for clarity). B. Non-treated stage 8+ HH embryo. HNK-1 positive putative neural crest cells now visible in the caudal rhombencephalic and spinal cord regions of the neural tube (arrows). C - D. Stage 8- HH embryos treated with 0.2% (C) and 0.3% (D) (v/v) ethanol; the embryos show near-identical HNK-1 immunoreactivity. E. Stage 8 HH embryo treated with 0.4% (v/v) ethanol, showing a pattern of HNK-1 immunoreactivity, similar to that at lower ethanol concentrations (C and D). F. Untreated Stage 9 HH embryo. HNK-1 immunoreactivity is present at all levels of the neuraxis. In B and F, the neural tube is outlined for clarity. Intensely-stained lower lateral regions of images represent non-specific staining of membranes (open arrows). Olympus inverted phase-contrast microscope. 40X.

Fig. 8 A-F. Phase-contrast micrographs of cranial regions of whole mount chick embryos immunostained with HNK-1 monoclonal antibody specific for neural crest cells. A. Non-treated stage 8+ HH embryo. HNK-1 immunoreactive cells can be seen at the crest of the neural folds (open arrowheads). B, C. Stage 8- HH embryo treated with 0.2% and 0.3% ethanol (v/v) respectively, with a similar pattern of HNK-1 immunoreactivity as control embryos. The band of immunoreactive cells (between arrowheads) appears to be thicker in the 0.3% (v/v) ethanol-treated embryo (C). D. Stage 8+ HH embryo treated with 0.4% ethanol (v/v). The pattern of HNK-1 immunoreactivity is similar to that in the untreated embryo (open arrowheads). However, compared to the control embryo, midline fusion of the neural tube is complete cranially (arrow). E. Non-treated stage 9 HH embryo. The neural tube is still outlined by HNK-1 positive reaction, but less so than in earlier stage (treated and untreated) embryos. The surface ectoderm contains bands of HNK-1 positive cells (arrows). F. Stage 10- HH embryo, treated with 0.4% ethanol (v/v). Bands of HNK-1 positive cells similar to those in E can be seen within the surface ectoderm (arrows). In addition a stream of HNK-1 positive cells appears between the neural tube and surface ectoderm (open arrowheads). Neural tube has been highlighted for clarity. Olympus phase-contrast microscope. 100X.

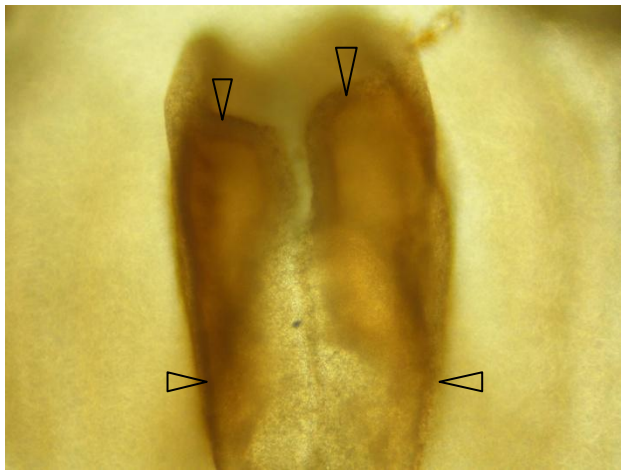

A

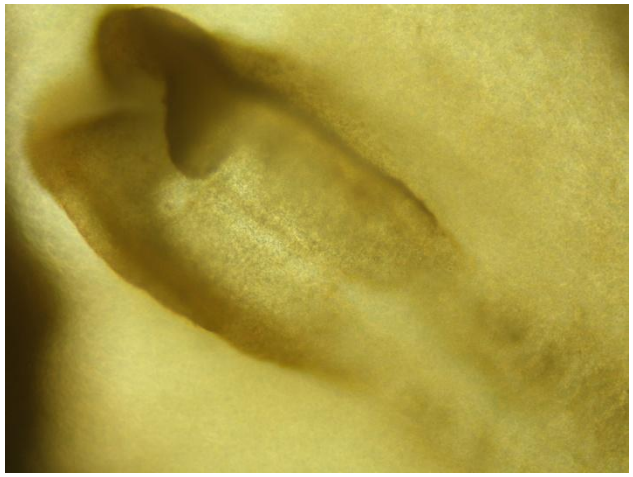

B

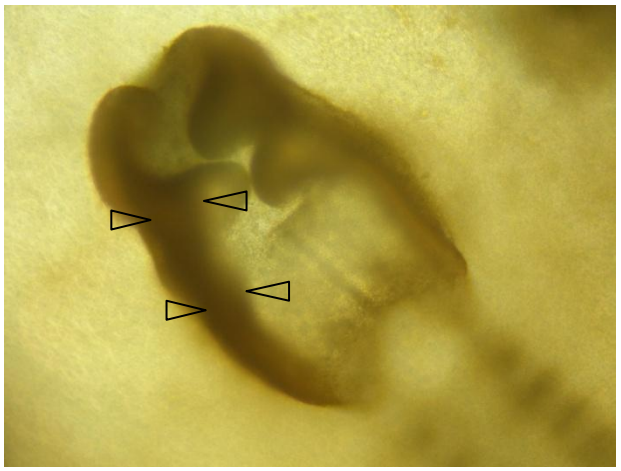

C

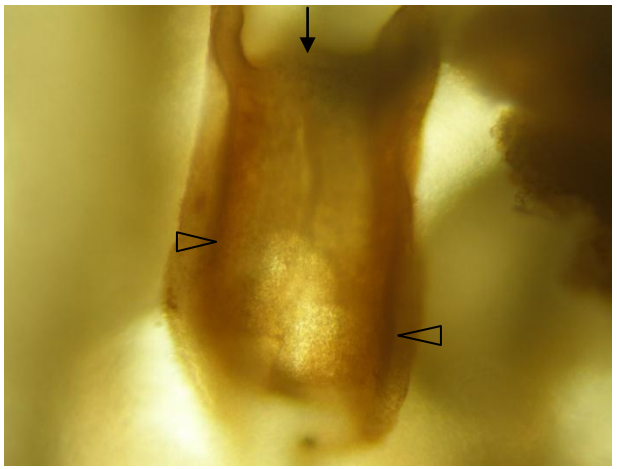

D

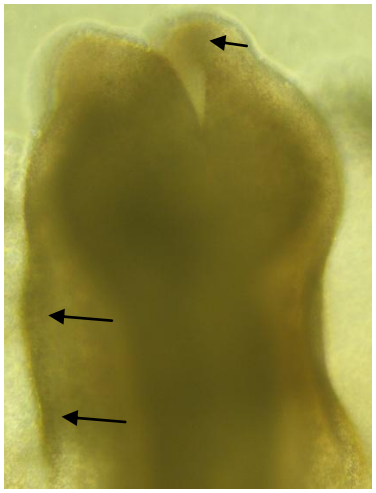

E

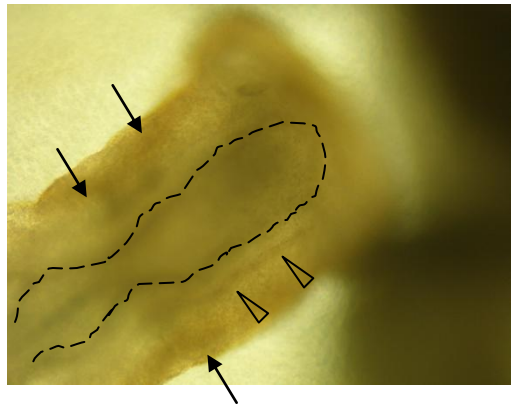

F

Fig. 8. See legend on the preceding page

3.7 Chick cranial neural crest cell morphology following ethanol exposure

3.7.1 Ethanol concentration of medium used to culture treated neural crest cells

Ethanol concentration in the ethanol-treated medium was determined from the absorbance values in the standard curve (Fig. 9). The mean ethanol values obtained came to within ± 0.05% (v/v) of the expected values (Table 12).

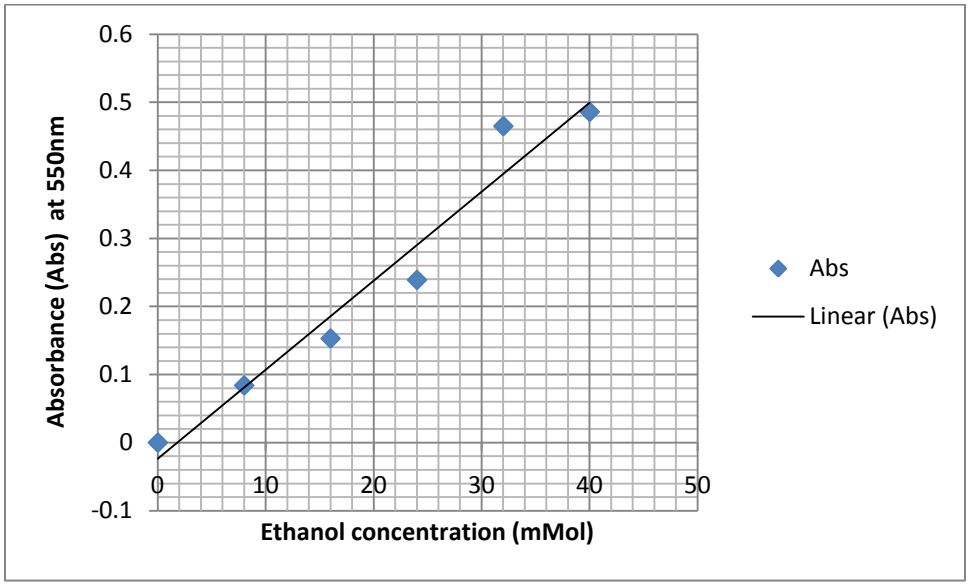

Fig. 9. Plot of ethanol concentration *in vitro* against absorbance (Abs)

Table 12. Determination of ethanol concentration in ethanol-treated cultures of chick cNCCs*

Sample	Sa (nmol)	Sv (ul)	Sa/Sv	Observed concentration, O (mM)	Expected concentration, E (mM)	Difference (O-E) (mM)	O-E (% v/v)
Control	99	25	3.96	7.92	0.0	+7.9	+0.046
0.2% ethanol	402	25	16.08	32.2	34.0	-1.8	-0.011
0.3% ethanol	59	7.3	8.08	48.5	51.0	-2.5	-0.015
0.4% ethanol	27	4.4	6.16	61.6	68.0	-6.4	-0.038

*Samples tested in triplicates. Mean values represented. (Sa = sample amount, Sv = sample volume)

3.7.2 Microscopic appearance of ethanol-exposed chick neural crest cells.

A notable observation with ethanol-treated, compared to untreated neural crest cells was their apparent change in morphology from typical spindle-shaped cells to a more flattened and cuboidal appearance (Fig. 10). This was most noticeable with increasing ethanol concentration and duration of culture (Fig. 10). There was also a striking apparent increase in proliferation of ethanol-treated cells (reported further in section 3.8).

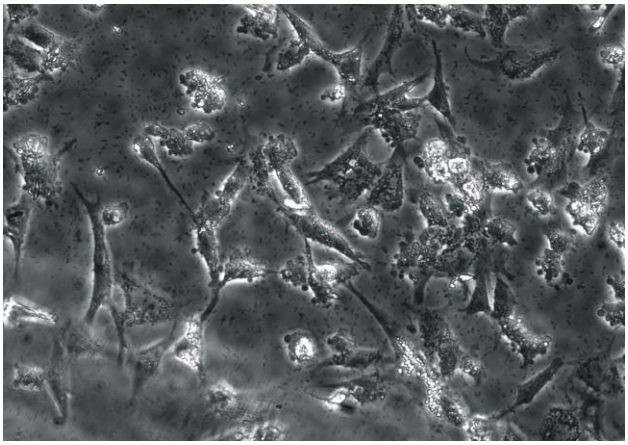

A

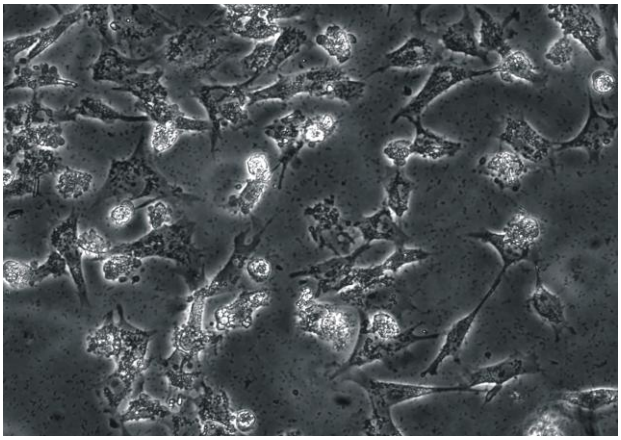

B

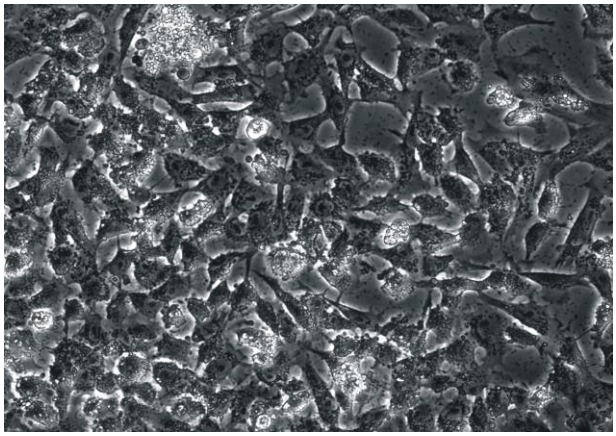

C

Fig. 10 A & B. Comparison of the morphology of neural crest cells on day 4 of continuous culture. Control cells are largely spindle shaped (A), while cells cultured in 0.2% (B) and 0.4% ethanol (v/v) appear epithelial in a dose-dependent manner. Note also the 'crowding' of treated cells, presumably due to increased proliferation (see section 3.8). (Inverted phase contrast microscope. 200X).

3.8 Proliferation of ethanol-treated chick cranial neural crest cells (Mitotic Index)

After 24hrs of ethanol exposure, a dose-dependent statistically significant increase in mitotic index (MI) was observed in ethanol-treated cells, compared to controls (Fig. 11). This ethanol-induced increase in proliferation of exposed cells relative to controls persisted at 48hrs (Fig. 11). However, when mitotic indices at 24hrs of culture were compared with values at 48hrs for the same cells, only control cNCCs and cells cultured in 0.2% ethanol showed a significant increase in proliferation at 48hrs, compared to 24hrs (Fig. 11). The increased MI at 24hrs compared to 48hrs, observed in cNCCs treated with 0.3% ethanol was not significant ($p=0.058$). Cranial NCCs cultured in 0.4% ethanol showed a decreased MI at 48hrs of culture compared to the index at 24hrs (Fig. 11). This decrease in MI was not significant ($p=0.359$).

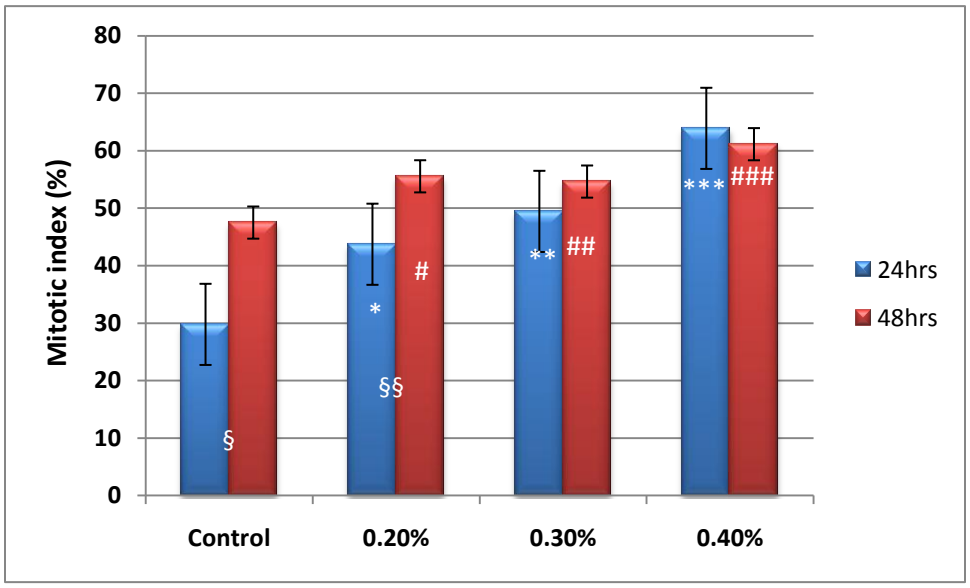

Fig. 11. Mean mitotic index (MI) of control and ethanol-treated cNCCs observed at 24- and 48hrs. An ethanol-induced dose-dependent increase in MI can be observed, particularly at 24hrs. The legend of symbols used in the graph to show differences that were significant is explained as follows

Samples	p-value 24hrs	p-value 48hrs
Control vs. 0.2% EtOH	$^{*}5.34\text{x}10^{-8}$	$^{\#}0.012$
Control vs. 0.3% EtOH	$^{**}3.6\text{x}10^{-7}$	$^{\#\#}0.021$
Control vs. 0.4% EtOH	$^{***}7.26\text{x}10^{-7}$	$^{\#\#\#}5\text{x}10^{-5}$
Control 24hrs vs. 48hrs	$^{\S}1.7\text{x}10^{-10}$	
0.2% EtOH 24hrs vs. 48hrs	$^{\S\S}7.4\text{x}10^{-5}$	

3.9.1 Distances migrated by chick neural crest cells after 24hrs of culture.

After 24hrs of culture, when the direction in which cNCCs migrated was considered, there was an increase in mean distance migrated along the x axis from 1.00 mm in control cells to 1.09 mm, 1.20 mm and 1.04 mm in 0.2%, 0.3% and 0.4% (v/v) ethanol-treated crest cells respectively. The increase at 0.3% ethanol-treatment was statistically significant (Table 13). In the y-axis, the mean distance migrated increased from 1.14 mm in control cNCCs to 1.18 mm and 1.28 mm in 0.2% and 0.3% (v/v) ethanol-treated cells respectively, but it decreased to 1.12 mm in 0.4% (v/v) ethanol-treated cNCCs. Neither the increased nor decreased mean distance of migration by ethanol-treated cNCCs along the y axis was significant (Table 13). The mean "vector distance" (vDistance), the vector sum of distance of migration along the x and y axes, increased from 1.53 mm in control cNCCs to 1.64 mm, 1.77 mm and 1.57 mm in 0.2%, 0.3% and 0.4% (v/v) ethanol-treated neural crest cells respectively (Fig. 12). However only the increase in vDistance of the cells cultured in 0.3% ethanol (v/v) was significant ($p=0.039$; Table 13).

Table 13. Mean distances migrated by alcohol-treated and untreated neural crest cells after 24 hours of culture*

	Control n=26		**0.2% ethanol n=13**		**0.3% ethanol n=10**		**0.4% ethanol n=24**	
	x-axis	**y-axis**	**x-axis**	**y-axis**	**x-axis**	**y-axis**	**x-axis**	**y-axis**
Dist dir (mm)	1.00	1.14	1.09	1.18	1.2	1.28	1.04	1.12
SD	0.356	0.301	0.416	0.336	0.219	0.324	0.373	0.404
p (x-axis vs y-axis)	0.057		0.255		0.25		0.229	
vDist ±SD (mm)	1.53±0.426		1.64±0.388		1.77±0.319		1.57±0.478	
p (control vs ethanol) dir			0.255	0.352	**0.025**	0.126	0.35	0.412
p (control vs ethanol) vDist			0.197		**0.039**		0.378	

*Significant differences are highlighted in **bold** type. Abbreviations: Dist dir, directional distance (along the x or y axis); vDist, sum of directional distance (as a vector quantity); p(control vs ethanol) dir, p value for difference in directional distance, comparing control versus ethanol-treated samples; p(control vs ethanol) vDist, p value for difference summative distance, comparing control versus ethanol-treated samples.

3.9.2 Distances migrated by chick neural crest cells after 48hrs of culture

Only the cells cultured in 0.4% ethanol showed a significant difference in the distance migrated along the x- compared to the y axis (Table 14). Furthermore, in the x axis, control cells migrated over a mean distance of 1.51 mm, compared to a distance of 0.98 mm, 1.10 mm and 1.42 mm for cells cultured in 0.2%, 0.3% and 0.4% ethanol (v/v) respectively. This decrease in migrated distance by ethanol-treated cells was significant in 0.2% and 0.3% but not 0.4% (v/v) ethanol (Table 14). The mean distance through which cNCCs migrated along the y axis showed a decrease from 1.38 mm in control cells to 1.20 mm and 1.35 mm in 0.2% and 0.3% (v/v) ethanol-treated cells respectively. The mean migrated distance was however increased to 1.72 mm with 0.4% (v/v) ethanol treatment. This increase was significant when compared to the controls (p=0.04l; Table 14). Vector summation of distances migrated by cNCCs at 48 hours revealed that vDistance was decreased non-significantly compared to controls, by treatment with 0.2% and 0.3% (v/v) ethanol, but increased by treatment with 0.4% ethanol (v/v), compared to the control cells. This increase was not statistically significant (Table 14).

3.9.3 Comparison between 24- and 48-hr distances migrated by chick neural crest cells

The mean distance migrated by control cells increased from 1.00 mm and 1.14 mm in the x and y axes respectively at 24hrs to 1.51 mm and 1.38mm in the x and y axes respectively at 48 hrs. This increase was significant in the x axis as well as when vector-summated (Table 14 and Fig. 12A). In the ethanol treatment groups, for both 0.2% and 0.3% ethanol-treated cNCCs, migrated distance decreased in the x axis but increased in

Table 14. Mean distances migrated by alcohol-treated and untreated neural crest cells after 48 hours of culture*

	Control n=15		**0.2% ethanol n=9**		**0.3% ethanol n=6**		**0.4% ethanol n=10**	
	x-axis	**y-axis**	**x-axis**	**y-axis**	**x-axis**	**y-axis**	**x-axis**	**y-axis**
Dist dir (mm)	1.51	1.378	0.982	1.202	1.103	1.351	1.428	1.716
SD	0.467	0.476	0.655	0.635	0.317	0.187	0.203	0.439
p (x-axis versus y-axis)	0.228		0.238		0.068		**0.041**	
vDist ±SD (mm)	2.07 ±0.574		1.56 ±0.887		1.50 ±0.725		2.25 ±0.379	
p (control vs ethanol) dir			**0.026**	0.242	**0.019**	0.427	0.282	**0.041**
p (control vs ethanol) vDist			0.075		0.050		0.175	
p (24hrs vs. 48hrs) (x-axis versus y-axis)	**0.001**	0.049	0.338	0.470	0.269	0.300	**0.000**	**0.001**
p (24hrs vs. 48hrs) vDist	**0.002**		0.398		0.195		**0.0001**	

*Significant differences are highlighted in **bold** type. Abbreviations: Dist dir, directional distance (along the x or y axis); vDist, sum of directional distance (as a vector quantity); p(control vs ethanol) dir, p value for difference in directional distance, comparing control versus ethanol-treated samples; p(control vs ethanol) vDist, p value for difference summative distance, comparing control versus ethanol-treated samples.

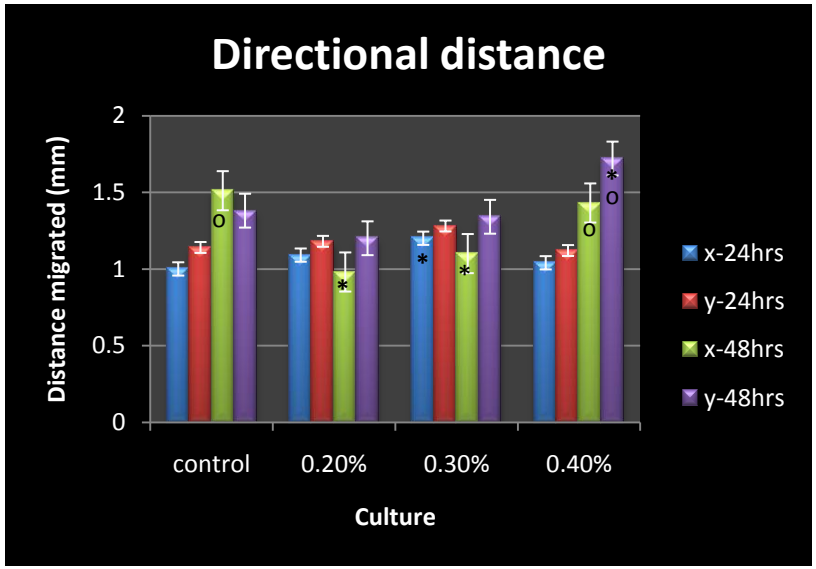

A

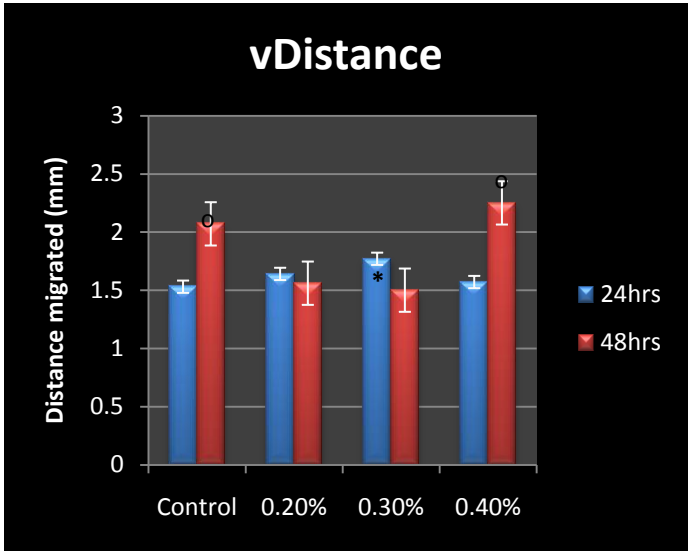

B

Fig. 12 A & B. Mean distance migrated by control and ethanol-treated cultured cNCCs at 24- and 48hrs. A. Mean distance measured in the direction parallel (x) or perpendicular (y) to the neural tube. B. Mean directional distance added as vector quantities (vDistance); Significant differences in the distance migrated by ethanol-treated compared to control cells are indicated by asterisk (*). Significant differences in the distance migrated by the same cells at 24hrs compared to 48hrs are marked by an open circle (○).

the y axis between 24- and 48hrs. These differences were not significant (Table 14). At 0.4% (v/v) ethanol concentration, a statistically significant increase occurred in the distance of migration at 48hrs compared to 24hrs in both axes of migration as well as when the axes were summated as vectors (Fig. 12B).

Summary of distance migrated by cNCCs at 24- and 48 hours

- With just one exception (y axis, 0.4% v/v ethanol-treated cells), after 24 hours of ethanol exposure, cNCCs tended to increase their migratory distance compared to control cells. When the distances migrated along the axes were added, ethanol treatment appeared to increase the distance of migration at all concentrations of treatment. However, only the increase observed in the 0.3% (v/v) ethanol-treated, x-axis-directed cNCCs was statistically significant compared to controls.
- By 48 hours of ethanol treatment, a reverse had occurred, with the majority of ethanol-treated cNCCs now showing a decrease in distance migrated compared to controls. However, this decrease was statistically significant only for cNCCs migrating along the x axis in 0.2% and 0.3% (v/v) ethanol cultures. Vector distance (vDistance) migrated by ethanol-treated cNCCs was similarly reduced in all but the cells cultured in 0.4% ethanol (v/v), although neither reduced nor increased vDistance at 48hrs was statistically significant compared to controls.
- At 48hours of migration cNCCs exposed to 0.4% (v/v) ethanol, migrating in the y axis showed a statistically significantly increased distance migrated, compared to controls.

- A comparison of migrated distance at 24- compared to 48 hours by the same cNCCs showed that:
    - Non-treated cNCCs had migrated further along the x axis and along the vector summation of both axes. This increased distance on the second compared to the first day of culture was statistically significant.
    - Similarly, cNCCs cultured in 0.4% (v/v) ethanol migrated over a statistical significantly greater distance at 48hrs than they did at 24hrs in both the x and y axes, as well as when both axes were vector summated.
    - Neural crest cells cultured in 0.2% (v/v) and 0.3% (v/v) ethanol both showed a decreased vDistance at 48- compared to 24hrs, although this decrease was not statistically significant.

3.9.4 The distance migrated by chick cranial neural crest cells in relation to the embryonic stage of development.

When the distances migrated by cranial neural crest cells were examined based on the Hamburger and Hamilton (1992) stage of development of the embryo (neural tube) from which the emigrant neural crest cells were derived, the following observations were made (Fig. 13 A-C and Fig. 14 A-C):

Stage 8 (HH) embryo-derived chick neural crest cells

Control stage 8 (HH) cNCCs showed a significant increase in mean distance migrated at 48hrs as compared to 24hrs in both x ($p=0.04$) and y ($p=0.000$) axes, as well as in the summation of the axes ($p=0.005$) (Fig. 13 A and Fig. 14A). Furthermore, after 24 hours of cell culture, cNCCs at stage 8 (HH), which had been exposed to 0.2% ethanol (v/v) manifested a slight (but statistically non-significant) mean increase in migrated distance along both x and y axes, compared to controls. At 48hrs, while the increase in migrated distance along the x axis persisted, cNCCs migrating in the y-axis showed a significant decrease in mean migrated distance, when compared to control cells ($p=0.04$; Fig. 13A). The mean "vector distance" (vDistance) of the 0.2% (v/v) ethanol-exposed cells at 24hrs increased (with no statistical significance) compared to controls, but decreased at 48hrs compared to control cells, also with no statistical significance (Fig. 14A).

With 0.4% (v/v) ethanol-exposure, cNCCs showed a very slight decrease in migrated distance along both axes at 24hrs compared to control cells, and both an increase (x axis) and a decrease (y axis) in migrated distance at 48hrs compared to control cNCCs. These differences were not statistically significant (Fig. 13A). Vectorial addition of the

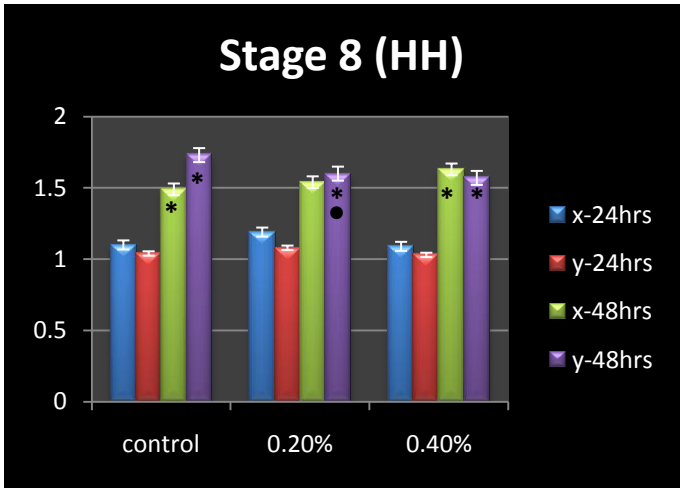

A

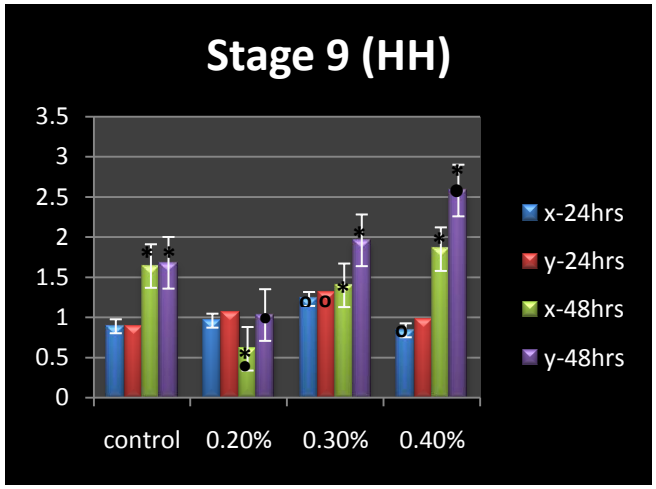

B

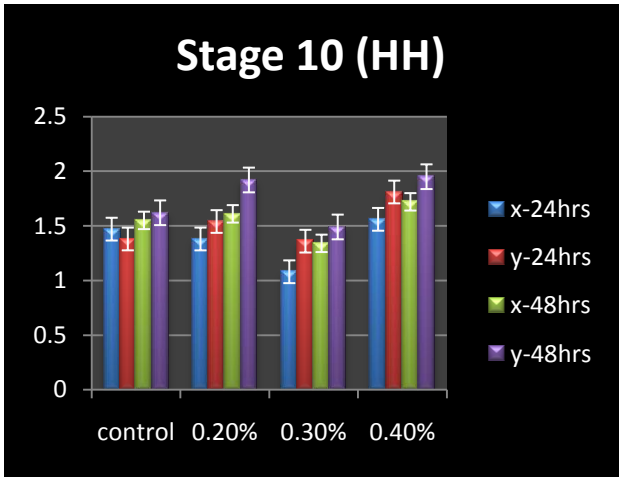

C

Fig. 13 A, B & C. Mean directional distance (mm) (along x and y axes) migrated by control and ethanol-treated cranial neural crest cells that were cultured from neural tubes removed from embryos at stages 8 (A), 9 (B) and 10 (C) (HH). Significant differences indicated by open circles (o) relate to comparisons between distance migrated by ethanol-treated cNCCs and control cells at 24hrs; significant differences indicated by solid circles (●) relate to comparisons between distance migrated by ethanol-treated cNCCs and control cells at 48hrs, and significant differences indicated by asterisks (*) relate to comparisons between the distance migrated at 24hrs versus that at 48 hrs.

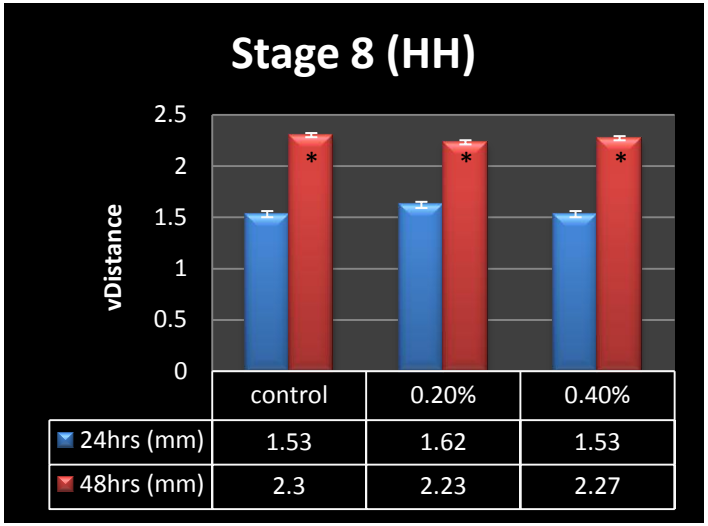

A

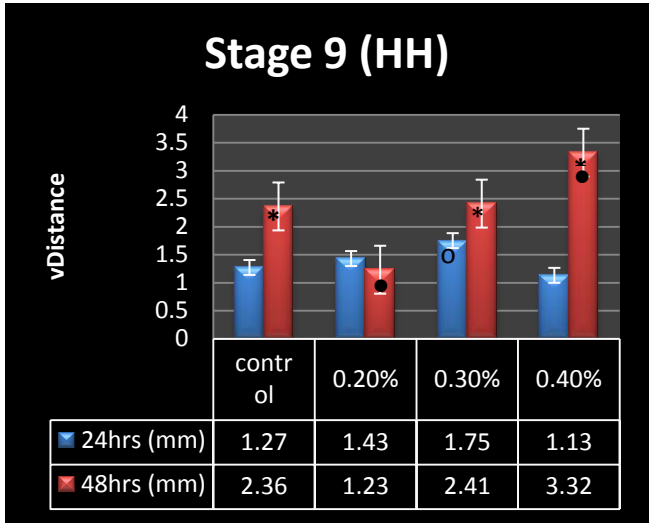

B

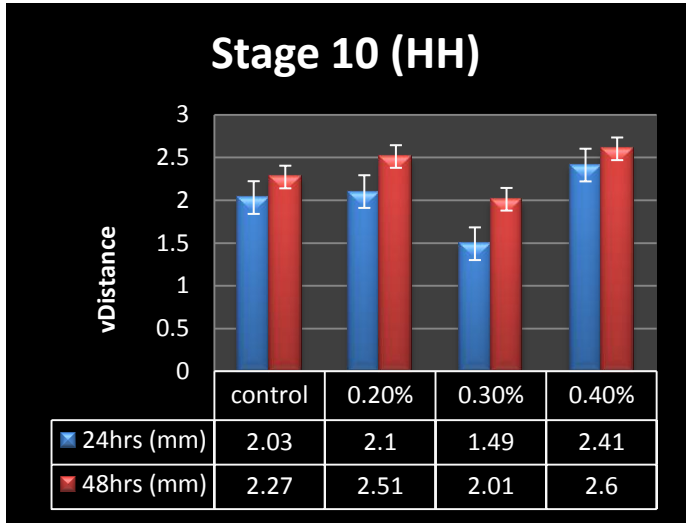

C

Fig. 14 A, B & C. Mean vDistance migrated by control and ethanol-treated cranial neural crest cells, cultured from neural tubes that were removed from embryos at stages 8 (A), 9 (B) and 10 (C) HH. Significant differences indicated by open circles (o) relate to comparisons between distance migrated by ethanol-treated cNCCs and control cells at 24hrs; significant differences indicated by solid circles (●) relate to comparisons between distance migrated by ethanol-treated cNCCs and control cells at 48hrs, and significant differences indicated by asterisks (*) relate to comparisons between the distance migrated at 24hrs versus that at 48 hrs.

displacement over the x and y axes for 0.4% (v/v) ethanol-treated cells showed that at both 24- and 48 hrs, cNCCs migrated over similar vDistances to those of control cNCCs without any statistically significant difference (Fig. 14A).

Stage 9 (HH) embryo-derived chick neural crest cells

Control cNCCs from stage 9 (HH) embryos migrated over significantly greater mean distances in the x axis ($p=0.031$), y axis ($p=0.004$) and combined axes ($p=0.012$) at 48hrs compared to 24hrs (Fig. 13B and Fig. 14B). With 0.2% (v/v) ethanol treatment, stage 9 (HH) cNCCs increased their mean distance of migration at 24hrs, along both x and y axes when compared to controls (with no statistical significance) (Fig 12B). At 48hrs, there was a significantly reduced distance migrated by 0.2% (v/v) ethanol-treated cNCCs in both x ($p=0.010$) and y ($p=0.011$) axes, as compared to controls. Summation of the axes showed that with 0.2% (v/v) ethanol exposure, vDistance increased at 24 hrs (with no statistical significance), but decreased significantly at 48hrs ($p=0.010$) (Fig. 14B).

Stage 9 (HH) cNCCs that were exposed to 0.3% (v/v) ethanol showed a significant increase in distance migrated in both x- ($p=0.035$) and y ($p=0.023$) axes after 24hrs of culture, compared to controls (Fig. 13B). The vDistance migrated by this treatment group of cNCCs was also significant compared to the vDistance migrated by control cells ($p=0.016$; Fig. 14B). After 48hrs of culture, 0.3% (v/v) ethanol-treated cells showed a non-statistically significant increase in the mean distance migrated compared to control cNCCs, along the y axis (Fig 12B). There was a non-statistically significant decrease in distance migrated along the x axis compared to control cells. The summated mean

vDistance migrated by 0.3% (v/v) ethanol-exposed cells at 48hrs of exposure was increased compared to control values, but with no statistical significance (Fig 13B).

Treatment of Stage 9 (HH) cNCCs with 0.4% (v/v) ethanol resulted in a slight decrease in migrated distance along the x-, but an increase along the y axis at 24hrs, neither of which was statistically significant compared to controls. The increase in mean vDistance observed for this treatment group at 24hrs was also not significant (p=0.446) (Fig. 14B). However after 48 hours of migration, 0.4% (v/v) ethanol-treated stage 9 (HH) cNCCs increased their distance of migration compared to controls, in both axes, with the y axis increase being significant (p=0.006; Fig. 13B). Furthermore, the mean vDistance migrated by 0.4% (v/v) ethanol-treated cNCCs at 48 hours of culture increased significantly compared to control values (p=0.027; Fig. 14B).

Stage 10 (HH) embryo-derived chick neural crest cells

There was a non-statistically significant increase in the distance migrated by control stage 10 (HH) cNCCs in the x and y axes and in both axes combined (vDistance) at 48hrs compared to 24hrs (Fig. 13C and Fig 13C). The treatment of stage 10 (HH) cNCCs with 0.2% (v/v) ethanol resulted in a reduction in migrated distance in the x axis, but an increase in distance migrated in the y axis after 24 hours, neither of which was significant (p, x axis = 0.41; p, y axis = 0.33; Fig. 13C). After 48 hrs of culture in 0.2% (v/v) ethanol, stage 10 (HH) cNCCs, showed a non-statistically significant increase in migrated distance in both axes, compared to control cells (Fig. 13C). The summated mean vDistance values migrated by 0.2% (v/v) ethanol-exposed cNCCs at 24- and at 48 hours

of observation were increased compared to controls but with no statistical significance (Fig. 14C).

With exposure to 0.3% (v/v) ethanol concentration, the mean distance migrated by stage 10 (HH) cNCCs was non-significantly reduced along both axes of migration (p, x axis=0.108; p, y axis=0.463) at 24hrs compared to control values (Fig. 13C). The mean vDistance migrated by the 0.3% (v/v) ethanol-treated cNCCs along the combined axes was also decreased at 24hrs, with no statistically significant difference (Fig. 14C). After 48hrs of culture, there was a non-statistically significant decrease in the distance migrated by 0.3% (v/v) ethanol-treated cNCCs along both the x and y axes, when compared to control cNCCs, as well as along the combined axes (vDistance) (Fig. 13C and Fig. 14C).

At an ethanol concentration of 0.4% (v/v), there were statistically non-significant increases in the mean distance migrated by stage 10 (HH) cNCCs compared to control cells, along all axes and at both time points at which they were observed (Fig. 13C). When the distances along the x- and y axes were summed, cNCCs obtained from stage 10 (HH) embryos and treated with 0.4% (v/v) ethanol, showed statistically non-significant increases in mean vDistance of migration compared to control cells at both 24- and 48 hours, (Fig. 14C).

Summary of HH stage-dependent distance of migration by cNCCs

- The most consistent finding was that at embryonic stage 9 (HH), there was an increase in mean vDistance among ethanol-treated cNCCs compared to controls, both at 24- and 48 hours of observation. This increase was observed at ethanol concentrations of 0.3% and 0.4%.
- Most of the statistically significant increases in distance migrated by ethanol-treated cNCCs compared to control cells occurred at 48hrs, in cNCCs derived at stage 9 (HH) which had been exposed to either 0.3% or 0.4% (v/v) ethanol
- Most of the significant reductions in distance migrated by ethanol-treated cNCCs compared to control cells also occurred at 48hrs, also in cNCCs derived at stage 9 (HH), which had been exposed to 0.2% (v/v) ethanol.

3.10 Time-lapse video microscopy of migrating chick cranial neural crest cells

Sample copies of the video recordings of two control and three ethanol-treated (two 0.2% and one 0.4% v/v) cultures of migrating neural crest cells, as well as the time-analysis of the recording of the migration of neural crest cells are available for viewing on the accompanying compact disc (Appendix H). The recordings highlight dynamic aspects of neural crest cell migration that were not available from still photographs.

Control cNCCs commenced their migration after about 2hrs (t+2) from the start of the video recording (t) and reached the defined end-point of migration (the edge of the microscope field of view) after 12hrs (t+14). At the end of the video recording (t+24), the morphology of control neural crest cells was mainly spindle-shaped (Appendix H). Compared to control cells, there was an average delay of about five hours in the time that it took 0.2% ethanol-treated cNCCs to emerge from the neural tube as they started to migrate at about t+7. In addition, this group of ethanol-treated cells reached the edge of the field of view about nine hours after control cells had reached the same point (t+23). At the end of the video recording, the morphology of the 0.2% (v/v) ethanol-treated cNCCs was mainly cuboidal. The neural crest cells which were exposed to 0.4% ethanol (v/v) appeared to emerge from the neural tube about one hour ahead of control cells (t+1), but failed to reach the end-point of migration observed in the control cells by the end of the video recording (Appendix H). Furthermore, at the termination of the video recording, in the 0.4% (v/v) ethanol-treated cultures, numerous round bodies were seen in the culture medium, atypical of normal neural crest cells.

Summary of time-lapse video microscopy observations

- There was an apparent delay in onset of cNCCs emigration from the neural tubes that were cultured in 0.2% ethanol (v/v), compared to control cells.
- There was an apparent acceleration of the onset of migration in 0.4% (v/v) ethanol-treated cNCCs compared to control cNCCs.
- At the end of the period of video recording, 0.2% ethanol-treated cNCCs consisted mostly of flattened cuboidal cells, while control cNCCs were mostly spindle-shaped
- Some cNCCs that were exposed to 0.4% ethanol (v/v), failed to assume the expected spindle-shaped morphology of neural crest cells (as seen in control cultures), but became small round bodies within the culture medium.

3.11 Effect of ethanol exposure on the actin cytoskeleton of chick neural crest cells.

Prior to visualization of their actin cytoskeleton by fluorescent microscopy, control and ethanol-exposed cNCCs were identified by HNK-1 immunolabelling of their cell membranes, using phase-contrast microscopy. The actin cytoskeleton of control cranial neural crest cells was well-defined, with an ordered microfilament structure. In addition, focal adhesions were clearly visible at points where the cells made contact with the substratum (Figs 14A, 15A and 16A). A number of features characterized the actin cytoskeleton of ethanol-treated cNCCs. At 48 hrs of culture, while non-treated cNCCs showed regularly arranged and clearly recognizable actin filaments, these filaments were not as well-defined in ethanol-treated cells (Fig. 15B). Another feature that was noted after 48 hrs of culture was that neural crest cells exposed to ethanol were characterized by prominent positive phalloidin immuno-fluorescence in the region of the presumptive nucleus - a feature largely absent in control cells (Fig. 15). Ethanol-treated cells also appeared more numerous and of smaller size than control NCCs (Fig. 15) (previously discussed in section 3.8). By 96 hrs of cell culture, actin microfilaments were visible in both control cells and in those exposed to ethanol. However, neural crest cells that were cultured in ethanol showed disarray in their cytoskeletal actin architecture, a feature that was well-observed at higher magnifications (Figs. 15 and 16). Furthermore, in ethanol-treated crest cells, irregular digitations were seen at leading edges of some cells, focal adhesions were fewer than what was observed in controls and ethanol-treated cells appeared to clump together and overlap each other (Fig. 16B). This was not observed in control cells. Many of the actin microfilaments in alcohol-treated cells were seen ‘end-

on', suggestive of their altered orientation (Fig. 17B). This feature was not a frequent observation in control cells.

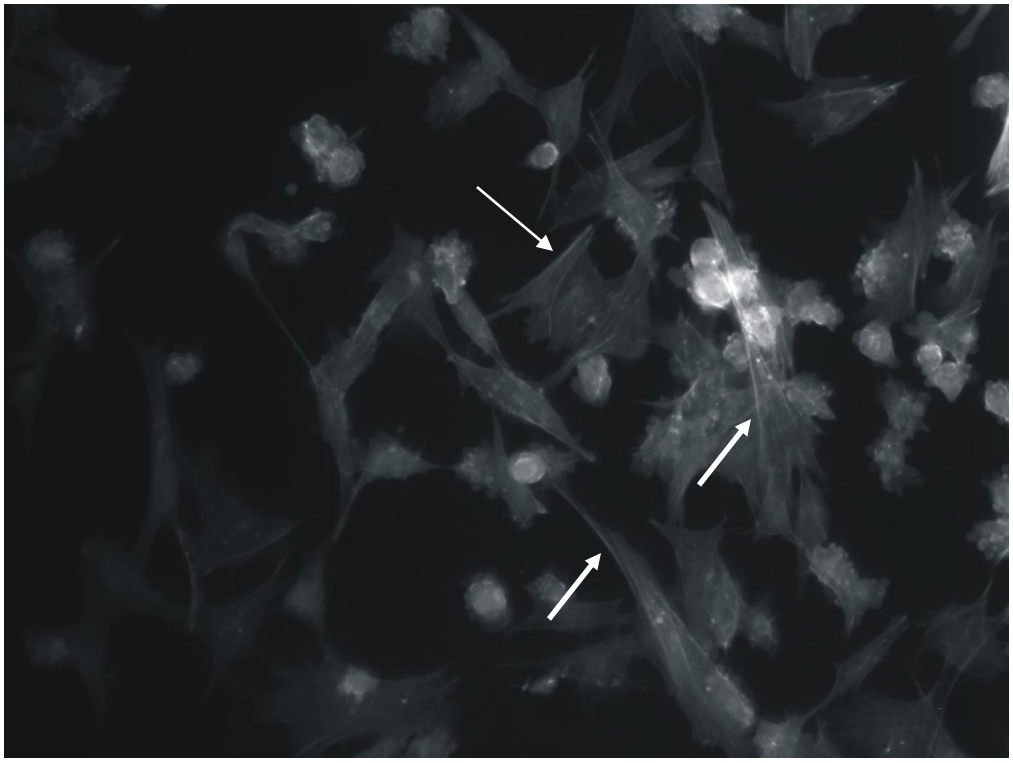

A

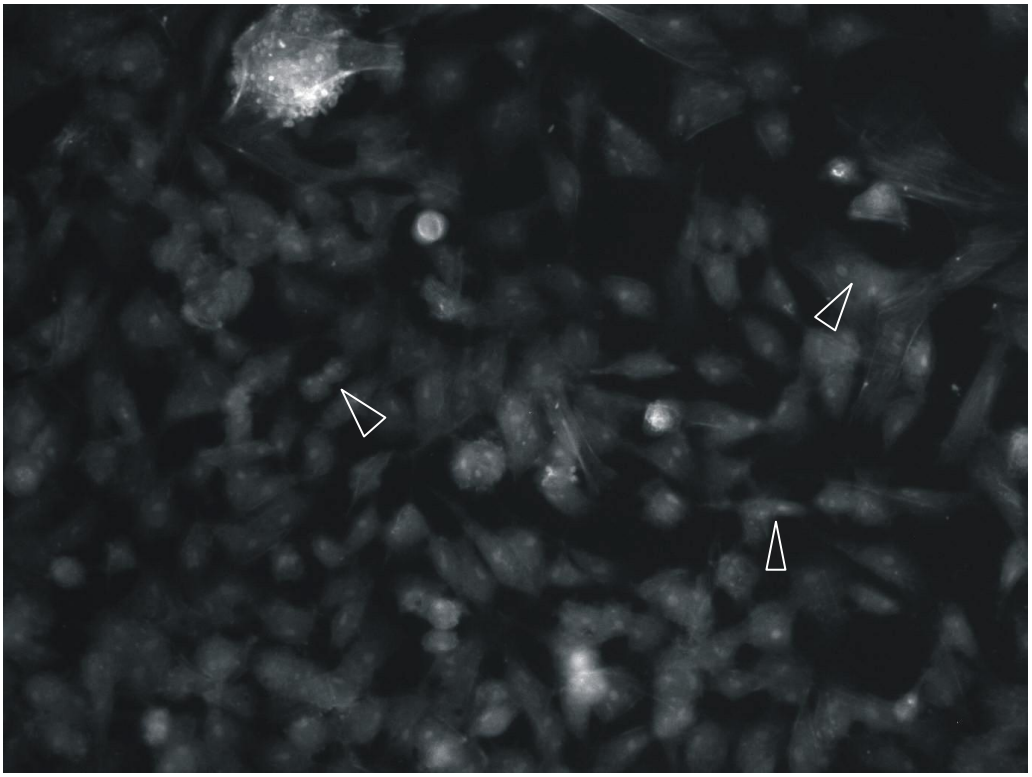

B

Fig. 15 A & B. Appearance of rhodamine immuno-labelled actin cytoskeleton of control (A) and 0.4% (v/v) ethanol-treated neural crest cells (B), after 2 days of culture. Even at this magnification, actin filaments are clearly seen in control cells (arrows), but not in ethanol-treated cells, which do not show extended processes. A phalloidin-positive entity within presumptive nuclei is a prominent feature of ethanol-treated crest cells. Many of the ethanol-treated cells appear to be in late mitosis (arrowheads). Olympus inverted microscope with epifluorescence200X.

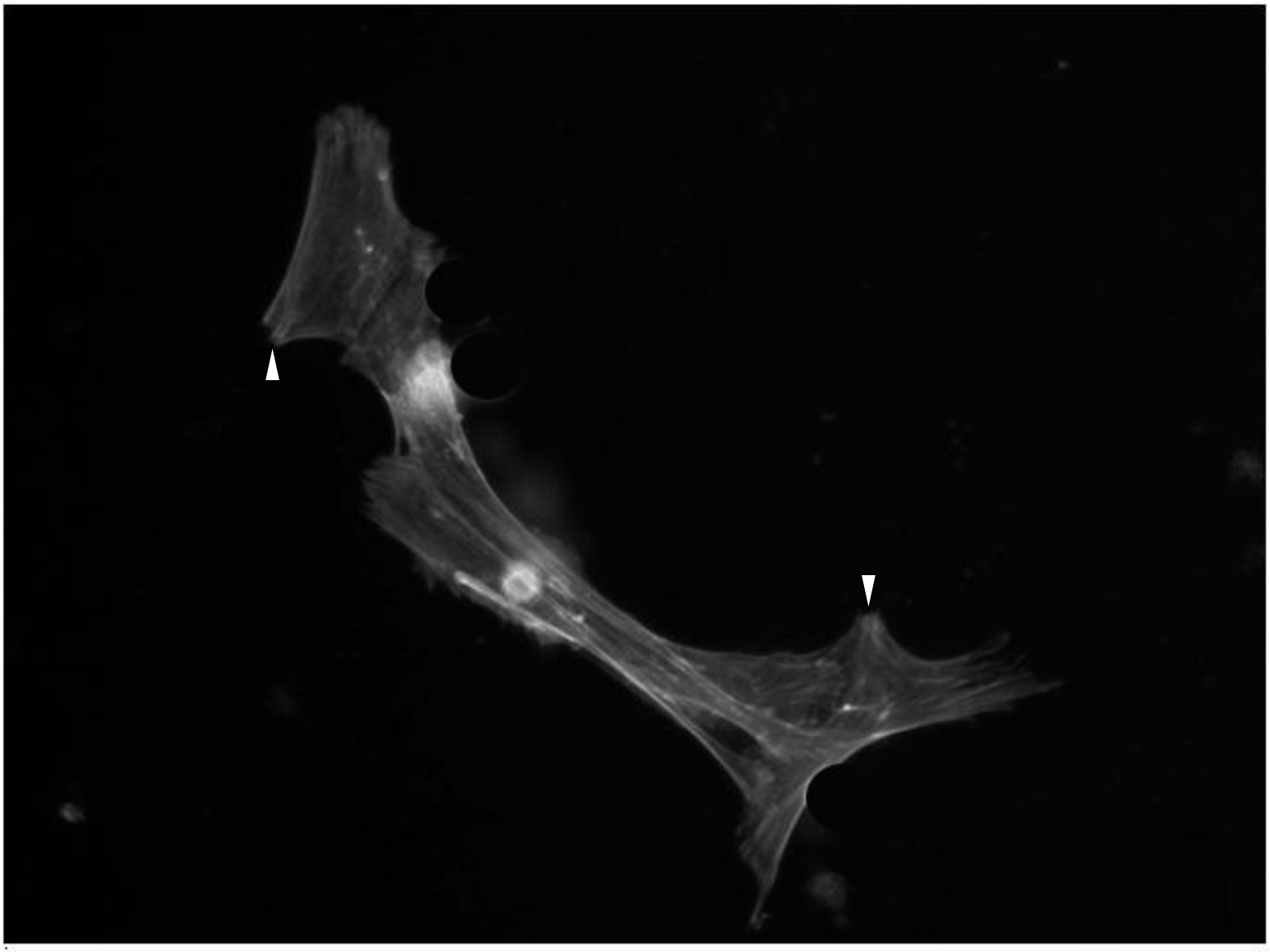

A

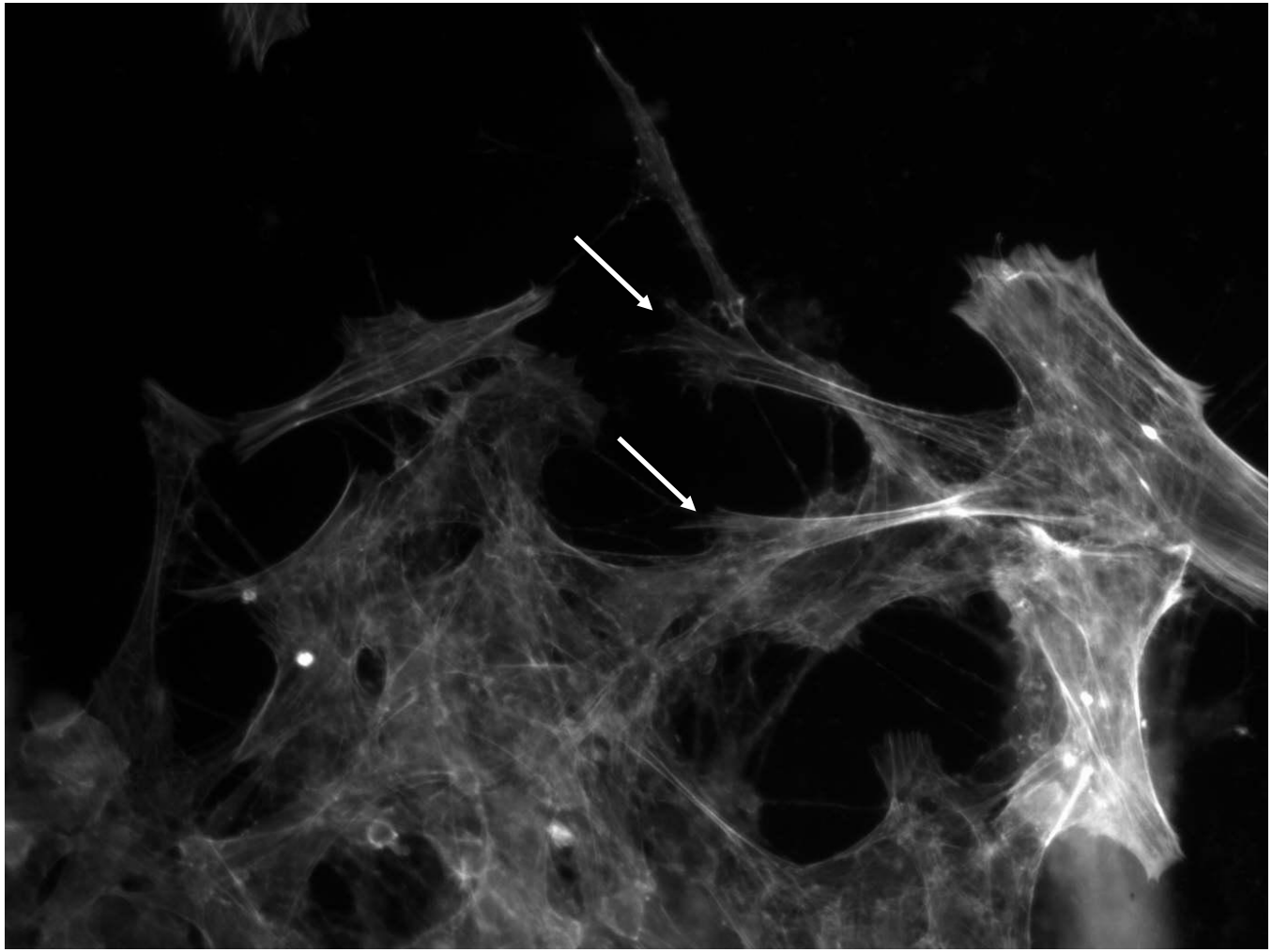

B

Fig. 16 A & B. Appearance of rhodamine immuno-labelled actin cytoskeleton of control (A) and 0.2% (v/v) ethanol-treated neural crest cells (B), after 4 days of culture. Actin filaments appear to be in disarray in ethanol-treated neural crest cells and lack focal adhesions in contrast to control cells (arrowheads in A). There are digitations of the actin cytoskeleton at leading edges of some treated cells (arrows) Ethanol-treated cells appear to be clumped together as they overlap and have migrated over each other. Olympus fluorescence microscope. 200X.

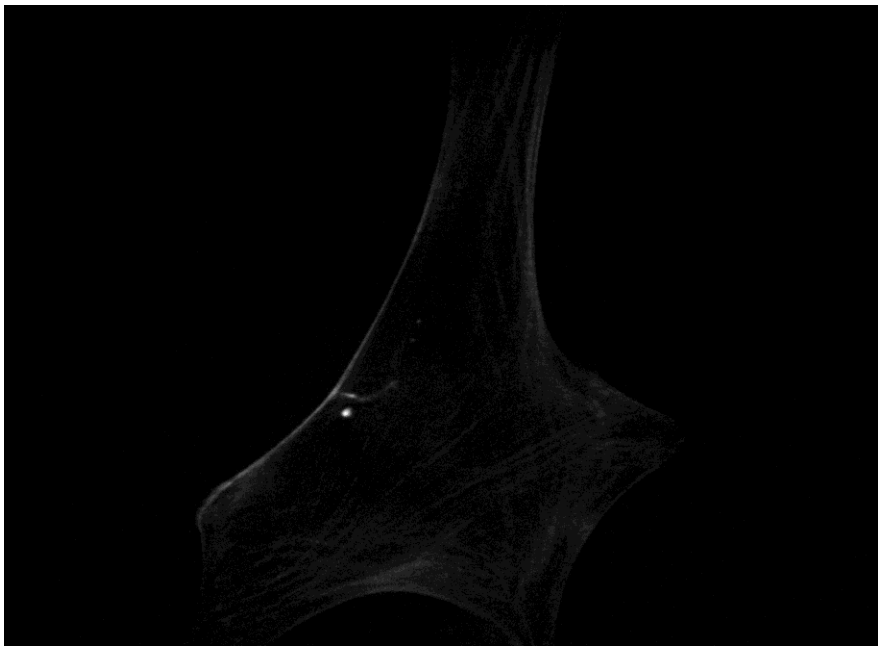

A

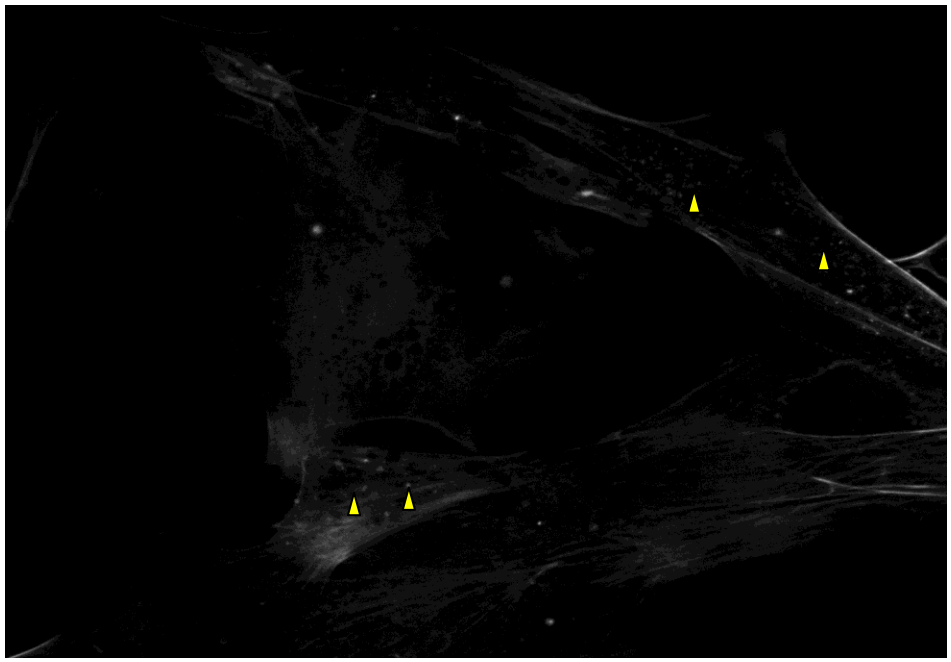

B

Fig. 17 A & B. Appearance of rhodamine immuno-labelled actin cytoskeleton of control (A) and 0.2% (v/v) ethanol-treated neural crest cells (B), after 6 days of culture. While the actin microfilaments are well-ordered in the control cell, they appear disorganized in treated cells. Some of the actin filaments are seen 'end on' (yellow arrowheads), indicative of their loss of proper orientation within the neural crest cell cytoplasm. Brighter white spots appear to be artefacts. Olympus fluorescence microscope. 400X.

Summary of observations on the actin cytoskeleton of ethanol-treated cNCCs

The actin cytoskeleton of ethanol-treated cranial neural crest cells showed

- Disorganization, irregularity and thinning, compared to controls
- Prominent intranuclear phalloidin immunofluorescence, which was not observed in control cNCCs
- Relative absence of focal adhesions

3.12 Surface ultrastructure of chick neural crest cells after exposure to ethanol

After 24 hrs of culture, low magnification scanning electron microscopy (SEM) revealed cranial neural crest cells which have been exposed to 0.2% (v/v) ethanol as having an epithelial, rather than a spindle-shaped mesenchymal appearance that was observed in non-treated neural crest cells (Fig. 18A). There also appears to be a reticular meshwork which was consistently present in ethanol-treated, but not control samples (arrows, Fig. 18B, C). Evidence of apoptosis (blebbing of the cell membrane) was observed in both control and ethanol-treated cells at 48hrs of culture (Fig. 19). Membrane protrusion ("blebbing") was more pronounced in neural crest cells cultured from neural tubes of younger embryos (stage 8 HH) than in those from older embryos (stage 10 HH), regardless of whether they were ethanol-exposed or not (Fig. 19). On the contrary, the appearance of a reticular meshwork was a feature of neural crest cells of stages 9 and 10 (HH) embryos, which had been exposed to ethanol. It was not found either in similar-stage control embryos, or in cultured crest cells from stage 8 embryos, whether or not these had been exposed to ethanol (Fig. 19), in spite of the fact that they were processed at the same time.

Another feature observed in ethanol-exposed neural crest cells, particularly those which were cultured from stage 8 (HH) derived neural tubes, was the presence of intercellular filamentous extensions between apoptotic cells (Fig. 19C). By the 6^{th} day of culture, some evidence of neural crest cell differentiation was observed, including the presence of nerve cells in control cultures (Fig. 20). Differentiation was also seen in ethanol-exposed neural crest cells, some of which showed extensive blebbing of the surface membrane (Fig.19B).

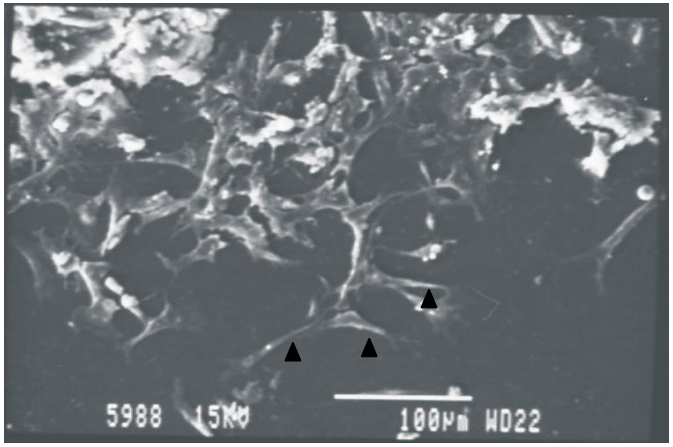

A

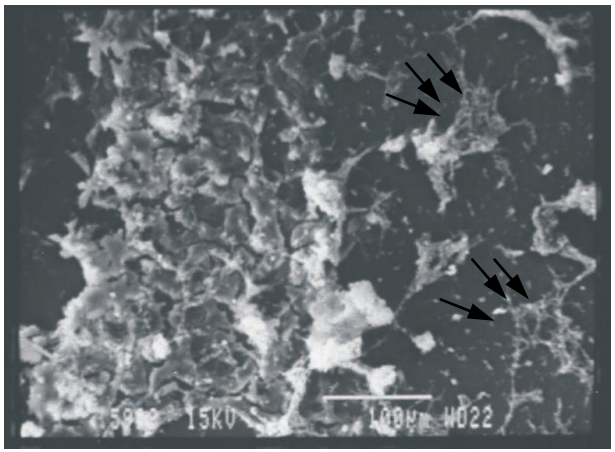

B

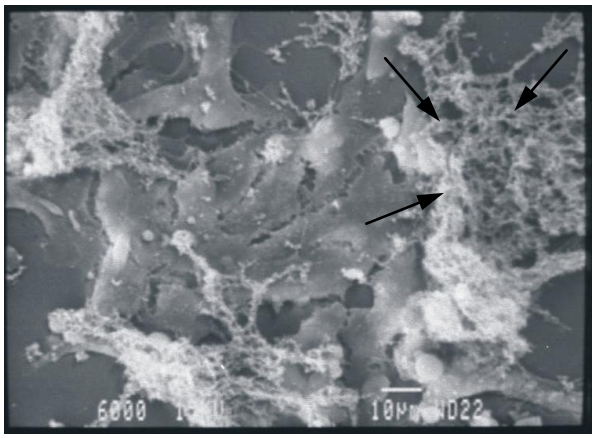

C

Fig. 18 A, B & C. Scanning electron micrographs of untreated neural crest cells (A) and cells cultured in 0.2% ethanol (v/v) for 24 hrs (B), and 4 days (C). While control cells are mesenchymal in appearance, with typical spinous processes (arrowheads), ethanol-treated cells are epithelial in shape. Treated cells also show a reticular meshwork (arrows in B, C), possibly remnants of apoptotic events. A, B 300X; C, 1000X.

Fig. 19 A – F. Scanning electron micrographs of non-treated (control) and ethanol-treated neural crest cells from neural tubes of stages 8-10 (HH) chick embryos at 48 hrs of culture. Membrane blebbing (arrows) featured prominently in both untreated (A) and ethanol-treated (B, C) cells cultured from neural tubes of stage 8 (HH) embryos (A, B and C), while the presence of a reticular meshwork characterized neural crest cells cultured from neural tubes of stage 9 (HH) (F) and stage 10 (HH) (D and E) embryos. At high ethanol concentration, intercellular extensions (arrowheads) are seen between neural crest cells (C). A, D, controls; B, 0.3% ethanol (v/v); E, 0.2% ethanol (v/v); C, F, 0.4% ethanol (v/v). A-E, 3000X. F, 2000X.

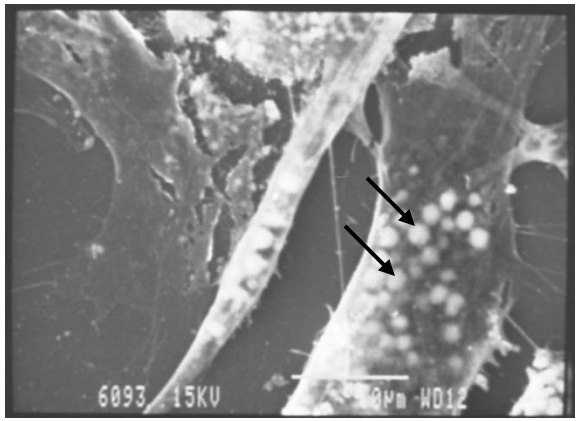

A

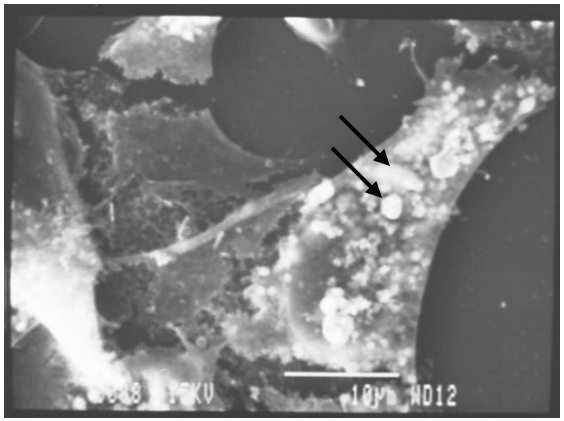

B

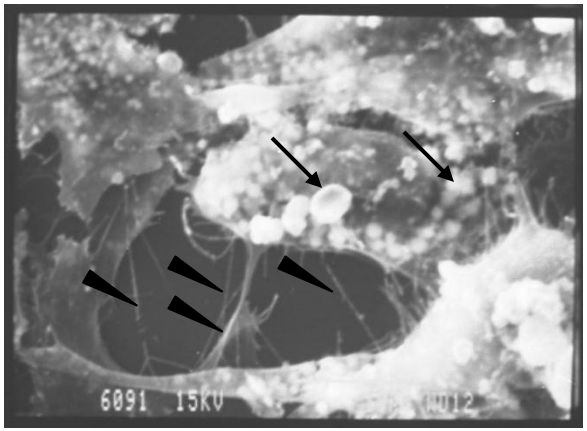

C

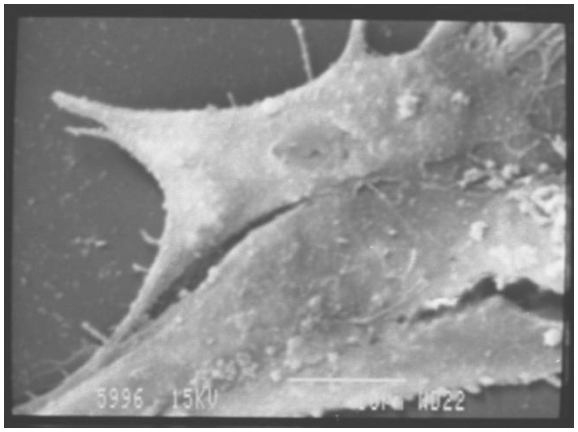

D

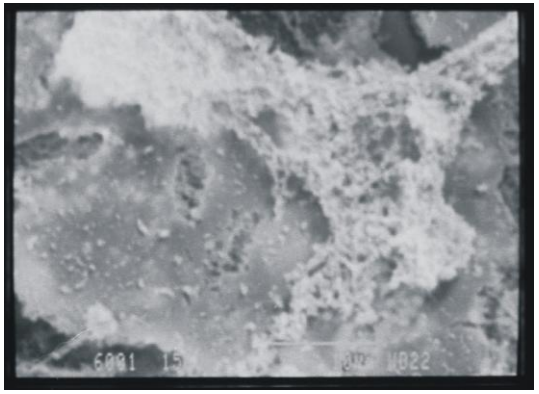

E

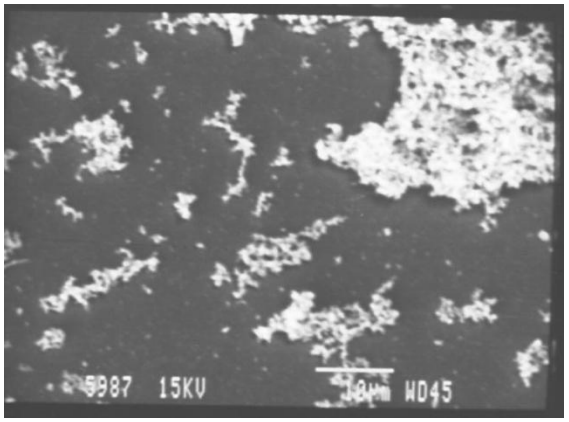

F

Fig. 19 A - F (See legend on preceding page).

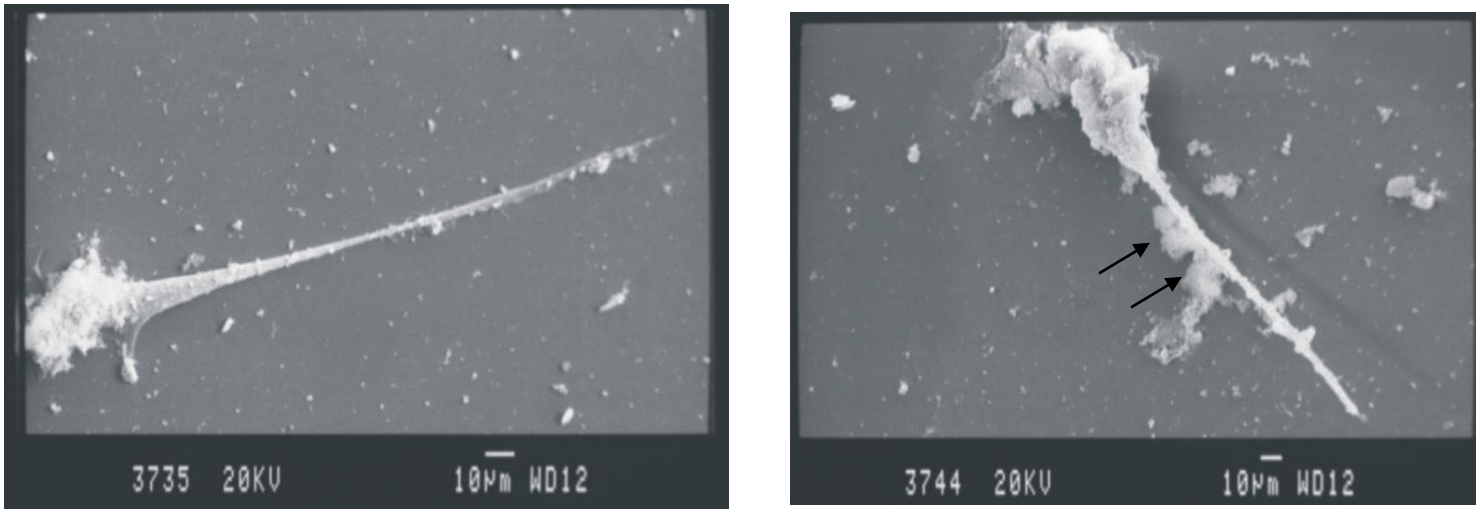

A B

Fig. 20 A & B. Control (A) and 0.2% (v/v) ethanol-treated chick neural crest cells in an advanced stage of differentiation into presumptive nerve cells, on the 6th day of cell culture. There are membrane blebs on the soma of both control and treated cells. However, there appears to be more "blebbing" on the ethanol-exposed cell and these blebs appear to extend from the long process of the cell (arrows). A, 600 X; B, 450 X.

Summary of SEM observation of surface ultrastructure of cNCCs

- Ethanol-treated cNCCs had an epithelial rather than mesenchymal shape
- The presence of membrane blebbing and a reticular meshwork appeared to be more prominent in ethanol-treated cNCCs, compared to control neural crest cells. The blebbing was more prominent at stage 8 (HH) while the meshwork was more prominent at stages 9-10 (HH).
- Ethanol-treated cNCCs that survived until the 6^{th} day of culture appeared to differentiate while showing evidence of generalized membrane blebbing.

3.13 Apoptosis in chick cNCCs *in vitro* following exposure to ethanol.

At 24 hrs of culture, there appeared to be no significant difference between control, 0.2% ethanol (v/v) and 0.4% (v/v) ethanol-treated cNCCs as indicated by the FITC marker for caspase-dependent apoptosis (Fig. 21 A-C). By 48 hrs of culture however, there was an increase in the number of cells which were positive for caspase-dependent immunofluorescence among the 0.2% (v/v) ethanol-treated cNCCs (Fig. 21E). A similar increase in caspase-dependent immunofluorescence was observed in cNCCs that were exposed to 0.4% ethanol (v/v) (Fig. 21F). Quantitation of the FITC-labelled relative to unlabelled cells (Table 15) confirmed the qualitative observations that were made using fluorescence microscopy. Although the number of FITC-labelled cells increased at 48hrs, there was no statistically significant increase in the number of fluorescent cells in ethanol-treated cNCCs over control neural crest cells either at 24- or 48hrs of cell culture (Table 15).

Summary of fluorescence microscopy results

There was no statistically significant increase in the number of FITC-labelled cNCCs (indicating caspase-dependent apoptosis) following exposure to either 0.2% or 0.4% (v/v) ethanol.

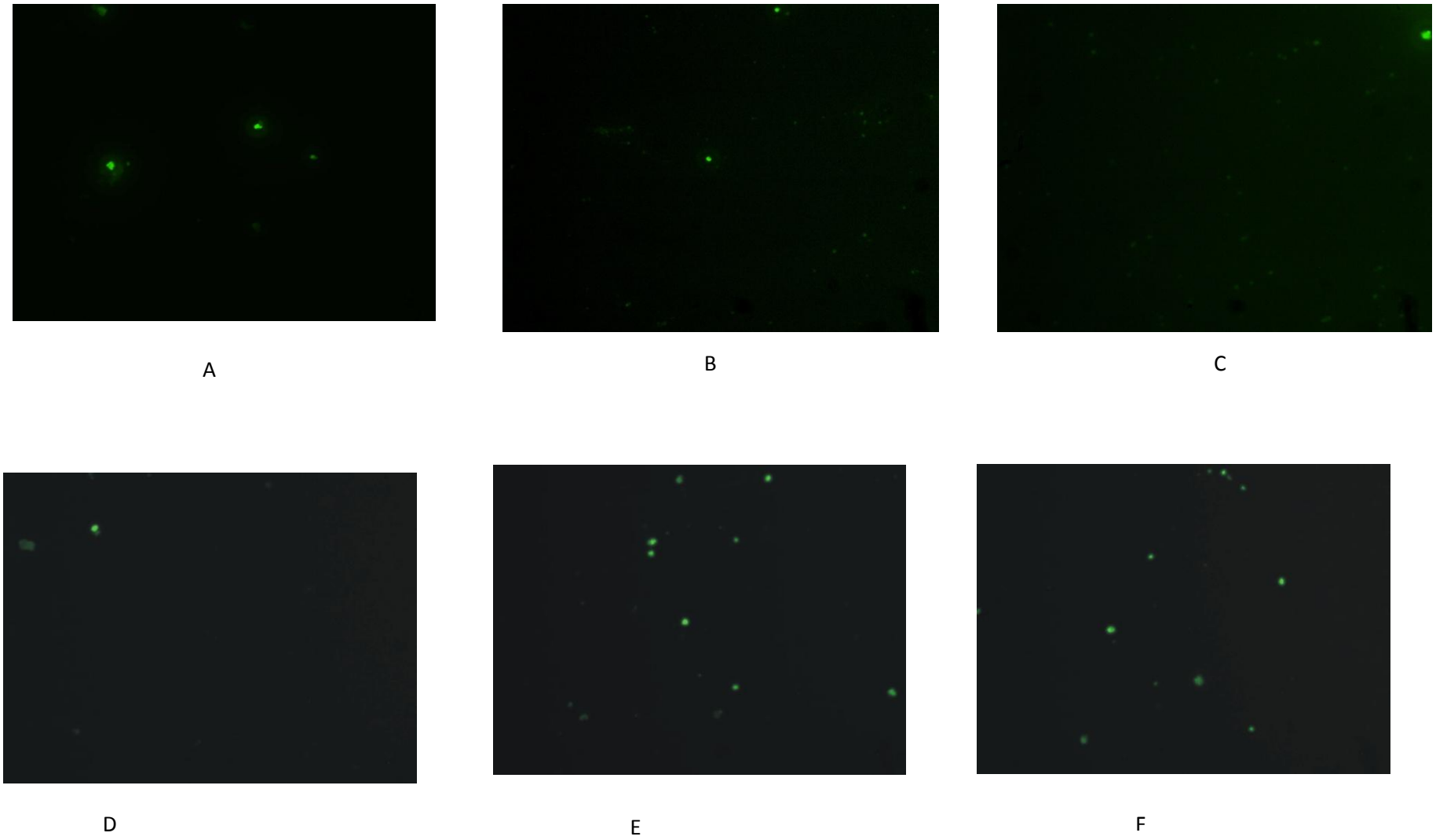

Fig. 21 A - F. Micrographs of FITC labelling of cells (indicating caspase-dependent apoptosis) in untreated (A, D) and ethanol-treated (B, C, E and F) neural crest cells at 24 hrs of culture. (A - C) and 48 hrs of culture (D - F). B, E, 0.2% ethanol (v/v); C, F, 0.4% ethanol (v/v). At 24 hrs, FITC labelling increased markedly in 0.2% ethanol (v/v) compared to control samples, but decreased on exposure to 0.4% ethanol. At 48 hrs, there were similar levels of slightly increased FITC labelling on exposure to both 0.2% and 0.4% ethanol (v/v). X200

Table 15. Mean number of FITC-labelled cells among control and ethanol-treated (Etoh) cranial neural crest cells.

	Labelled n (%)		**Unlabelled n (%)**		**Total n (%)**	
	24 hrs	**48hrs**	**24hrs**	**48hrs**	**24hrs**	**48hrs**
Control	3 (1.2)	10 (4.1)	240 (98.8)	236 (95.9)	243 (100)	246 (100)
0.2% Etoh	2 (0.6)	11 (3.8)	341 (99.4)	275 (96.2)	343 (100)	286 (100)
0.4% Etoh	1 (0.5)	15 (4.3)	197 (99.5)	337 (95.7)	198 (100)	352 (100)
p =0.398 (control versus 0.2% Etoh)			p =0.897 (control versus 0.2% Etoh)			
p =0.422 (control versus 0.4% Etoh)			p =0.906 (control versus 0.4% Etoh)			

3.14 Effect of ethanol on the expression of three candidate genes derived from chick neural crest cells

β-actin

After 24hrs of cNCCs culture in 0.3% (v/v) ethanol, the expression of actin was not detectable. However, by 48hrs of exposure to the same concentration of ethanol, the actin gene was upregulated to a mean of more than twofold that of control values. This was however not significant (p=1.00). With exposure to 0.4%, (v/v) ethanol, the actin gene was initially up-regulated compared to controls by a mean factor of almost six (Fig. 22A). By 48hrs of continuous exposure to this ethanol concentration however, this high level of expression was down-regulated to a level of about 2.5 times that of controls (Fig. 22B). All the changes in the expression of the actin gene following exposure to 0.4% (v/v) ethanol were not significant (p=0.423).

Rho B

The mean level of expression of the Rho B gene in cranial neural crest cells exposed to 0.3% (v/v) ethanol concentrations after 24 hrs was 1.6 times that of controls. This level of gene expression was down-regulated to control levels at 48hrs. Neither of these levels of relative Rho b expression was statistically significant when compared to control values. Exposure to 0.4% (v/v) concentration of ethanol changed from an initial down-regulation of the cNCCs Rho B gene (a mean of half of the control levels), to a mean level of expression of 1.3 times control values at 48hrs of ethanol exposure. This increase in gene expression was not significant (p=0.09; Fig. 22A and B).

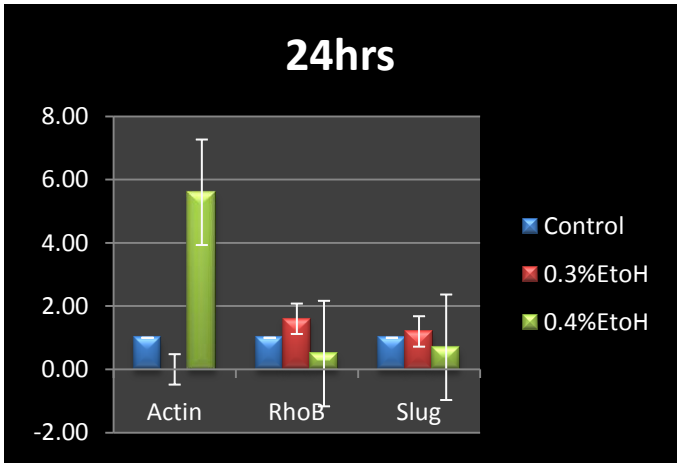

A

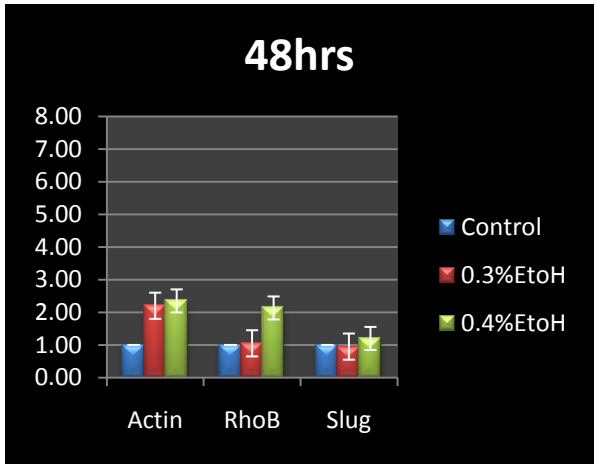

B

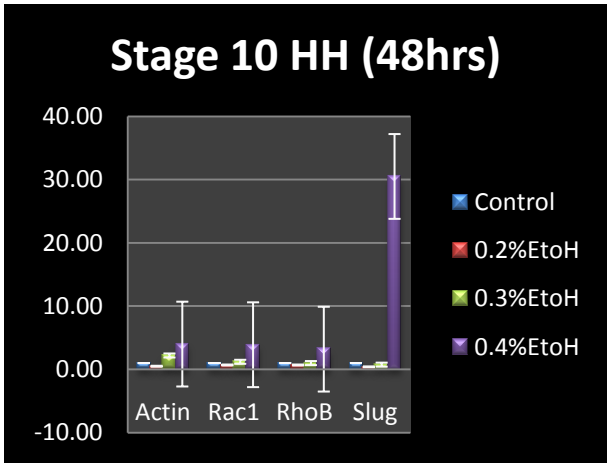

C

Fig. 22 A, B & C. Effect of different ethanol concentrations on the relative gene expression of selected neural crest cell genes at 24hrs (A), 48hrs (B) and in stage 10 (HH) neural crest cells, which were examined at 48hrs of migration.

Slug

The cNCCs *slug* gene showed only a slight (1.2X) mean increase in expression after exposure to 0.3% ethanol (v/v) for 24hrs, and a reduced (0.7X) gene expression with exposure to 0.4% ethanol (v/v) at 24hrs (Fig. 22). Following 48hrs of 0.3% ethanol exposure, the *slug gene* showed a level of expression that was similar to controls (mean of 0.95X). Cranial neural crest cells which were treated with 0.4% ethanol (v/v) also had a level of *slug* gene expression that was similar to that of control cells (mean of 1.2X; Fig. 22).

Relative gene expression of selected chick cNCCs genes at stage HH 10

From the results of section 3.9.4, we observed that migration of stage 10 (HH) chick cNCCs appeared not to be significantly affected by ethanol treatment, either after 24- or 48 hrs of culture. This group of cNCCs was therefore chosen for further gene expression analysis in order to observe whether there were more subtle changes at the molecular level that were being missed from the analysis of cell migration alone. Neural crest cells from the 48-hr culture sample were chosen to allow time for such an effect, if present to be observed.

The relative gene expression compared to controls was highest when stage 10 (HH) derived cNCCs were exposed to 0.4% ethanol (v/v) for all the genes examined (Actin, Rac 1, Rho B and *slug*) (Fig. 22C). The greatest amount of up-regulation occurred for the cNCCs *slug* gene, which was up-regulated by a mean of more than 30 times compared to control values following exposure of the cNCCs to 0.4% ethanol (v/v).

Summary of the results for cNCCs gene expression

- Except for the expression of β-actin after 24hrs of exposure to 0.4% ethanol, exposure of cNCCs to ethanol for 24hrs and 48hrs did not have a significant effect on gene expression.
- However, the *slug* gene of stage 10 (HH) cNCCs was upregulated by a mean of 30-fold by exposure to 0.4% ethanol (v/v), while the Rac 1, Rho B and actin genes of cNCCs from the same embryonic stage were only upregulated by a mean of about 5 times..

4.0 DISCUSSION

4.1 Ethanol may have dormant embryotoxic effects – possible role for cephalometry

That alcohol is a teratogen to unborn fetuses, even in single acute doses, is no longer in doubt. What remains is the attempt to understand how the embryotoxic effects are accomplished with a view to ultimate prevention in children born to alcoholic mothers (Spong *et al*., 2001). A preliminary step to understanding how craniofacial abnormalities are produced in children suffering from FAS could be the measurement of these effects as accurately as possible by means of cephalometry. Ward (1989) argued that simple head measurements using relatively inexpensive tools still provide a valuable adjunct to clinical observation, despite the wide availability of sophisticated computerized techniques. An example of the usefulness of cephalometry is how Peltomaki *et al*. (1989) showed significant differences in linear and angular measurements of the skull base in Turner syndrome patients. Such measurements could perhaps reveal patterns that mere subjective evaluations fail to make obvious. With only a few exceptions (Schwetz *et al*., 1978), the effect of acute or chronic alcohol exposure on fetal viability, litter size, birth weight, and postnatal growth on offspring in both animal and human models appears to be consistently deleterious (Chernoff, 1977; Streissguth *et al*., 1980; Sulik and Johnston, 1983; Webster *et al*., 1983; Brown, 1990; Spong *et al*., 2001). The findings of this study in the murine model demonstrated reduced fetal viability and increased fetal reabsorptions, but not a significantly reduced litter size or fetal birth weight in ethanol-treated animals as compared to controls. Similarly and perhaps related to this, is the fact that unlike some previous studies (Giglio *et al*., 1987; Edwards and Dow-Edwards, 1991; Hernandez-Guerrero *et al*., 1998) where ethanol-fed dams either lost weight or did not gain as much weight as the controls, the ethanol-treated dams in the present study continued to gain weight in a pattern similar to that of control animals. This was probably due to the fact that in this study food and water were withheld from control dams

during the time that the ethanol-fed ones were unable to feed due to alcohol intoxication. That the birth weight of the neonate animal should be related to the weight gain or lack thereof of its dam appears to be a reasonable assumption and could explain the lack of a significant difference in birth weight between the groups of fetuses in our series, especially as both treated and untreated dams had the same average litter size. Tze and Lee (1975) observed a similar pattern of weight gain in treated and untreated animals as was found in this study. In the series of Giglio *et al*. (1987), the offspring from rat dams that were pair fed with caloric and volume equivalents to their ethanol-fed counterparts had a lower (although not significantly reduced) birth weight than controls that were allowed to feed *ad libitum*. Randall and Taylor (1979) found no significant differences in the birth weight of mice from either ethanol-fed or pair-fed dams, a result similar to that in the present study.

Concerning the facial appearance of individuals suffering from FAS, it has been suggested by some investigators that such dysmorphic features represent only one of the ways in which alcohol disrupts embryonic development, and that perhaps it is not the most serious pathology arising from *in utero* alcohol exposure (Webster and Ritchie, 1991). If, as these authors claim, ‘‘facial development is not peculiarly sensitive to alcohol,’’ then the more exact the determination of facial anomalies arising from suspected FAS, the better the characterization will be of any abnormalities in the facial appearance of offspring of alcoholic mothers. Giglio *et al*. (1987) highlighted the usefulness of cephalometry in depicting the effect of alcohol on the developing head even in the absence of the typical FAS features. Their work showed that elements of the mandible, including the mandibular base, condylar process, and coronoid process were reduced when measured at 21 days postpartum in treated rats. Interestingly, mandibular width was not altered in these animals, again highlighting the fact that the craniofacial effects of alcohol could be complex, subtle, and multifactorial, as also suggested by Su *et al*. (2001) from their work on chick embryos. Hernandez-Guerrero *et al*. (1998) have

shown similar results. In their study, cephalometry revealed postnatal reductions in skull and mandibular lengths in mice that had been prenatally exposed to alcohol. The fact that the present study did not find significant differences between cranial measurements of ethanol-treated mice compared to controls, may not be as contradictory to previous results as the case may first appear to be. Giglio *et al*. (1987) and Hernandez-Guerrero *et al*. (1998) conducted their measurements on postnatal animals, on average 21 days after delivery. It is possible that differences that were not apparent at birth would progressively become obvious later on. Streissguth *et al*. (1980) make the point that ‘‘the growth deficiency typical of FAS is of prenatal onset and postnatal catch-up growth generally does not occur.’’ Furthermore, these authors assert that as FAS-affected children develop, the reduced adipose tissue becomes more pronounced, thus highlighting the pre-existing growth deficiency. Studies in the rat have previously shown that this rodent’s skull grows more during postnatal than prenatal life (Moss, 1958 cited in Edwards and Dow-Edwards, 1991). In the present study, skeletal staining revealed that mice, which had no obvious gross abnormalities at term showed minor cranial defects, as well as ossification at stages that lagged behind that in control pups of similar ages. Although the latter results were not statistically significant, they at least point to the need to investigate the argument more rigorously that latent effects of FAS become more prominent after birth, probably due to pre-existing but occult defects (Streissguth *et al*., 1980). Interestingly, even though the level of fetal abnormalities observed in our series stopped just short statistical significance, a clear trend emerged where the overwhelming majority (86%) of abnormalities occurred in ethanol-exposed fetuses. Future studies with larger samples may be able to demonstrate that birth defects occurring in mice offspring treated with a series of acute ethanol doses may become more overt prenatally rather than postnatally. This, in the light of previous studies that showed multiple abnormalities in the skeleton of animal fetuses that were exposed to ethanol in utero (Chernoff, 1977; Schwetz *et*

al., 1978; Randall and Taylor, 1979). In contrast, however, to these postulations is the observation made by Su *et al*. (2001), who showed that chick embryos were able to compensate for ethanol-induced cranial deficits by the seventh day following hatching. As far as is currently known, such recovery from a preterm ethanol insult has not been previously demonstrated in rodents or other mammals. An ideal study would be to conduct serial cephalometry on ethanol-exposed animals at defined intervals *in utero* and postnatally, to assess critical head and face changes in an accurate manner. With the advent of ultrasound scanning and similar modern technology, this is not an inconceivable suggestion.

4.2 Teratogenic dose of blood alcohol concentration remains variable

Much has been previously written about the role of blood ethanol levels in the aetiology of FAS. However, there appears to be a lack of consensus in the literature about the actual teratogenic dose. Webster and Ritchie (1991) observed that the doses of maternal alcohol and resultant peak blood alcohol levels required to cause teratogenesis in experimental animals was in the region of 400-800 mg/100 ml blood. This contrasts with results from the study by Randall and Taylor (1979) which demonstrated significant birth defects in fetuses that had been exposed to ethanol concentrations just exceeding 100 mg/ml for two out of the 5 days for which they were fed with an ethanol diet. Other studies (Schwetz *et al*., 1978; Mooney and Miller, 2001) did not find malformations in pups even though blood ethanol values that were attained in their dams were between 200 and 400 mg/dl. Mean BEC peaked at just above 180 mg/dl in the present study, although levels as high as 260 mg/dl were achieved in some animals. The fact that, similar to some previously published work (Schwetz *et al*., 1978; Mooney and Miller, 2001), the present study did not find significant ethanol-induced gross congenital malformations at these levels may reflect the need for a more thorough understanding of the mechanisms of the teratogenicity of ethanol. There was no evidence in

this study that the food deprivation suffered by treated mice during their state of intoxication produced any harmful effects, as these animals showed an overall weight gain pattern similar to that observed in controls. Both the control and ethanol-treated groups of animals showed certain unexplained swings in their feeding patterns, which did not exceed 24 h at any given time. We did not find any evidence that these changes significantly affected the outcomes of this study.

4.3 Teratogenic mechanisms of ethanol: a combination of apoptosis and proliferation

Cranial neural crest cells (cNCCs), emigrating from the embryonic regions of mid-diencephalon to the level of the 5th somite contribute significantly to forming cranial and dentofacial structures (Le Douarin and Kalchiem, 1999; Sant'Anna and Tosello, 2006). It is widely accepted that the teratogenic effects of ethanol can be explained, at least in part, because it targets these migrating cells (Cartwright and Smith 1995a; Cartwright and Smith 1995b; Smith and Debelak-Kragtorp, 2005). The precise way in which ethanol affects neural crest cells is still under intense investigation and is by no means fully elucidated, but ethanol has been shown to amplify the normal process of apoptosis (Cartwright and Smith 1995a; Smith, 1997). Ethanol-induced apoptosis is thought to be triggered by, among other mechanisms, oxidative stress (Wentzel and Eriksson, 2009), free radical damage (Davis *et al*., 1990; Chen and Sulik, 1996; Chen and Sulik, 2000), alteration of calcium signalling (Messing *et al*., 1986; Debelak-Kragtorp *et al*., 2003; Garic-Stankovic *et al*., 2005a; Garic-Stankovic *et al*., 2006) and perturbations of DNA (Davis *et al*. 1990; Giles *et al*. 2008).

Given the overwhelming reports in the literature, of the increase in ethanol-induced apoptosis in brain cells generally and cNCCs in particular (Kotch and Sulik, 1992a; Kotch and Sulik, 1992b; Cartwright and Smith, 1995a; Cartwright and Smith, 1995b; Miller, 1996; Smith, 1997; Cartwright *et al*., 1998; Dunty *et al*., 2001), the finding in the present study of no

significant increase in caspase-dependent apoptosis in ethanol-exposed cNCCs compared to controls is somewhat surprising. It may be noteworthy to consider that with a few exceptions (Davis *et al*., 1990; Rovasio and Battiato, 2002), the pivotal reports that demonstrated the expanded apoptosis of embryonic cells, particularly cNCCs, arose from *in-ovo* ethanol administration in chick (Cartwright and Smith, 1995a; Garic-Stankovic *et al*., 2005a; Garic-Stankovic *et al*., 2005b) and *in utero* treatment in mouse embryos (Sulik *et al*., 1988; Gage and Sulik, 1991; Johnston and Bronsky, 1991). Furthermore and significantly, previous workers (Sulik *et al*., 1988; Cartwright *et al*., 1998) have noted that the vulnerability of cNCCs populations to ethanol-induced apoptosis is related to how close affected cells are *in vivo* to regions of normal programmed cell death. Graham *et al*. (1993; 1995) have elegantly described how neural crest cell apoptosis occurs in rhombomeres 3 and 5 of the chick hindbrain in the presence, but not in the absence of the neighbouring rhombomeres 2, 4 and 6. Such a "proximity effect" may not be easily replicated for *in vitro* cultures. More work is needed to illuminate the conditions under which ethanol-induced cNCCs apoptosis may be optimally demonstrated *in vitro*.

Considering the reported deleterious effects of ethanol, it was a surprise finding in this study that ethanol had an apparent proliferative effect on cNCCs, as observed subjectively from the apparent increase in number of ethanol-treated cNCCs in culture and the qualitatively thicker cNCCs columns in ethanol-exposed whole-mount immunolabelled embryos compared to control embryos. An ethanol-induced proliferation of cNCCs in the present study was however quantified as we found a significant increase in the mitotic index of ethanol-treated neural crest cells compared to control cells. Certain authors (Cartwright *et al*., 1998) have previously commented on the "well-documented" ability of ethanol to promote proliferation in neural cells in general and in neural crest cells in particular (Rovasio and Battiato, 1995). Significantly, the latter author described a high "cell density" of cNCCs when treated with

ethanol, which caused them to migrate abnormally into the neural tube lumen. However, the aforementioned authors (Cartwright *et al*., 1998) concluded that such increased proliferation was either not statistically significant or otherwise was caused by their "intrinsic proliferative behaviour" (Rovasio and Battiato, 1995). On the other hand, Vaglia and Hall (1999), reviewing the phenomenon of regeneration – the mechanism by which extirpated undifferentiated embryonic cells are replaced by other undifferentiated cells, comment that "increased cell division in response to neural crest ablation is likely more common than has been reported". Yet another group of authors (Hoffman and Kulyk, 1999) have described how ethanol promotes quantitatively increased formation of cartilage *in vitro*, from the culture of ectomesenchymal cells from facial primordia (maxillary, mandibular, frontonasal, and hyoid processes), which are of cNCCs origin. It is apparent that at least under certain conditions, ethanol does promote neural crest cell proliferation. This increased proliferation, it may be postulated, may cause migrating cNCCs to be directed into ectopic sites (Rovasio and Battiato 1995), or to miss crucial spatial and temporal cues along their migratory route (Le Douarin, 1986; Dupin *et al*., 1993; Sieber-Blum and Zhang, 1997; Duband, 2006). The misdirected cNCCs would then be removed by apoptosis or other cell protective mechanisms, eventually contributing to the FAS phenotype (Arends and Wyllie, 1991; White, 1996).

Contrary to the above scenario where an ethanol-induced increase in cell numbers could direct cNCCs into ectopic migratory pathways, we observed from time-lapse video microscopy that in a few ethanol-treated cultures, cNCCs exhibited a late onset of migration and a prolonged duration of migration, compared to control cells. A plausible explanation may be that there was an initial ethanol-induced delayed migration with subsequent recovery of the type described by Cartwright and Smith (1995b). The latter authors found that although older embryos showed evidence of cNCC cell death caused by ethanol, they also showed that an increased capacity for recovery. In the present study, cNCCs which were slow to emigrate

from the neural tube were comparable to those attributed with "ethanol-induced depletion, but increased capacity for recovery" by Cartwright *et al*. (1995b). Due to the constraints of our experiments, our slow-migrating cultures were only observed for 24 hours, a time frame that perhaps did not allow such a potential recovery to be recorded. The method of ethanol administration, *in ovo* by Cartwright and Smith (1995b) versus our *in vitro* ethanol application, as well as the final ethanol concentration achieved, may also have contributed to the apparent differences in the results obtained between the present study and that of others.

4.4 Ethanol's effect on neural crest cell migratory potential and surface morphology appears to target embryonic stages 9-10 (HH)

Furthermore regarding stage-specific effects of ethanol on cNCCs, one result in the present study was that cNCCs obtained from stage 9 (HH) embryos appeared to be more susceptible, at least in terms of their migration, to the deleterious effects of ethanol than cNCCs obtained from stages 8 or 10 (HH) embryos. This was inferred from the significant differences in the distances migrated by ethanol-treated stage 9 (HH) cNCCs compared to controls. While several authors have explored stage-dependent ethanol teratogenesis on other aspects of neural crest function (Cartwright and Smith, 1995b; Cavieres and Smith, 2000; Giles *et al*., 2008), to our knowledge, this is the first time that an attempt has been made to ascertain whether the toxicity of ethanol as pertains to the distance migrated by cNCCs is restricted to, or even predominant at any given embryonic stage. Related to this is the fact that the present study found, again perhaps for the first time, that cNCCs from different stage embryos appear to respond differently to an ethanol challenge by the type of surface modifications that they produce. While it has been known for some time that migrating neural crest cells lose their surface projections, variably termed "microvilli", "villi" or "arborized dendrites", and develop membrane "blebs", (Hassler and Moran 1986; Davis *et al*. 1990; Rovasio and

Battiato 2002), we have described in this work the presence of cNCCs surface "meshworks", which appear to be consistently present on ethanol-challenged, but not control cNCCs, particularly of neural crest cells derived from embryos of stages 9-10 (HH). The exact nature of these "meshworks" is presently unclear. To our knowledge, these "meshworks" have never been described before in the literature, probably due to the fact that the majority of the morphological studies into apoptosis in comparison to necrosis have understandably employed transmission electron microscopy, which enables the visualisation of internal rather than surface cell features (Uller *et al*., 2004; do Vale *et al*., 2007; Silva *et al*., 2008). It is known that apoptotic bodies are continuously undergoing degradation and phagocytosis by surrounding cells (Hengartner, 2001; Ziegler and Groscurth, 2004). If not phagocytosed, apoptotic bodies continue to degrade and the process will morphologically resemble necrosis – the so called secondary necrosis - with rupture of the cell membrane, excessive chromatin shrinkage and leakage of cell contents (Uller *et al*., 2004; Ziegler and Groscurth, 2004; Rydell-Tormanen *et al*., 2006; do Vale *et al*., 2007; Silva *et al*., 2008). Indeed forms of cell death that display morphological features similar to both necrosis and apoptosis are known. As these become better understood, it is becoming clear, that when cells are challenged chemically or otherwise, stereotyped outcomes either as apoptosis or necrosis cannot always be expected (Ziegler and Groscurth, 2004).

4.5 Does ethanol have an effect on nuclear actin?

The disorganized actin cytoskeleton that was observed in ethanol-exposed cells in this study has been recognized for some time as a result of the treatment of cNCCs with ethanol (Hassler and Moran 1986; Rovasio and Battiato 2002). What has seemingly not been described before is the prominent phalloidin staining within presumptive nuclei of ethanol treated cNCCs. There is now no doubt among researchers (Rando *et al*., 2000; Pederson and

Aebi, 2002; Bettinger *et al*., 2003; Pollard and Borisy, 2003; Franke, 2004; Winder and Ayscough, 2005; Jockusch *et al*., 2006; Pederson, 2008; Hofmann *et al*., 2009) that actin does exist within the nucleus and that it is involved in events such as transcription by RNA polymerases, chromatin remodelling, spindle formation and nuclear transport of RNA and proteins. The literature appears to be unanimous in the opinion that phalloidin does not recognise polymeric F-actin under physiological conditions (Rando *et al*., 2000; Hofmann and de Lanerolle, 2006). However, under conditions of cell stress, including experimental treatment with membrane active compounds, heat shock or toxins, nuclear actin is rendered susceptible to phalloidin immunoreactivity (Fukui, 1978; Fukui and Katsumaru, 1979; Sanger *et al*., 1980; Iida *et al*., 1986; Kushnaryov *et al*., 1990; Jockusch *et al*., 2006). It is likely that exposure of cNCCs to ethanol in the present study may have rendered their nuclear actin immunoreactive to phalloidin, probably by exposing phalloidin-binding sites on the protein, or otherwise changing the phalloidin-insensitive conformation of nuclear actin (Gonsior *et al*., 1999; Schoenenberger *et al*., 2005).

4.6 The regulation of cranial neural crest cell β-actin, Rac 1, RhoB and *slug* genes by ethanol depends on the concentration and duration of exposure

A large body of work (McCauley and Bronner-Fraser, 2006; McCabe and Bronner-Fraser, 2009; Nikitina *et al*., 2009) has been devoted in the literature to describing the genetic and molecular factors that underlie cNCCs delamination, migration and fate determination using amphibian, chick and mouse models. Not only are the molecular factors and pathways which regulate normal neural crest cells being investigated, but those that are involved in abnormal neural crest function and ethanol-induced teratogenicity in humans and in animal models are also receiving sustained scholarly attention (Johnston and Bronsky, 1991; Downing and Gilliam, 1999; Dick and Foroud, 2003; Lombard *et al*., 2007; Downing *et al*., 2009a;

Downing *et al*., 2009b; Ouko *et al*., 2009). In the present study, we chose to investigate the effect of ethanol on three cNCCs genes that have been implicated in cNCCs induction, survival, epithelial to mesenchymal transformation, migration and cell lineage determination (LaBonne and Bronner-Fraser, 2000; Adams *et al*., 2008). Our results shows that the β-actin gene, which codes for all cytoplasmic actin (Sparrow and Laing, 2008), from ethanol-treated stages 8 – 10 (HH) cNCCs was upregulated at high (0.4% v/v) ethanol concentrations compared to controls at 24 hours. This observation accords with the results of our migration assay, which showed that cNCCs treated with 0.4% ethanol (v/v) migrated further than control cells. However, there was a lack of concordance between the relative regulation of the β-actin gene and the distance migrated by cNCCs treated with 0.3% ethanol (v/v). Even though β-actin transcripts were not detectable relative to controls, 0.3% ethanol-treated cNCCs migrated significantly further than control cells at 24 hours. Conversely at 48 hours, while 0.3% (v/v) ethanol-treated cNCCs did not migrate as far as control cells, the β-actin gene in these cells was upregulated relative to control levels. This discordance between β-actin gene expression and cytoskeleton-dependent migration is difficult to explain, given the synergy observed between these two parameters at 0.4% ethanol concentration. Presumably, these effects reflect ethanol concentration-dependent alterations. However the actual cellular events producing these observations may be more complex. They may involve molecular interactions, rate-limiting steps and feedback loops between β-actin gene transcription, β-actin mRNA translation and β-actin polymerization into cytoskeletal actin. It is known that β-actin polymerization is increased at the growing ends of axons (Lund *et al*., 2002) and at the leading or "barbed" edges of migrating cells (Shestakova *et al*., 2001; Ridley *et al*., 2003; Raftopoulou and Hall, 2004). It may be that an optimal level of β-actin protein synthesis is needed to achieve cell migration. The different concentrations of ethanol employed in this study may affect this optimal level variably.

Rho B, another protein that has wide-ranging roles in actin cytoskeletal assembly, maintenance of cell shape and the integrity of cell junctions, among other functions (Hall and Nobes, 1992; Nobes and Hall, 1999; Bishop and Hall, 2000; Etienne-Manneville and Hall, 2002), also exhibited varying levels of mRNA regulation compared to controls, depending on ethanol concentration and treatment duration. Again, these disparate results may reflect concentration-dependent effects of ethanol. The fact that all the three genes studied were up-regulated to varying extents in 0.4% ethanol (v/v) at 48 hours of treatment may also indicate the effect of duration of ethanol exposure on cNCCs gene expression, such that the genes may be over-expressed during long-term ethanol exposure. This over-expression may relate to attempts at recovery by ethanol-exposed cNCCs. Ahlgren *et al*. (2002) found that the exogenous over-expression of the Sonic hedgehog gene protected cNCCs from apoptosis. Ultimately however, these effects may be due to factors that are yet to be elucidated. Debelak and Smith (2000) stated that the heterogeneity in alcohol's effects suggested a complex aetiology for FAS. We believe that this complexity has its roots at the cellular and molecular levels.

Another observation in the present study was that the *slug* gene exhibited a 30-fold up-regulation compared to controls, in cNCCs which were derived from stage 10 (HH) embryos and cultured in 0.4% ethanol (v/v). This once again may reflect the stage-dependent effects of ethanol, with a potentially interesting implication. In Xenopus and Gallus species, *Slug* is expressed in premigratory and migratory neural crest cells (Carl *et al*., 1999; LaBonne and Bronner-Fraser, 1999; Christiansen *et al*., 2000; LaBonne and Bronner-Fraser, 2000). In the light of the 30-fold up-regulation of *slug* by ethanol which we observed, it is interesting that previous workers have noted that when *slug* is experimentally overexpressed, NCC-forming regions are expanded *in vivo*, there is an increase in the number of NCCs and supernumerary melanocytes (derivatives of NCCs) are produced, particularly when other signalling

molecules (FGFs, Wnts) are also present (LaBonne and Bronner-Fraser, 1998; LaBonne and Bronner-Fraser, 1999; Christiansen *et al*., 2000). We observed an increase in cNCCs (proliferation) in this study which was greatest at 0.4% ethanol concentration. This may be due to the up-regulation of *slug.* The significantly increased distance migrated by cNCCs, particularly at 0.4% ethanol concentration may also reflect the ethanol-induced increase in activity of the *slug* gene. This is because the over expression (up-regulation) of slug (or its analogue s*nail*) has been demonstrated to encourage epithelial to mesenchymal transformation *in vitro* and *in vivo*, principally by inhibiting the cell adhesion molecule E-cadherin (Cano *et al*., 2000; Savagner, 2001; Savagner *et al*., 2005; Moreno-Bueno *et al*., 2006). Thus free of cell-to-cell adhesion, induced cNCCs will be free to migrate relatively unhindered, compared to cNCCs expressing *slug* with normal activity. It should be interesting to discover whether cNCCs derived from stages 8 and 9 (HH) embryos which were not selectively evaluated for *slug* expression in this study also show a similar activity of this gene at the same or other ethanol levels.

The study of the effect of ethanol on cNCCs gene expression, even when a limited number of genes are considered, is intricate because of the multiple factors that are involved. Ahlgren *et al*. (2002) showed that ethanol down-regulated the expression of chick *Sonic Hedgehog* (*Shh*), a gene that is required for normal craniofacial development (Chiang *et al*., 1996; Helms *et al*., 1997; Ahlgren and Bronner-Fraser, 1999; Ahlgren *et al*., 2002; Jeong *et al*., 2004). The authors however also found that when *Shh* RNA transcripts were retrovirally transferred into chick head regions which were then exposed to ethanol, the *Shh* completely prevented cNCCs apoptosis, however at artificially elevated *Shh* levels.

Debelak and Smith (2000) observed that the genetic strain of chicks strongly influence whether the cNCCs of these animals die or not in response to a single dose of ethanol. In that regard, they categorised their chick strains into high, moderate and low responders

respectively (Debelak and Smith, 2000). It would be interesting to determine whether the *Potch koek koek* chick strain used in this study is a high, moderate or low ethanol responder, in the pattern similar to the animals described by Debelak and Smith (2000). One may propose that *Potch koek koek* birds are either moderate or low ethanol-responders, given the results of our *in vitro* assay for cNCCs ethanol-induced apoptosis in this chick strain, which showed non-significant differences between control and ethanol-treated cNCCs.

In a follow-up study to that of Debelak and Smith (2000), Su *et al*. (2001) examined whether the pattern of chick facial deficits following ethanol-induced apoptosis was also related to their genetic strain. Their results showed that although chick genetic strain determined the (high or low) patterns of cNCCs loss, ethanol's depletion of cNCCs did not necessarily result in decreased craniometric measurements or altered facial appearance in the ethanol-treated animals (Su *et al*., 2001). Finally, Kim and Shukla (2006), working on 8 week old rats showed that histone H3, a member of the family of proteins that render chromatin accessible to transcription factors, was significantly acetylated in some, but not all the rat tissues, which they tested. Interestingly the protein was not altered in the brain and heart – structures which receive significant neural crest cell contributions (Kim and Shukla, 2006). These results reinforce the point that the intellectual effort to characterise the genetic, cellular and molecular mechanisms that determine cNCCs loss or malfunction in response to exposure to ethanol is a work in progress.

4.7 Conclusion: overall effects of acute fetal ethanol exposure

We have demonstrated in this study that when C57 BL mice are treated with ethanol *in utero*, they suffer significantly in fetal viability and survival rate as well as show some defects in cranial skeleton and delayed ossification, but their body, head and facial measurements appear unaffected. Furthermore, chick cranial neural crest cells cultured in the presence of

ethanol become epithelial rather than spindle-shaped, and their surface morphology shows membrane blebbing; they also lose their ordered cytoskeleton, but appear to proliferate and migrate further distances than control cells when exposed to 0.3% and 0.4% (v/v) ethanol. Other observed differences in migration between treated and untreated cNCCs vary with the concentration of ethanol and the stage of development of the embryo from which the cNCCs were cultured. Specifically, stage 9 (HH) derived cNCCs migrate over significantly increased distances than controls after exposure to 0.3% and 0.4% ethanol, but the same cells migrate over significantly reduced distances following exposure to 0.2% ethanol. Ethanol exposure to cNCCs also results in significant proliferation of these cells at 24- and 48hrs, while the *slug* gene transcripts obtained from these cells show a 30-fold up-regulation. More work is needed to reconcile previous *in vivo* and the present *in vitro* results on the effects of ethanol on cNCCs apoptosis, and characterise the genetic and molecular mechanisms which underpin these interesting observations more precisely.

APPENDIX A

Spreadsheet showing an example of calculations used to validate Vertico-mental length (VM) and Mandibular length (MANL), using the Lin's coefficient of concordance method (Lin, 2001). Concordance values (in **bold** type) between 0.9 and 1.0 validate the accuracy of the measurements.

Serial no	ID	VM1	VM2	Y1-Y2	$(Y1-Y2)^2$
1	13Mar#A1L	5.678	5.68	-0.002	4E-06
2	13Mar#A1R	5.789	5.746	0.043	0.001849
3	13Mar#A2L	5.762	5.746	0.016	0.000256
4	13Mar#A2R	5.938	5.951	-0.013	0.000169
5	13Mar#A3L	5.962	5.951	0.011	0.000121
6	13Mar#A3R	6.108	5.986	0.122	0.014884
7	13Mar#A4R	5.803	5.797	0.006	3.6E-05
8	13Mar#A5R	5.633	5.643	-0.01	1E-04
9	13Mar#A6R	5.694	5.711	-0.017	0.000289
10	15Mar#A10	6.029	6.363	-0.334	0.111556
11	15Mar#A11	4.969	4.991	-0.022	0.000484
12	15Mar#A12	6.116	6.106	0.01	1E-04
13	15Mar#A13	5.456	5.454	0.002	4E-06
14	15Mar#A14	5.109	5.094	0.015	0.000225
15	15Mar#A15	5.89	5.9	-0.01	0.0001
16	15Mar#A4	5.794	5.797	-0.003	9E-06
17	15Mar#A5	5.803	5.644	0.159	0.025281
18	15Mar#A8	5.265	5.265	0	0
19	15Mar#C1	5.612	5.626	-0.014	0.000196
20	15Mar#C2	5.856	5.351	0.505	0.255025
21	15Mar#C3	6.412	6.432	-0.02	0.0004
22	16DEC#A1	5.941	5.941	0	0
23	16DEC#A2	6.239	6.249	-0.01	1E-04
24	16DEC#A3	6.066	5.9	0.166	0.027556
25	16DEC#A4	5.447	5.407	0.04	0.0016
26	16DEC#A5	6.16	6.131	0.029	0.000841
27	17NOV#A1	5.856	5.823	0.033	0.001089
28	17NOV#A10	5.527	5.491	0.036	0.001296
29	17NOVA12	6.43	6.439	-0.009	8.1E-05
30	17NOVA13	5.579	5.562	0.017	0.000289
31	17NOVA14	6.083	5.858	0.225	0.050625
32	17NOVA14a	5.874	6.036	-0.162	0.026244
33	17NOVA15	5.648	5.716	-0.068	0.004624
34	17NOVA16	5.915	5.906	0.009	8.1E-05
35	17NOVA17	6.03	6.024	0.006	3.6E-05
36	17NOVA18	5.527	5.289	0.238	0.056644
37	17NOVA19	5.942	5.929	0.013	0.000169
38	17NOV#A2	5.596	5.597	-0.001	1E-06
39	17NOVA20	5.716	5.716	0	0
40	17NOVA21	5.907	5.941	-0.034	0.001156
41	17NOVA22	5.438	5.396	0.042	0.001764
42	17NOVA24	5.693	5.657	0.036	0.001296
43	17NOVA25	6.03	6.012	0.018	0.000324
44	17NOVA26	6.411	6.131	0.28	0.0784
45	17NOV#A3	6.013	5.989	0.024	0.000576
46	17NOV#A5	5.7	5.704	-0.004	1.6E-05
47	17NOV#A6	5.728	5.74	-0.012	0.000144
48	17NOV#A7	5.63	5.407	0.223	0.049729
49	17NOV#A8	5.735	5.692	0.043	0.001849
50	17NOV#A9	5.37	5.751	-0.381	0.145161
51	17NOVC15	6.116	6.083	0.033	0.001089
52	17NOVCo1	5.977	5.965	0.012	0.000144
53	17NOVCo10	5.484	5.739	-0.255	0.065025
54	17NOVCo11	5.577	5.68	-0.103	0.010609
55	17NOVCo12	6.203	6.178	0.025	0.000625
56	17NOVCo13	5.125	5.087	0.038	0.001444
57	17NOVCo14	5.786	5.775	0.011	0.000121
58	17NOVCo2	6.099	5.87	0.229	0.052441
59	17NOVCo3	5.942	6.238	-0.296	0.087616
60	17NOVCo4	5.803	5.821	-0.018	0.000324

61	17NOVCo6	5.925	5.917	0.008	6.4E-05
62	17NOVCo7	5.786	5.775	0.011	0.000121
63	17NOVCo8	5.56	5.704	-0.144	0.020736
64	17NOVCo9	5.368	5.704	-0.336	0.112896
65	20MAY#A2	5.749	5.74	0.009	8.1E-05
66	20MAY#A3	5.794	5.787	0.007	4.9E-05
67	20MAY#A4	5.943	5.941	0.002	4E-06
68	20MAY#A5	6.03	6	0.03	0.0009
69	21MAYC1	6.203	6.202	0.001	1E-06
70	21MAYC10	6.151	6.154	-0.003	9E-06
71	21MAYC2	6.343	6.356	-0.013	0.000169
72	21MAYC5	6.368	6.368	0	0
73	21MAYC6	6.064	6.036	0.028	0.000784
74	21MAYC7	5.665	5.585	0.08	0.0064
75	21MAYC9	5.751	5.953	-0.202	0.040804
76	26AugRHDam4#2	4.83	4.974	-0.144	0.020736
77	26AugRHDam4#4	4.917	5.317	-0.4	0.16
78	30JUNEC1	5.96	5.917	0.043	0.001849
79	30JUNEC10	6.064	5.822	0.242	0.058564
80	30JUNEC11	5.786	5.728	0.058	0.003364
81	30JUNEC12	5.752	5.728	0.024	0.000576
82	30JUNEC13	6.325	6.309	0.016	0.000256
83	30JUNEC14	5.387	5.372	0.015	0.000225
84	30JUNEC2	5.56	5.538	0.022	0.000484
85	30JUNEC3	5.873	5.87	0.003	9E-06
86	30JUNEC4	5.751	5.775	-0.024	0.000576
87	30JUNEC5	5.838	5.467	0.371	0.137641
88	30JUNEC6	5.873	5.739	0.134	0.017956
89	30JUNEC7	5.821	5.929	-0.108	0.011664
90	30JUNEC8	5.751	5.704	0.047	0.002209
91	30JUNEC9	6.23	5.656	0.574	0.329476
92	31JUL#A1L	5.699	5.729	-0.03	0.0009
93	31JUL#A1R	6.186	6.192	-0.006	3.6E-05
94	31JUL#A3	6.134	6.119	0.015	0.000225
95	31JUL#C1R	5.56	5.466	0.094	0.008836
96	31JUL#C2L	5.786	5.68	0.106	0.011236
97	31JUL#C2R	5.664	5.811	-0.147	0.021609
98	31JUL#C3L	6.116	6.106	0.01	1E-04
99	31JUL#C4L	6.186	6.19	-0.004	1.6E-05
100	31JUL#C4R	5.768	5.775	-0.007	4.9E-05
101	31JUL#C5R	5.699	5.846	-0.147	0.021609
102	9SEP#A1L	5.293	5.289	0.004	1.6E-05
103	9SEP#A1R	5.365	5.36	0.005	2.5E-05
104	9SEP#A2L	5.436	5.396	0.04	0.0016
105	9SEP#A2R	5.561	5.526	0.035	0.001225
106	9SEP#A3R	5.613	5.574	0.039	0.001521
					2.079823
	Mean	5.797217	5.78518868	0.00014468	
	StDev	0.3195126	0.30770648		
	StDev2	0.1020883	0.09468328		
	Lin's coefficient	**0.9003588**			

Serial no	ID	MANL2	MANL1	Y1-Y2	(Y1-Y2)2
1	13Mar#A1L	2.605	2.986	-0.381	0.145161
2	13Mar#A2L	2.41	2.419	-0.009	8.1E-05
3	13Mar#A2R	1.289	1.304	-0.015	0.000225
4	13Mar#A3L	1.41	1.423	-0.013	0.000169
5	13Mar#A4R	2.164	2.229	-0.065	0.004225
6	13Mar#A5R	3.138	3.107	0.031	0.000961
7	13Mar#A6R	2.578	2.585	-0.007	4.9E-05
8	15Mar#A4	3.187	3.107	0.08	0.0064
9	15Mar#A5	2.991	3.226	-0.235	0.055225
10	15Mar#A8	3.475	3.51	-0.035	0.001225
11	15Mar#A11	3.378	3.368	0.01	0.0001
12	15Mar#A12	2.605	2.585	0.02	0.0004
13	15Mar#A13	3.093	3.486	-0.393	0.154449
14	15Mar#A14	3.822	3.581	0.241	0.058081
15	15Mar#A15	2.571	2.988	-0.417	0.173889
16	15Mar#C1	3.753	3.676	0.077	0.005929
17	15Mar#C2	3.232	3.724	-0.492	0.242064
18	15Mar#C3	2.745	2.941	-0.196	0.038416
19	26AugRHDam4#4	1.563	0.925	0.638	0.407044
20	26AugRHDam4#2	2.536	1.542	0.994	0.988036
21	31JUL#A1L	2.223	2.182	0.041	0.001681
22	31JUL#A1R	1.423	1.648	-0.225	0.050625
23	31JUL#C1R	2.189	2.597	-0.408	0.166464
24	31JUL#C2L	2.431	2.526	-0.095	0.009025
25	31JUL#C2R	2.536	1.98	0.556	0.309136
26	31JUL#C3L	2.223	2.336	-0.113	0.012769
27	31JUL#C4R	2.814	2.644	0.17	0.0289
28	31JUL#C5R	3.023	2.81	0.213	0.045369
	Mean	2.62167857	2.62267857	1E-06	2.906098
	StDev	0.67133317	0.76112145		
	StDev2	0.45068823	0.57930586		
	Lin's coefficient	**0.91182913**			

APPENDIX B

Mast head of the cover page of the publication arising from this thesis

ELSEVIER

Alcohol 42 (2008) 21–27

ALCOHOL

Acute ethanol administration causes malformations but does not affect cranial morphometry in neonatal mice

Olusegun Olufemi Oyedele*, Beverley Kramer

Embryonic Differentiation and Development Research Programme, School of Anatomical Sciences, Faculty of Health Sciences, University of the Witwatersrand, 7 York Road Parktown, Johannesburg, Gauteng, 2193 South Africa

Received 7 August 2006; received in revised form 21 August 2007; accepted 18 October 2007

APPENDIX C

Skeletal staining solutions (Menegola *et al*., 2001)

Acid staining solution (pH 2.8)
0.14% Alcian blue dissolved in 70% ethanol, 5 parts;
0.12% Alizarin red S dissolved in 96% ethanol, 1 part;
Glacial acetic acid, 8 parts, and 70% ethanol, 50 parts.

Basic staining solution
0.7% Potassium hydroxide dissolved in distilled water, 250 parts;
0.5% Alizarin red S dissolved in distilled water, 1 part.

Clearing solution
70% ethanol, 2 parts
Glycerin 2 parts
Benzyl alcohol, 1 part

Conservation solution
70% ethanol, 1 part
Glycerine, 1 part

APPENDIX D

Working solutions

Chick Ringer solution

NaCl 8.5g
KCl 0.42g
$CaCl_2$ 0.25g
1000ml distilled water

2.5% Fibronectin solution
25µl Fibronectin (Sigma)
975µl sterile distilled water

Phosphate Buffered Saline
To 800mldistlitted water add
NaCl 8.0g
KCl 0.2g
Na_2HPO_4 1.44g
KH_2PO_4 0.24g
Adjust pH to 7.4
Adjust volume to 1L with distilled water

APPENDIX E

PCNA (Proliferating Cell Nuclear Antigen) Kit, BioAssay™ (US Biologicals, Massachusetts)
Catalog Number: P3115-11G

Kit Components
P3115-11G1: Blocking Solution, 1x6ml
P3115-11G2: PCNA Mab (Biotin), 1x6ml
P3115-11G3: Streptavidin (HRP), 1x6ml
P3115-11G4: Substrate Buffer (20X), 1x2ml
P3115-11G5: DAB (20X), 1x2ml
P3115-11G6: 0.6% Hydrogen Peroxide (20X), 1x2ml
P3115-11G7: Hematoxylin, 1x6ml
P3115-11G8: Histomount™, 1x6ml
P3115-11G9: Control slides, 1x5 (1 stained, 4 unstained)

Protocol for staining culture cells and cells in suspension
Preparation of Cells:
1. Fix cells in 70% alcohol or acid-ethanol for 15-30 minutes at 4°C. Acetone or Methacarn fixatives also can be used.
2. If necessary, block for endogenous peroxidase activity with 3% hydrogen peroxide in methanol for 10 minutes.
3. Wash in 3 changes of PBS for 2 minutes each.

Staining Procedures:
1. Apply sufficient quantity of P3115-11G1, 2 drops or ~100ul to cover specimen. Incubate at room temperature for 10 minutes.
Drain or blot off the solution. DO NOT RINSE.
2. Add sufficient antibody P3115-11G2, 2 drops or ~100ul to cover specimen. Incubate at room temperature for 30-60 minutes.
Rinse with PBS (2 min, 3 times).
3. Add sufficient Streptavidin (HRP) P3115-11G3, 2 drops or ~100ul to cover specimen. Incubate at room temperature for 10 minutes. Rinse with PBS (2 min, 3 times).
4. Prepare DAB mixture as follows: add 1 drop or ~50ul each of P3115-11G4, P3115-11G5 and P3115-11G6 to 1ml of ddH2O. Mix well, protecting from light. Use with in 1 hour.
5. Add sufficient quantity, 2 drops or ~100ul of the DAB MIXTURE to cover specimen. Incubate for 2-5 minutes.
6. Counterstain with sufficient quantity, 2 drops or ~100ul of P3115-11G7 HEMATOXYLIN to cover specimen. Incubate for 1-2 minutes. Wash slides in tap water. Put slides into PBS until sections turn blue (approx. 30 seconds).
7. Rinse in distilled water.
8 Dehydrate slides in a graded series of alcohol, and clear with xylene.
9. Add 2 drops of P3115-11G8 Histomount™ and coverslip.

APPENDIX F

Examples of NanoDrop™ print-out of RNA samples

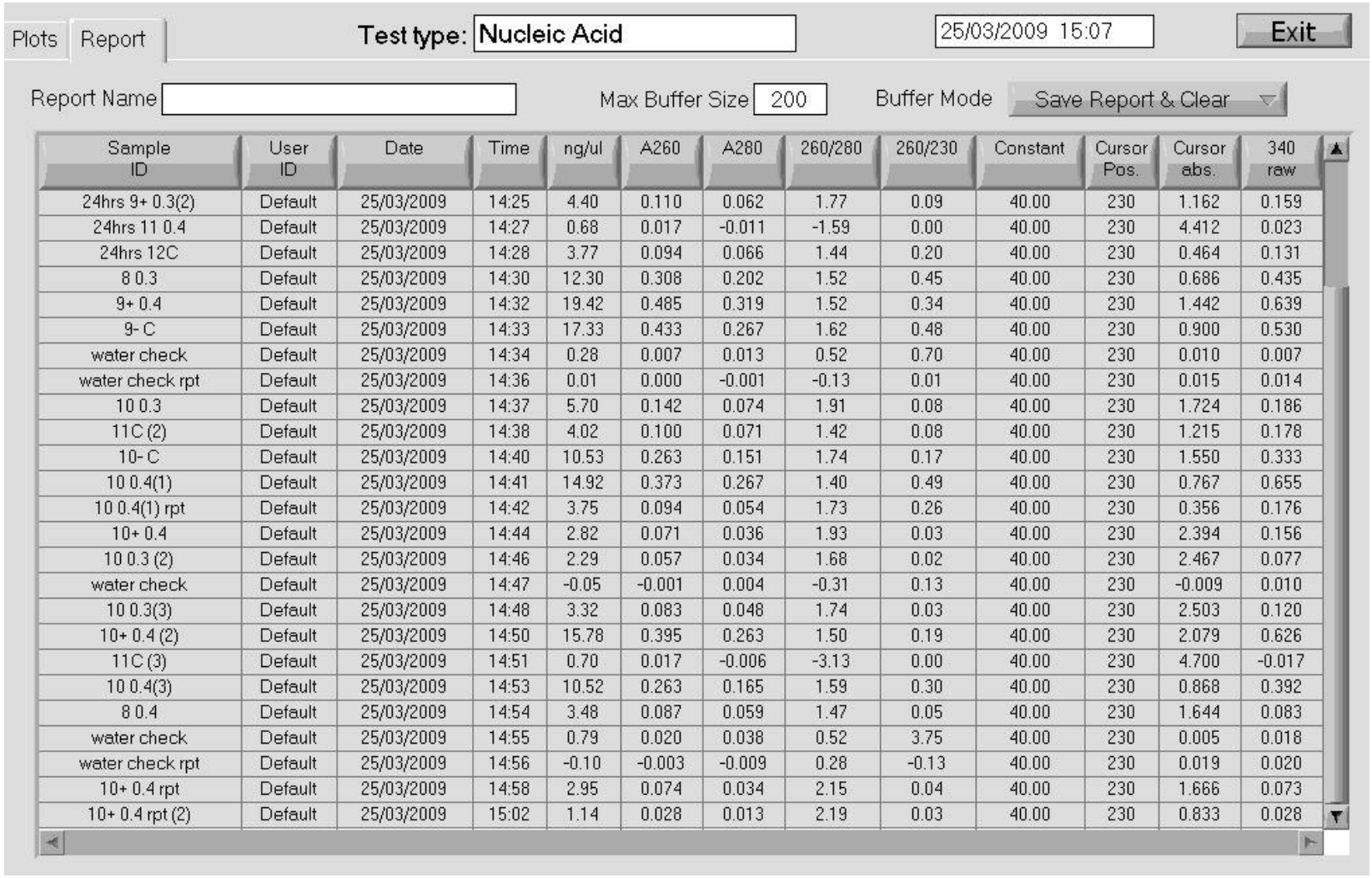

Plots | Report

Test type: Nucleic Acid

25/03/2009 15:07

Exit

Report Name

Max Buffer Size 200

Buffer Mode Save Report & Clear

Sample ID	User ID	Date	Time	ng/ul	A260	A280	260/280	260/230	Constant	Cursor Pos.	Cursor abs.	340 raw
24hrs 9+ 0.3(2)	Default	25/03/2009	14:25	4.40	0.110	0.062	1.77	0.09	40.00	230	1.162	0.159
24hrs 11 0.4	Default	25/03/2009	14:27	0.68	0.017	-0.011	-1.59	0.00	40.00	230	4.412	0.023
24hrs 12C	Default	25/03/2009	14:28	3.77	0.094	0.066	1.44	0.20	40.00	230	0.464	0.131
8 0.3	Default	25/03/2009	14:30	12.30	0.308	0.202	1.52	0.45	40.00	230	0.686	0.435
9+ 0.4	Default	25/03/2009	14:32	19.42	0.485	0.319	1.52	0.34	40.00	230	1.442	0.639
9- C	Default	25/03/2009	14:33	17.33	0.433	0.267	1.62	0.48	40.00	230	0.900	0.530
water check	Default	25/03/2009	14:34	0.28	0.007	0.013	0.52	0.70	40.00	230	0.010	0.007
water check rpt	Default	25/03/2009	14:36	0.01	0.000	-0.001	-0.13	0.01	40.00	230	0.015	0.014
10 0.3	Default	25/03/2009	14:37	5.70	0.142	0.074	1.91	0.08	40.00	230	1.724	0.186
11C (2)	Default	25/03/2009	14:38	4.02	0.100	0.071	1.42	0.08	40.00	230	1.215	0.178
10- C	Default	25/03/2009	14:40	10.53	0.263	0.151	1.74	0.17	40.00	230	1.550	0.333
10 0.4(1)	Default	25/03/2009	14:41	14.92	0.373	0.267	1.40	0.49	40.00	230	0.767	0.655
10 0.4(1) rpt	Default	25/03/2009	14:42	3.75	0.094	0.054	1.73	0.26	40.00	230	0.356	0.176
10+ 0.4	Default	25/03/2009	14:44	2.82	0.071	0.036	1.93	0.03	40.00	230	2.394	0.156
10 0.3 (2)	Default	25/03/2009	14:46	2.29	0.057	0.034	1.68	0.02	40.00	230	2.467	0.077
water check	Default	25/03/2009	14:47	-0.05	-0.001	0.004	-0.31	0.13	40.00	230	-0.009	0.010
10 0.3(3)	Default	25/03/2009	14:48	3.32	0.083	0.048	1.74	0.03	40.00	230	2.503	0.120
10+ 0.4 (2)	Default	25/03/2009	14:50	15.78	0.395	0.263	1.50	0.19	40.00	230	2.079	0.626
11C (3)	Default	25/03/2009	14:51	0.70	0.017	-0.006	-3.13	0.00	40.00	230	4.700	-0.017
10 0.4(3)	Default	25/03/2009	14:53	10.52	0.263	0.165	1.59	0.30	40.00	230	0.868	0.392
8 0.4	Default	25/03/2009	14:54	3.48	0.087	0.059	1.47	0.05	40.00	230	1.644	0.083
water check	Default	25/03/2009	14:55	0.79	0.020	0.038	0.52	3.75	40.00	230	0.005	0.018
water check rpt	Default	25/03/2009	14:56	-0.10	-0.003	-0.009	0.28	-0.13	40.00	230	0.019	0.020
10+ 0.4 rpt	Default	25/03/2009	14:58	2.95	0.074	0.034	2.15	0.04	40.00	230	1.666	0.073
10+ 0.4 rpt (2)	Default	25/03/2009	15:02	1.14	0.028	0.013	2.19	0.03	40.00	230	0.833	0.028

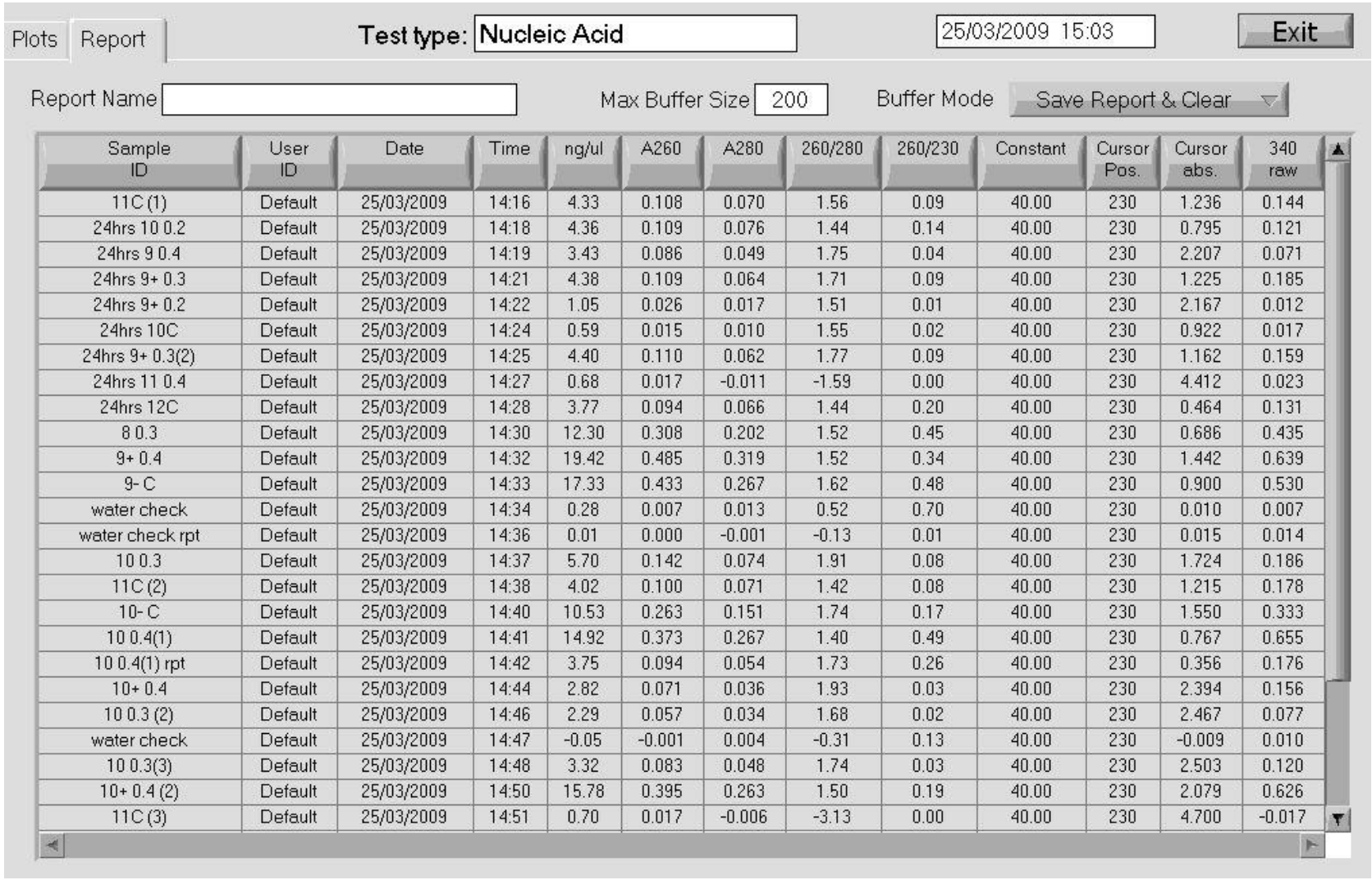
Plots Report

Test type: Nucleic Acid

25/03/2009 15:03

Exit

Report Name

Max Buffer Size 200

Buffer Mode Save Report & Clear

Sample ID	User ID	Date	Time	ng/ul	A260	A280	260/280	260/230	Constant	Cursor Pos.	Cursor abs.	340 raw
11C (1)	Default	25/03/2009	14:16	4.33	0.108	0.070	1.56	0.09	40.00	230	1.236	0.144
24hrs 10 0.2	Default	25/03/2009	14:18	4.36	0.109	0.076	1.44	0.14	40.00	230	0.795	0.121
24hrs 9 0.4	Default	25/03/2009	14:19	3.43	0.086	0.049	1.75	0.04	40.00	230	2.207	0.071
24hrs 9+ 0.3	Default	25/03/2009	14:21	4.38	0.109	0.064	1.71	0.09	40.00	230	1.225	0.185
24hrs 9+ 0.2	Default	25/03/2009	14:22	1.05	0.026	0.017	1.51	0.01	40.00	230	2.167	0.012
24hrs 10C	Default	25/03/2009	14:24	0.59	0.015	0.010	1.55	0.02	40.00	230	0.922	0.017
24hrs 9+ 0.3(2)	Default	25/03/2009	14:25	4.40	0.110	0.062	1.77	0.09	40.00	230	1.162	0.159
24hrs 11 0.4	Default	25/03/2009	14:27	0.68	0.017	-0.011	-1.59	0.00	40.00	230	4.412	0.023
24hrs 12C	Default	25/03/2009	14:28	3.77	0.094	0.066	1.44	0.20	40.00	230	0.464	0.131
8 0.3	Default	25/03/2009	14:30	12.30	0.308	0.202	1.52	0.45	40.00	230	0.686	0.435
9+ 0.4	Default	25/03/2009	14:32	19.42	0.485	0.319	1.52	0.34	40.00	230	1.442	0.639
9- C	Default	25/03/2009	14:33	17.33	0.433	0.267	1.62	0.48	40.00	230	0.900	0.530
water check	Default	25/03/2009	14:34	0.28	0.007	0.013	0.52	0.70	40.00	230	0.010	0.007
water check rpt	Default	25/03/2009	14:36	0.01	0.000	-0.001	-0.13	0.01	40.00	230	0.015	0.014
10 0.3	Default	25/03/2009	14:37	5.70	0.142	0.074	1.91	0.08	40.00	230	1.724	0.186
11C (2)	Default	25/03/2009	14:38	4.02	0.100	0.071	1.42	0.08	40.00	230	1.215	0.178
10- C	Default	25/03/2009	14:40	10.53	0.263	0.151	1.74	0.17	40.00	230	1.550	0.333
10 0.4(1)	Default	25/03/2009	14:41	14.92	0.373	0.267	1.40	0.49	40.00	230	0.767	0.655
10 0.4(1) rpt	Default	25/03/2009	14:42	3.75	0.094	0.054	1.73	0.26	40.00	230	0.356	0.176
10+ 0.4	Default	25/03/2009	14:44	2.82	0.071	0.036	1.93	0.03	40.00	230	2.394	0.156
10 0.3 (2)	Default	25/03/2009	14:46	2.29	0.057	0.034	1.68	0.02	40.00	230	2.467	0.077
water check	Default	25/03/2009	14:47	-0.05	-0.001	0.004	-0.31	0.13	40.00	230	-0.009	0.010
10 0.3(3)	Default	25/03/2009	14:48	3.32	0.083	0.048	1.74	0.03	40.00	230	2.503	0.120
10+ 0.4 (2)	Default	25/03/2009	14:50	15.78	0.395	0.263	1.50	0.19	40.00	230	2.079	0.626
11C (3)	Default	25/03/2009	14:51	0.70	0.017	-0.006	-3.13	0.00	40.00	230	4.700	-0.017

APPENDIX G

Oligonucleotide primer sequences

Gallus gallus GTP-binding protein (rhoB) mRNA

Primer Set 3

Forward Primer

Primer Sequence:	TCTTTGAGAACTACGTGGCCGACA		
Primer Start Position:	406	Primer Length:	24
Primer T_M:	59.8 ºC	Primer Self Any:	4.0
Primer GC %:	50.0 %	Primer Self End:	3.0
Primer End Stability:	6.36	Primer Penalty:	0.20

Reverse Primer

Primer Sequence:	TGTCCACTGAGAAGCACATGAGGA		
Primer Start Position:	555	Primer Length:	24
Primer T_M:	59.6 ºC	Primer Self Any:	4.0
Primer GC %:	50.0 %	Primer Self End:	3.0
Primer End Stability:	5.72	Primer Penalty:	0.40

Primer Pair/Product

Primer Pair Penalty:	0.60	Primer Pair Comp Any:	4.0
Primer Product Size:	150	Primer Pair Comp End:	0.0

Gallus sp. B-Actin mRNA

GallusBactinF: 5’- ACCCCAAAGCCAACAGA- 3’

GallusBactinR: 5’- CCAGAGTCCATCACAATACC- 3’

Gallus sp. GAPDH mRNA

GallusGAPDHF: 5’-GTTCTGTTCCCTTCTGTCTC- 3’

GallusGAPDHR: 5’-GTTTCTATCAGCCTCTCCCA-3’

Gallus sp. Slug mRNA

Primer Set 3

Forward Primer

Primer Sequence:	TCCTCCAAAGATCACAGCGGTTCA		
Primer Start Position:	294	Primer Length:	24
Primer T_M:	60.0 ºC	Primer Self Any:	4.0
Primer GC %:	50.0 %	Primer Self End:	1.0
Primer End Stability:	5.19	Primer Penalty:	0.04

Reverse Primer

Primer Sequence:	TGTGTTTGGCCAACCCAGAGAAAG		
Primer Start Position:	450	Primer Length:	24
Primer T_M:	59.6 ºC	Primer Self Any:	8.0
Primer GC %:	50.0 %	Primer Self End:	0.0
Primer End Stability:	4.58	Primer Penalty:	0.37

Primer Pair/Product

Primer Pair Penalty:	0.40	Primer Pair Comp Any:	5.0
Primer Product Size:	157	Primer Pair Comp End:	0.0

Gallus gallus ras-related C3 botulinum toxin substrate 1 (rho family, small GTP binding protein Rac1) (RAC1), mRNA

Primer Set 2

Forward Primer

Primer Sequence:	ACGAAGCTATCCGAGCAGTTCTGT		
Primer Start Position:	527	Primer Length:	24
Primer T_M:	59.7 ºC	Primer Self Any:	4.0
Primer GC %:	50.0 %	Primer Self End:	3.0
Primer End Stability:	5.47	Primer Penalty:	0.30

Reverse Primer

Primer Sequence:	TTCTGAGCAAAGCACAGGGTTTGG		
Primer Start Position:	641	Primer Length:	24
Primer T_M:	59.8 ºC	Primer Self Any:	5.0
Primer GC %:	50.0 %	Primer Self End:	3.0
Primer End Stability:	5.29	Primer Penalty:	0.17

Primer Pair/Product

Primer Pair Penalty:	0.47	Primer Pair Comp Any:	4.0
Primer Product Size:	115	Primer Pair Comp End:	0.0

APPENDIX H

Compact Disc containing time-lapse video recordings of the migration of cranial neural crest cells and the time-analysis of the migration.

REFERENCES

1. Abel EL (1995) An update on incidence of FAS: FAS is not an equal opportunity birth defect. Neurotoxicol Teratol 17:437-443.

2. Adams MS, Gammill LS, Bronner-Fraser M (2008) Discovery of transcription factors and other candidate regulators of neural crest development. Dev Dyn 237:1021-1033.

3. Agrawal A, Lynskey MT (2008) Are there genetic influences on addiction: evidence from family, adoption and twin studies. Addiction 103:1069-1081.

4. Ahlgren SC, Bronner-Fraser M (1999) Inhibition of sonic hedgehog signaling in vivo results in craniofacial neural crest cell death. Curr Biol 9:1304-1314.

5. Ahlgren SC, Thakur V, Bronner-Fraser M (2002) Sonic hedgehog rescues cranial neural crest from cell death induced by ethanol exposure. Proc Natl Acad Sci U S A 99:10476-10481.

6. Ahlgren S (2008) Cell Division, Differentiation, and Death in Avian Embryos, in *Avian Embryology,* Vol. 87, (Bronner-Fraser M ed), pp 153-165. Elsevier, New York, USA.

7. Arends MJ, Wyllie AH (1991) Apoptosis: mechanisms and roles in pathology. Int Rev Exp Pathol 32:223-254.

8. Astley SJ, Magnuson SI, Omnell LM, Clarren SK (1999) Fetal alcohol syndrome: changes in craniofacial form with age, cognition, and timing of ethanol exposure in the macaque. Teratology 59:163-172.

9. Baker CV, Bronner-Fraser M (1997) The origins of the neural crest. Part I: embryonic induction. Mech Dev 69:3-11.

10. Bar-Sagi D, Hall A (2000) Ras and Rho GTPases: a family reunion. Cell 103:227-238.

11. Basch ML, Bronner-Fraser M (2006) Neural crest inducing signals. Adv Exp Med Biol 589:24-31.

12. Becker HC, Diaz-Granados JL, Randall CL (1996) Teratogenic actions of ethanol in the mouse: a minireview. Pharmacol Biochem Behav 55:501-513.

13. Bettinger BT, Gilbert DM, Amberg DC (2003) Actin up in the nucleus. Biol 23:1358-1367.

14. Bishop AL, Hall A (2000) Rho GTPases and their effector proteins. Biochem J 348 Pt 2:241-255.

15. Blader P, Strahle U (1998) Ethanol impairs migration of the prechordal plate in the zebrafish embryo. Dev Biol 201:185-201.

16. Bolande RP (1974) The neurocristopathies: A unifying concept of disease arising in neural crest maldevelopment. Human Pathol 5:409-429.

17. Bonthius DJ, West JR (1990) Alcohol-induced neuronal loss in developing rats: Increased brain damage with binge exposure. Alcohol Clin Exp Res 14:107-118.

18. Bowman PD, Ennis SR, Rarey KE, Betz AL, Goldstein GW (1983) Brain microvessel endothelial cells in tissue culture: a model for study of blood-brain barrier permeability. Ann Neurol 14:396-402.

19. Bronner-Fraser M (1994) The FASEB jornal. FASEB J 8:699-706.

20. Bronner-Fraser M (1987) Perturbation of cranial neural crest migration by the HNK-1 antibody. Dev Biol 123:321-331.

21. Bronner-Fraser M (1986) Analysis of the early stages of trunk neural crest migration in avian embryos using monoclonal antibody HNK-1. Dev Biol 115:44-55.

22. Bronner-Fraser M (1985) Alterations in neural crest migration by a monoclonal antibody that affects cell adhesion. J Cell Biol 101:610-617.

23. Bronner-Fraser M, Sauka-Spengler T (2009) Neural Crest Induction and Evolution. Annu Rev Cell Dev Biol .

24. Brown NA (1990) Routine assessment of morphology and growth: scoring systems and measurements of size. in *Postimplantation Mammalian Embryos: A Practical Approach*, (Copp AJ, Cockroft DL eds), pp 93-108. Oxford University Press, New York.

25. Bryson PD (1996) Ethyl Alcohol, in *Comprehensive Review in Toxicology for Emergency Clinicians,* (Anonymous), pp 386-386. Taylor and Francis, Washington, D.C. USA.

26. Bustin SA (2002) Quantification of mRNA using real-time reverse transcription PCR (RT-PCR): trends and problems. J Mol Endocrinol 29:23-39.

27. Bustin SA, Benes V, Garson JA, Hellemans J, Huggett J, Kubista M, Mueller R, Nolan T, Pfaffl MW, Shipley GL, Vandesompele J, Wittwer CT (2009) The MIQE guidelines: minimum information for publication of quantitative real-time PCR experiments. Clin Chem 55:611-622.

28. Calhoun F, Warren K (2007) Fetal alcohol syndrome: historical perspectives. Neurosci Biobehav Rev 31:168-171.

29. Cano A, Pérez-Moreno MA, Rodrigo I, Locascio A, Blanco MJ, del Barrio MG, Portillo F, Nieto MA (2000) The transcription factor snail controls epithelial–mesenchymal transitions by repressing E-cadherin expression. Nat Cell Biol 2:76-83.

30. Carl TF, Dufton C, Hanken J, Klymkowsky MW (1999) Inhibition of neural crest migration in Xenopus using antisense slug RNA. Dev Biol 213:101-115.

31. Carlier MF, Laurent V, Santolini J, Melki R, Didry D, Xia GX, Hong Y, Chua NH, Pantaloni D (1997) Actin depolymerizing factor (ADF/cofilin) enhances the rate of filament turnover: implication in actin-based motility. J Cell Biol 136:1307-1322.

32. Cartwright MM, Smith SM (1995a) Increased cell death and reduced neural crest cell numbers in ethanol-exposed embryos: partial basis for the fetal alcohol syndrome phenotype. Alcohol Clin Exp Res 19:378-386.

33. Cartwright MM, Smith SM (1995b) Stage-dependent effects of ethanol on cranial neural crest cell development: partial basis for the phenotypic variations observed in fetal alcohol syndrome. Alcohol Clin Exp Res 19:1454-1462.

34. Cartwright MM, Tessmer LL, Smith SM (1998) Ethanol-induced neural crest apoptosis is coincident with their endogenous death, but is mechanistically distinct. Alcohol Clin Exp Res 22:142-149.

35. Cavieres MF, Smith SM (2000) Genetic and developmental modulation of cardiac deficits in prenatal alcohol exposure. Alcohol Clin Exp Res 24:102-109.

36. Chen SY, Sulik KK (2000) Iron-mediated free radical injury in ethanol-exposed mouse neural crest cells. J Pharmacol Exp Ther 294:134-140.

37. Chen SY, Sulik KK (1996) Free radicals and ethanol-induced cytotoxicity in neural crest cells. Alcohol Clin Exp Res 20:1071-1076.

38. Chernoff GF (1977) The fetal alcohol syndrome in mice: an animal model. Teratology 15:223-229.

39. Chhabra D, dos Remedios CD (2008) Actin: An Overview of Its Structure and Function, in *Actin-Binding Proteins and Disease,* Vol. 8, (Chhabra D, dos Remedios CD eds), pp 1-15. Springer Science+Business Media LLC, New York, USA.

40. Chiang C, Litingtung Y, Lee E, Young KE, Corden JL, Westphal H, Beachy PA (1996) Cyclopia and defective axial patterning in mice lacking Sonic hedgehog gene function. Nature 383:407-413.

41. Christiansen JH, Coles EG, Wilkinson DG (2000) Molecular control of neural crest formation, migration and differentiation. Curr Opin Cell Biol 12:719-724.

42. Clarren SK, Smith DW (1978) The fetal alcohol syndrome. N Engl J Med 298:1063-1067.

43. Colangelo W, Jones DG (1982) The fetal alcohol syndrome: a review and assessment of the syndrome and its neurological sequelae. Prog Neurobiol 19:271-314.

44. Connolly KM, Bogdanffy MS (1993) Evaluation of proliferating cell nuclear antigen (PCNA) as an endogenous marker of cell proliferation in rat liver: a dual-stain comparison with 5-bromo-2'-deoxyuridine. J Histochem Cytochem 41:1-6.

45. Cook CS, Nowotny AZ, Sulik KK (1987) Fetal alcohol syndrome. Eye malformations in a mouse model. Arch Ophthalmol 105:1576-1581.

46. Couly GF, Coltey PM, Le Douarin NM (1993) The triple origin of skull in higher vertebrates: a study in quail-chick chimeras. Development 117:409-429.

47. Croxford J, Viljoen D (1999) Alcohol consumption by pregnant women in the Western Cape. S Afr Med J 89:962-965.

48. Cudd TA (2005) Animal model systems for the study of alcohol teratology. Exp Biol Med (Maywood) 230:389-393.

49. Davis WL, Crawford LA, Cooper OJ, Farmer GR, Thomas DL, Freeman BL (1990) Ethanol induces the generation of reactive free radicals by neural crest cells in vitro. J Craniofac Genet Dev Biol 10:277-293.

50. Debelak KA, Smith SM (2000) Avian genetic background modulates the neural crest apoptosis induced by ethanol exposure. Alcohol Clin Exp Res 24:307-314.

51. Debelak-Kragtorp KA, Armant DR, Smith SM (2003) Ethanol-induced cephalic apoptosis requires phospholipase C-dependent intracellular calcium signaling. Alcohol Clin Exp Res 27:515-523.

52. Deltour L, Ang HL, Duester G (1996) Ethanol inhibition of retinoic acid synthesis as a potential mechanism for fetal alcohol syndrome. FASEB J 10:1050-1057.

53. Dick DM, Foroud T (2003) Candidate genes for alcohol dependence: a review of genetic evidence from human studies. Alcohol Clin Exp Res 27:868-879.

54. Dickinson ME, Selleck MA, McMahon AP, Bronner-Fraser M (1995) Dorsalization of the neural tube by the non-neural ectoderm. Development 121:2099-2106.

55. Dietrich DR (1993) Toxicological and pathological applications of proliferating cell nuclear antigen (PCNA), a novel endogenous marker for cell proliferation. Crit Rev Toxicol 23:77-109.

56. do Vale A, Costa-Ramos C, Silva DS, Macedo PM, Fernandes R, Sampaio P, Dos Santos NM, Silva MT (2007) Cytochemical and ultrastructural study of anoikis and secondary necrosis in enterocytes detached in vivo. Apoptosis 12:1069-1083.

57. Downing C, Balderrama-Durbin C, Broncucia H, Gilliam D, Johnson TE (2009a) Ethanol teratogenesis in five inbred strains of mice. Alcohol Clin Exp Res 33:1238-1245.

58. Downing C, Balderrama-Durbin C, Hayes J, Johnson TE, Gilliam D (2009b) No effect of prenatal alcohol exposure on activity in three inbred strains of mice. Alcohol Alcohol 44:25-33.

59. Downing C, Gilliam D (1999) Cytoplasmic factors do not contribute to a maternal effect on ethanol teratogenesis. Behav Genet 29:31-39.

60. Driscoll CD, Streissguth AP, Riley EP (1990) Prenatal alcohol exposure: comparability of effects in humans and animal models. Neurotoxicol Teratol 12:231-237.

61. Duband JL (2006) Neural crest delamination and migration: integrating regulations of cell interactions, locomotion, survival and fate. Adv Exp Med Biol 589:45-77.

62. Duester G (1998) Alcohol dehydrogenase as a critical mediator of retinoic acid synthesis from vitamin A in the mouse embryo. J Nutr 128:459S-462S.

63. Duester G (1991) A hypothetical mechanism for fetal alcohol syndrome involving ethanol inhibition of retinoic acid synthesis at the alcohol dehydrogenase step. Alcohol Clin Exp Res 15:568-572.

64. Dunty WC,Jr., Chen SY, Zucker RM, Dehart DB, Sulik KK (2001) Selective vulnerability of embryonic cell populations to ethanol-induced apoptosis: implications for alcohol-related birth defects and neurodevelopmental disorder. Alcohol Clin Exp Res 25:1523-1535.

65. Dunty WC,Jr., Zucker RM, Sulik KK (2002) Hindbrain and cranial nerve dysmorphogenesis result from acute maternal ethanol administration. Dev Neurosci 24:328-342.

66. Dupin E, Sextier-Sainte-Claire Deville F, Nataf V, Le Douarin NM (1993) The ontogeny of the neural crest. C R Acad Sci III, Sci Vie 316:1062-1081.

67. Edwards DC, Sanders LC, Bokoch GM, Gill GN (1999) Activation of LIM-kinase by Pak1 couples Rac/Cdc42 GTPase signalling to actin cytoskeletal dynamics. Nat Cell Biol 1:253-259.

68. Edwards HG, Dow-Edwards DL (1991) Craniofacial alterations in adult rats prenatally exposed to ethanol. Teratology 44:373-378.

69. Erickson CA, Loring JF, Lester SM (1989) Migratory pathways of HNK-1-immunoreactive neural crest cells in the rat embryo. Dev Biol 134:112-118.

70. Etienne-Manneville S, Hall A (2002) Rho GTPases in cell biology. Nature 420:629-635.

71. Evangelista M, Blundell K, Longtine MS, Chow CJ, Adames N, Pringle JR, Peter M, Boone C (1997) Bni1p, a yeast formin linking cdc42p and the actin cytoskeleton during polarized morphogenesis. Science 276:118-122.

72. Fleige S, Pfaffl MW (2006) RNA integrity and the effect on the real-time qRT-PCR performance. Mol Aspects Med 27:126-139.

73. Franke WW (2004) Actin's many actions start at the genes. Nat Cell Biol 6:1013-1014.

74. Fukui Y (1978) Intranuclear actin bundles induced by dimethyl sulfoxide in interphase nucleus of Dictyostelium. J Cell Biol 76:146.

75. Fukui Y, Katsumaru H (1979) Nuclear actin bundles in Amoeba, Dictyostelium and human HeLa cells induced by dimethyl sulfoxide. Exp Cell Res 120:451.

76. Gage JC, Sulik KK (1991) Pathogenesis of ethanol-induced hydronephrosis and hydroureter as demonstrated following in vivo exposure of mouse embryos. Teratology 44:299-312.

77. Gans C, Northcutt RG (1983) Neural Crest and the Origin of Vertebrates: A New Head. Science 220:268-273.

78. Garcia-Castro MI, Marcelle C, Bronner-Fraser M (2002) Ectodermal Wnt function as a neural crest inducer. Science 297:848-851.

79. Garic-Stankovic A, Hernandez M, Flentke GR, Smith SM (2006) Structural constraints for alcohol-stimulated Ca2+ release in neural crest, and dual agonist/antagonist properties of n-octanol. Alcohol Clin Exp Res 30:552-559.

80. Garic-Stankovic A, Hernandez MR, Chiang PJ, Debelak-Kragtorp KA, Flentke GR, Armant DR, Smith SM (2005a) Ethanol triggers neural crest apoptosis through the selective activation of a pertussis toxin-sensitive G protein and a phospholipase Cbeta-dependent Ca2+ transient. Alcohol Clin Exp Res 29:1237-1246.

81. Garic-Stankovic A, Hernandez MR, Chiang PJ, Debelak-Kragtorp KA, Flentke GR, Armant DR, Smith SM (2005b) Ethanol triggers neural crest apoptosis through the selective activation of a pertussis toxin-sensitive G protein and a phospholipase Cbeta-dependent Ca2+ transient. Alcohol Clin Exp Res 29:1237-1246.

82. Giglio MJ, Vieiro M, Friedman S, Bozzini CE (1987) Effect of prenatal ethanol exposure on the growth of rat mandible skeletal units. J Biol Buccale 15:211-216.

83. Giles S, Boehm P, Brogan C, Bannigan J (2008) The effects of ethanol on CNS development in the chick embryo. Reprod Toxicol 25:224-230.

84. Gonsior SM, Platz S, Buchmeier S, Scheer U, Jockusch BM, Hinssen H (1999) Conformational difference between nuclear and cytoplasmic actin as detected by a monoclonal antibody. J Cell Sci 112:797.

85. Goodlett CR, Horn KH, Zhou FC (2005) Alcohol teratogenesis: mechanisms of damage and strategies for intervention. Exp Biol Med (Maywood) 230:394-406.

86. Graham A, Heyman I, Lumsden A (1993) Even-numbered rhombomeres control the apoptotic elimination of neural crest cells from odd-numbered rhombomeres in the chick hindbrain. Development 119:233-245.

87. Graham A, Koentges G, Lumsden A (1996) Neural crest apoptosis and the establishment of craniofacial pattern: an honorable death. Mol Cell Neurosci 8:76-83.

88. Gray EG, Whittaker VP (1962) The isolation of nerve endings from brain: an electron-microscopic study of cell fragments derived by homogenization and centrifugation. J Anat 96:79-88.

89. Gurniak CB, Perlas E, Witke W (2005) The actin depolymerizing factor n-cofilin is essential for neural tube morphogenesis and neural crest cell migration. Dev Biol 278:231-241.

90. Hall A (1998) Rho GTPases and the actin cytoskeleton. Science 279:509-514.

91. Hall A, Nobes CD (2000) Rho GTPases: molecular switches that control the organization and dynamics of the actin cytoskeleton. Philos Trans R Soc Lond B Biol Sci 355:965-970.

92. Hall A, Nobes CD (1992) Rho GTPases: molecular switches that control the organization and dynamics of the actin cytoskeleton. Philosophical Transactions of the Royal Society B 355:965-970.

93. Hamburger V, Hamilton HL (1992) A series of normal stages in the development of the chick embryo. 1951. Dev Dyn 195:231-272.

94. Hassler JA, Moran DJ (1986a) The effects of ethanol on embryonic actin: a possible role in teratogenesis. Experientia 42:575-577.

95. Hassler JA, Moran DJ (1986b) Effects of ethanol on the cytoskeleton of migrating and differentiating neural crest cells: possible role in teratogenesis. J Craniofac Genet Dev Biol Suppl 2:129-136.

96. Helms JA, Kim CH, Hu D, Minkoff R, Thaller C, Eichele G (1997) Sonic hedgehog participates in craniofacial morphogenesis and is down-regulated by teratogenic doses of retinoic acid. Dev Biol 187:25-35.

97. Hengartner MO (2001) Apoptosis Corralling the Corpses. Cell 104:325-328.

98. Hernandez-Guerrero JC, Ledesma-Montes C, Loyola-Rodriguez JP (1998) Effects of maternal ethanol intake on second alcoholic generation murine skull and mandibular size. Arch Med Res 29:297-302.

99. Hoffman LM, Kulyk WM (1999) Alcohol promotes in vitro chondrogenesis in embryonic facial mesenchyme. Int J Dev Biol 43:167-174.

100. Hofmann WA, Arduini A, Nicol SM, Camacho CJ, Lessard JL, Fuller-Pace FV, de Lanerolle P (2009) SUMOylation of nuclear actin. J Cell Biol 186:193.

101. Hofmann WA, de Lanerolle P (2006) Nuclear actin: to polymerize or not to polymerize. J Cell Biol 172:495.

102. Horan R, Lavelle M. Basic Mathematics: Introduction to Vectors. December 21, 2004, 2004. Accessed January 14, 2009.

103. Horstadius S (1950)

The Neural Crest: its Properties and Derivatives in the Light of Experimental Research. Oxford University Press, London.

104. Hoyme HE, May PA, Kalberg WO, Kodituwakku P, Gossage JP, Trujillo PM, Buckley DG, Miller JH, Aragon AS, Khaole N, Viljoen DL, Jones KL, Robinson LK (2005) A practical clinical approach to diagnosis of fetal alcohol spectrum disorders: clarification of the 1996 institute of medicine criteria. Pediatrics 115:39-47.

105. Iida K, Iida H, Yahara I (1986) Heat shock induction of intranuclear actin rods in cultured mammalian cells. Exp Cell Res 165:207.

106. Jeong J, Mao J, Tenzen T, Kottmann AH, McMahon AP (2004) Hedgehog signaling in the neural crest cells regulates the patterning and growth of facial primordia. Genes Dev 18:937-951.

107. Jockusch BM, Schoenenberger CA, Stetefeld J, Aebi U (2006) Tracking down the different forms of nuclear actin. Trends Cell Biol 16:391-396.

108. Johnston MC, Bronsky PT (1991) Animal models for human craniofacial malformations. J Craniofac Genet Dev Biol 11:277-291.

109. Jones KL (1986) Fetal alcohol syndrome. Pediatr Rev 8:122-126.

110. Jones KL, Hoyme HE, Robinson LK, del Campo M, Manning MA, Bakhireva LN, Prewitt LM, Chambers CD (2009) Developmental pathogenesis of short palpebral fissure length in children with fetal alcohol syndrome. Birth defects research 85:695-699.

111. Jones KL, Smith DW (1973) Recognition of the fetal alcohol syndrome in early infancy. Lancet 302:999-1001.

112. Jones KL, Smith DW, Hanson JW (1976) The fetal alcohol syndrome: clinical delineation. Ann N Y Acad Sci 273:130-139.

113. Jones MW, Bass WT (2003) Fetal alcohol syndrome. Neonatal Netw 22:63-70.

114. Kaufman MH (1990) Morphological stages of postimplantation embryonic development, in *Postimplantation Mammalian Embryos: A Practical Approach*, (Copp AJ, Cockroft DL eds), pp 81-91. Oxford University Press, New York.

115. Kim JS, Shukla SD (2006) Acute in vivo effect of ethanol (binge drinking) on histone H3 modifications in rat tissues. Alcohol Alcohol 41:126-132.

116. Kost TA, Theodorakis N, Hughes SH (1983) The nucleotide sequence of the chick cytoplasmic beta-actin gene. Nucleic Acids Res 11:8287-8301.

117. Kotch LE, Sulik KK (1992a) Experimental fetal alcohol syndrome: proposed pathogenic basis for a variety of associated facial and brain anomalies. Am J Med Genet 44:168-176.

118. Kotch LE, Sulik KK (1992b) Patterns of ethanol-induced cell death in the developing nervous system of mice; neural fold states through the time of anterior neural tube closure. Int J Dev Neurosci 10:273-279.

119. Kubben FJ, Peeters-Haesevoets A, Engels LG, Baeten CG, Schutte B, Arends JW, Stockbrugger RW, Blijham GH (1994) Proliferating cell nuclear antigen (PCNA): a new marker to study human colonic cell proliferation. Gut 35:530-535.

120. Kurki P, Ogata K, Tan EM (1988) Monoclonal antibodies to proliferating cell nuclear antigen (PCNA)/cyclin as probes for proliferating cells by immunofluorescence microscopy and flow cytometry. J Immunol Methods 109:49-59.

121. Kushnaryov VM, Sedmak JJ, Markwald RR, Faculjak ML, Loo PM (1990) Actin and lamin comprised filaments in the nuclei of Chinese hamster ovary cells affected with Clostridium difficile enterotoxin A. Cytobios 64:181.

122. LaBonne C, Bronner-Fraser M (1999) Molecular mechanisms of neural crest formation. Annu Rev Cell Dev Biol 15:81-112.

123. LaBonne C, Bronner-Fraser M (2000) Snail-related transcriptional repressors are required in Xenopus for both the induction of the neural crest and its subsequent migration. Dev Biol 221:195-205.

124. LaBonne C, Bronner-Fraser M (1998) Neural crest induction in Xenopus: evidence for a two-signal model. Development 125:2403-2414.

125. Le Douarin NM (2004) The avian embryo as a model to study the development of the neural crest: a long and still ongoing story. Mech Dev 121:1089-1102.

126. Le Douarin NM (1986) Cell line segregation during peripheral nervous system ontogeny. Science (New York, N Y 231:1515-1522.

127. Le Douarin, N. M. Kalchiem, C. (1999) *The Neural Crest.* 2nd ed. Cambridge University Press, Cambridge, UK.

128. Lee VM, Lwigale PY (2008) Neural Crest, Sensory Neuron, and Muscle Cultures, in *Methods in Cell Biology,* Vol. 87, (Bronner-Fraser M ed), pp 115-133. Elsevier, New York, USA.

129. Lemoine P, Harousseau H, Borteyru JP, Menuet JC (2003) Children of alcoholic parents--observed anomalies: discussion of 127 cases. Ther Drug Monit 25:132-136.

130. Leung AY, Leung JC, Chan LY, Ma ES, Kwan TT, Lai KN, Meng A, Liang R (2005) Proliferating cell nuclear antigen (PCNA) as a proliferative marker during embryonic and adult zebrafish hematopoiesis. Histochem Cell Biol 124:105-111.

131. Liem KF,Jr, Tremml G, Roelink H, Jessell TM (1995) Dorsal differentiation of neural plate cells induced by BMP-mediated signals from epidermal ectoderm. Cell 82:969-979.

132. Lin LI (1989) A concordance correlation coefficient to evaluate reproducibility. Biometrics 45:255-268.

133. Lombard Z, Tiffin N, Hofmann O, Bajic VB, Hide W, Ramsay M (2007) Computational selection and prioritization of candidate genes for fetal alcohol syndrome. BMC Genomics 8:389.

134. Loucks EJ, Ahlgren SC (2009) Deciphering the role of Shh signaling in axial defects produced by ethanol exposure. Birth Defects Res A Clin Mol Teratol 85:556-567.

135. Lumsden A, Sprawson N, Graham A (1991) Segmental origin and migration of neural crest cells in the hindbrain region of the chick embryo. Development 113:1281.

136. Lund LM, Machado VM, McQuarrie IG (2002) Increased [beta]-Actin and Tubulin Polymerization in Regrowing Axons: Relationship to the Conditioning Lesion Effect. Exp Neurol 178:306-312.

137. Luo T, Lee YH, Saint-Jeannet JP, Sargent TD (2003) Induction of neural crest in Xenopus by transcription factor AP2alpha. Proc Natl Acad Sci U S A 100:532-537.

138. Maekawa M, Ishizaki T, Boku S, Watanabe N, Fujita A, Iwamatsu A, Obinata T, Ohashi K, Mizuno K, Narumiya S (1999) Signaling from Rho to the actin cytoskeleton through protein kinases ROCK and LIM-kinase. Science 285:895-898.

139. Maloney MT, Kinley AW, Pak , Bamburg JR (2008) ADF/Cofilin, Actin Dynamics, and Disease, in *Protein Reviews,* (Atassi MZ ed), pp 83-185. Springer Science+Business Media, LLC, New York, USA.

140. Mancilla A, Mayor R (1996a) Neural crest formation in Xenopus laevis: mechanisms of Xslug induction. Dev Biol 177:580-589.

141. Mancilla A, Mayor R (1996b) Neural crest formation in Xenopus laevis: mechanisms of Xslug induction. Dev Biol 177:580-589.

142. Matsuo T, Osumi-Yamashita N, Noji S, Ohuchi H, Koyama E, Myokai F, Matsuo N, Taniguchi S, Doi H, Iseki S (1993) A mutation in the Pax-6 gene in rat small eye is associated with impaired migration of midbrain crest cells. Nat Genet 3:299-304.

143. Matthews PC (1998) Vectors and scalars, in *Springer Undergraduate Mathematics Series: Vector Calculus,* (Anonymous), pp 1-4. Springer-Veriag, London, UK.

144. Mattson SN, Riley EP, Gramling L, Delis DC, Jones KL (1998) Neuropsychological comparison of alcohol-exposed children with or without physical features of fetal alcohol syndrome. Neuropsychology 12:146-153.

145. Mattson SN, Riley EP, Gramling L, Delis DC, Jones KL (1997) Heavy prenatal alcohol exposure with or without physical features of fetal alcohol syndrome leads to IQ deficits. J Pediatr 131:718-721.

146. May PA, Brooke L, Gossage JP, Croxford J, Adnams C, Jones KL, Robinson L, Viljoen D (2000) Epidemiology of fetal alcohol syndrome in a South African community in the Western Cape Province. Am J Public Health 90:1905-1912.

147. May PA, Gossage JP, Brooke LE, Snell CL, Marais AS, Hendricks LS, Croxford JA, Viljoen DL (2005) Maternal risk factors for fetal alcohol syndrome in the Western cape province of South Africa: a population-based study. Am J Public Health 95:1190-1199.

148. May PA, Gossage JP, Marais AS, Adnams CM, Hoyme HE, Jones KL, Robinson LK, Khaole NC, Snell C, Kalberg WO, Hendricks L, Brooke L, Stellavato C, Viljoen DL (2007) The epidemiology of fetal alcohol syndrome and partial FAS in a South African community. Drug Alcohol Depend 88:259-271.

149. Mayor R, Aybar MJ (2001a) Induction and development of neural crest in Xenopus laevis. Cell Tissue Res 305:203-209.

150. Mayor R, Aybar MJ (2001b) Induction and development of neural crest in Xenopus laevis. Cell Tissue Res 305:203-209.

151. Mayor R, Morgan R, Sargent MG (1995) Induction of the prospective neural crest of Xenopus. Development 121:767-777.

152. McBride WJ, Li TK (1998) Animal models of alcoholism: neurobiology of high alcohol-drinking behavior in rodents. Crit Rev Neurobiol 12:339-369.

153. McCabe KL, Bronner-Fraser M (2009) Molecular and tissue interactions governing induction of cranial ectodermal placodes. Dev Biol 332:189-195.

154. McCauley DW, Bronner-Fraser M (2006) Importance of SoxE in neural crest development and the evolution of the pharynx. Nature 441:750-752.

155. Menegola E, Broccia ML, Giavini E (2001) Atlas of rat fetal skeleton double stained for bone and cartilage. Teratology 64:125-133.

156. Messing RO, Carpenter CL, Diamond I, Greenberg DA (1986) Ethanol regulates calcium channels in clonal neural cells. Proc Natl Acad Sci U S A 83:6213-6215.

157. Miller MW (1996) Mechanisms of ethanol induced neuronal death during development: from the molecule to behavior. Alcohol Clin Exp Res 20:128-132.

158. Mooney SM, Miller MW (2001) Episodic exposure to ethanol during development differentially affects brainstem nuclei in the macaque. J Neurocytol 30:973-982.

159. Moreno-Bueno G, Cubillo E, Sarrió D, Peinado H, Rodríguez-Pinilla SM, Villa S, Bolós V, Jordá M, Fabra A, Portillo F (2006) Genetic profiling of epithelial cells expressing E-cadherin repressors reveals a distinct role for Snail, Slug, and E47 factors in epithelial-mesenchymal transition. Cancer Res 66:9543.

160. Morris-Kay G, Tan SS (1987) Mapping cranial neural crest cell migration pathways in mammalian embryos. Trends in Genetics 3:257-261.

161. Nakajima-Iijima S, Hamada H, Reddy P, Kakunaga T (1985) Molecular structure of the human cytoplasmic beta-actin gene: interspecies homology of sequences in the introns. Proc Natl Acad Sci U S A 82:6133-6137.

162. Nakatsuji N (1983) Craniofacial malformation in Xenopus laevis tadpoles caused by the exposure of early embryos to ethanol. Teratology 28:299-305.

163. Nikitina N, Sauka-Spengler T, Bronner-Fraser M (2009) Chapter 1. Gene regulatory networks in neural crest development and evolution. Curr Top Dev Biol 86:1-14.

164. Nobes CD, Hall A (1999) Rho GTPases Control Polarity, Protrusion, and Adhesion during Cell Movement. The Journal of cell biology 144:1235-1244.

165. Ouko LA, Shantikumar K, Knezovich J, Haycock P, Schnugh DJ, Ramsay M (2009) Effect of alcohol consumption on CpG methylation in the differentially methylated regions of H19 and IG-DMR in male gametes: implications for fetal alcohol spectrum disorders. Alcohol Clin Exp Res 33:1615-1627.

166. Oyedele OO, Kramer B (2008) Acute ethanol administration causes malformations but does not affect cranial morphometry in neonatal mice. Alcohol (Fayetteville, N Y 42:21-27.

167. Palmgren S, Vartiainen M, Lappalainen P (2002) Twinfilin, a molecular mailman for actin monomers. J Cell Sci 115:881-886.

168. Pederson T (2008) As functional nuclear actin comes into view, is it globular, filamentous, or both? J Cell Biol 180:1061.

169. Pederson T, Aebi U (2002) Actin in the nucleus: what form and what for? J Struct Biol 140:3-9.

170. Peltomaki T, Alvesalo L, Isotupa K (1989) Shape of the craniofacial complex in 45,X females: cephalometric study. J Craniofac Genet Dev Biol 9:331-338.

171. Peng Y, Yang PH, Guo Y, Ng SS, Liu J, Fung PC, Tay D, Ge J, He ML, Kung HF, Lin MC (2004a) Catalase and peroxiredoxin 5 protect Xenopus embryos against alcohol-induced ocular anomalies. Invest Ophthalmol Vis Sci 45:23-29.

172. Peng Y, Yang PH, Ng SS, Wong OG, Liu J, He ML, Kung HF, Lin MC (2004b) A critical role of Pax6 in alcohol-induced fetal microcephaly. Neurobiol Dis 16:370-376.

173. Pollard TD, Borisy GG (2003) Cellular motility driven by assembly and disassembly of actin filaments. Cell 112:453-465.

174. Raftopoulou M, Hall A (2004) Cell migration: Rho GTPases lead the way. Dev Biol 265:23-32.

175. Randall CL, Taylor WJ (1979) Prenatal ethanol exposure in mice: teratogenic effects. Teratology 19:305-311.

176. Rando OJ, Zhao K, Crabtree GR (2000) Searching for a function for nuclear actin. Trends Cell Biol 10:92-97.

177. Rickmann M, Fawcett JW, Keynes RJ (1985) The migration of neural crest cells and the growth of motor axons through the rostral half of the chick somite. J Embryol Exp Morphol 90:437-455.

178. Ridley AJ, Schwartz MA, Burridge K, Firtel RA, Ginsberg MH, Borisy G, Parsons JT, Horwitz AR (2003) Cell migration: integrating signals from front to back. Science 302:1704.

179. Rovasio RA, Battiato NL (2002) Ethanol induces morphological and dynamic changes on in vivo and in vitro neural crest cells. Alcohol Clin Exp Res 26:1286-1298.

180. Rovasio RA, Battiato NL (1995) Role of early migratory neural crest cells in developmental anomalies induced by ethanol. Int J Dev Biol 39:421-422.

181. Rydell-Tormanen K, Uller L, Erjefalt JS (2006) Direct evidence of secondary necrosis of neutrophils during intense lung inflammation. Eur Respir J 28:268-274.

182. Sadaghiani B, Vielkind JR (1990) Distribution and migration pathways of HNK-1-immunoreactive neural crest cells in teleost fish embryos. Development 110:197-209.

183. Sanders JL (2009) Were our forebears aware of prenatal alcohol exposure and its effects? A review of the history of fetal alcohol spectrum disorder. Can J Clin Pharmacol 16:e288-95.

184. Sanger JW, Sanger JM, Kreis TE, Jockusch BM (1980) Reversible translocation of cytoplasmic actin into the nucleus caused by dimethyl sulfoxide. Proceedings of the National Academy of Sciences 77:5268.

185. Sant'Anna LB, Tosello DO (2006) Fetal alcohol syndrome and developing craniofacial and dental structures--a review. Orthodontics & craniofacial research 9:172-185.

186. Savagner P (2001) Leaving the neighborhood: molecular mechanisms involved during epithelial-mesenchymal transition. Bioessays 23:912-923.

187. Savagner P, Kusewitt DF, Carver EA, Magnino F, Choi C, Gridley T, Hudson LG (2005) Developmental transcription factor slug is required for effective re-epithelialization by adult keratinocytes. J Cell Physiol 202:858-866.

188. Schoenenberger CA, Buchmeier S, Boerries M, SÃ¼tterlin R, Aebi U, Jockusch BM (2005) Conformation-specific antibodies reveal distinct actin structures in the nucleus and the cytoplasm. J Struct Biol 152:157-168.

189. Schwetz BA, Smith FA, Staples RE (1978) Teratogenic potential of ethanol in mice, rats and rabbits. Teratology 18:385-392.

190. Sefton M, Sanchez S, Nieto MA (1998) Conserved and divergent roles for members of the Snail family of transcription factors in the chick and mouse embryo. Development 125:3111-3121.

191. Serbedzija GN, Bronner-Fraser M, Fraser SE (1992) Vital dye analysis of cranial neural crest cell migration in the mouse embryo. Development 116:297-307.

192. Shestakova EA, Singer RH, Condeelis J (2001) The physiological significance of β-actin mRNA localization in determining cell polarity and directional motility. Proc Natl Acad Sci U S A 98:7045.

193. Sieber-Blum M, Zhang JM (1997) Growth factor action in neural crest cell diversification. J Anat 191 (Pt 4):493-499.

194. Silva MT, do Vale A, dos Santos NM (2008) Secondary necrosis in multicellular animals: an outcome of apoptosis with pathogenic implications. Apoptosis 13:463-482.

195. Smith SM (2008) The avian embryo in fetal alcohol research. Methods Mol Biol 447:75-84.

196. Smith SM (1997) Alcohol-induced cell death in the embryo. Alcohol Health Res World 21:287-297.

197. Smith SM, Debelak-Kragtorp KA (2005) Neural crest and alcohol exposure, in *The Developing Brain: Lessons Learned from Alcohol and Nicotine Exposures,* (Miller MW ed), Oxford University Press, New York, NY.

198. Sparrow JC, Laing NG (2008) Actin Genetic Diseases, in *Protein Reviews,* Vol. 8, (dos Remedios C, Chhabra D eds), pp 16. Springer Science+Business Media LLC, New York, USA.

199. Spiegel MR (1959) Vectors and scalars, in *Schaum's Outlines: Vector Analysis and an Introduction to Tensor Analysis,* (Anonymous), pp 1-15. McGraw-Hill, USA.

200. Spong CY, Abebe DT, Gozes I, Brenneman DE, Hill JM (2001) Prevention of fetal demise and growth restriction in a mouse model of fetal alcohol syndrome. J Pharmacol Exp Ther 297:774-779.

201. Stern CD (2005) The chick; a great model system becomes even greater. Developmental cell 8:9-17.

202. Streissguth AP, Clarren SK, Jones KL (1985) Natural history of the fetal alcohol syndrome: a 10-year follow-up of eleven patients. Lancet 2:85-91.

203. Streissguth AP, Landesman-Dwyer S, Martin JC, Smith DW (1980) Teratogenic effects of alcohol in humans and laboratory animals. Science (New York, N Y 209:353-361.

204. Su B, Debelak KA, Tessmer LL, Cartwright MM, Smith SM (2001) Genetic influences on craniofacial outcome in an avian model of prenatal alcohol exposure. Alcohol Clin Exp Res 25:60-69.

205. Sulik KK (2005) Genesis of alcohol-induced craniofacial dysmorphism. Exp Biol Med (Maywood) 230:366-375.

206. Sulik KK, Cook CS, Webster WS (1988) Teratogens and craniofacial malformations: relationships to cell death. Development 103 Suppl:213-231.

207. Sulik KK, Johnston MC (1983) Sequence of developmental alterations following acute ethanol exposure in mice: craniofacial features of the fetal alcohol syndrome. Am J Anat 166:257-269.

208. Sulik KK, Johnston MC, Webb MA (1981) Fetal alcohol syndrome: embryogenesis in a mouse model. Science (New York, N Y 214:936-938.

209. Sun HQ, Kwiatkowska K, Yin HL (1995) Actin monomer binding proteins. Curr Opin Cell Biol 7:102-110.

210. Tanguay RL, Reimers MJ (2008) Analysis of ethanol developmental toxicity in zebrafish. Methods Mol Biol 447:63-74.

211. Tapon N, Hall A (1997) Rho, Rac and Cdc42 GTPases regulate the organization of the actin cytoskeleton. Curr Opin Cell Biol 9:86-92.

212. Thapa A, Miller DC, Webster TJ, Haberstroh KM (2003) Nano-structured polymers enhance bladder smooth muscle cell function. Biomaterials 24:2915-2926.

213. The Institute of Medicine (1996) *Epidemiology and surveillance of fetal alcohol syndrome.* National Academy Press, Washington, D.C. USA.

214. Trainor PA, Tam PP (1995) Cranial paraxial mesoderm and neural crest cells of the mouse embryo: co-distribution in the craniofacial mesenchyme but distinct segregation in branchial arches. Development 121:2569-2582.

215. Trentin A, Glavieux-Pardanaud C, Le Douarin NM, Dupin E (2004) Self-renewal capacity is a widespread property of various types of neural crest precursor cells. Proc Natl Acad Sci U S A 101:4495-4500.

216. Tucker GC, Aoyama H, Lipinski M, Tursz T, Thiery JP (1984) Identical reactivity of monoclonal antibodies HNK-1 and NC-1: conservation in vertebrates on cells derived from the neural primordium and on some leukocytes. Cell Differ 14:223-230.

217. Tze WJ, Lee M (1975) Adverse effects of maternal alcohol consumption on pregnancy and foetal growth in rats. Nature 257:479-480.

218. Uller L, Andersson M, Greiff L, Persson CG, Erjefalt JS (2004) Occurrence of apoptosis, secondary necrosis, and cytolysis in eosinophilic nasal polyps. Am J Respir Crit Care Med 170:742-747.

219. Vaglia JL, Hall BK (1999) Regulation of neural crest cell populations: occurrence, distribution and underlying mechanisms. Int J Dev Biol 43:95-110.

220. Van Maele-Fabry G, Gofflot F, Clotman F, Picard JJ (1995) Alterations of mouse embryonic branchial nerves and ganglia induced by ethanol. Neurotoxicol Teratol 17:497-506.

221. Vandekerckhove J, Weber K (1978) Mammalian cytoplasmic actins are the products of at least two genes and differ in primary structure in at least 25 identified positions from skeletal muscle actins. Proc Natl Acad Sci U S A 75:1106-1110.

222. Vartiainen MK, Mustonen T, Mattila PK, Ojala PJ, Thesleff I, Partanen J, Lappalainen P (2002) The three mouse actin-depolymerizing factor/cofilins evolved to fulfill cell-type-specific requirements for actin dynamics. Mol Biol Cell 13:183-194.

223. Viljoen D, Croxford J, Gossage JP, Kodituwakku PW, May PA (2002) Characteristics of mothers of children with fetal alcohol syndrome in the Western Cape Province of South Africa: a case control study. J Stud Alcohol 63:6-17.

224. Ward RE (1989) Facial morphology as determined by anthropometry: keeping it simple. J Craniofac Genet Dev Biol 9:45-60.

225. Warner RH, Rosett HL (1975) The effects of drinking on offspring: an historical survey of the American and British literature. J Stud Alcohol 36:1395-1420.

226. Waterman RE (1976) Topographical changes along the neural fold associated with neurulation in the hamster and mouse. Am J Anat 146:151-171.

227. Webster WS, Ritchie HE (1991) Teratogenic effects of alcohol and isotretinoin on craniofacial development: an analysis of animal models. J Craniofac Genet Dev Biol 11:296-302.

228. Webster WS, Walsh DA, McEwen SE, Lipson AH (1983) Some teratogenic properties of ethanol and acetaldehyde in C57BL/6J mice: implications for the study of the fetal alcohol syndrome. Teratology 27:231-243.

229. Welch MD, Mallavarapu A, Rosenblatt J, Mitchison TJ (1997) Actin dynamics in vivo. Curr Opin Cell Biol 9:54-61.

230. Wentzel P, Eriksson UJ (2009) Altered gene expression in neural crest cells exposed to ethanol in vitro. Brain Res .

231. Werler MM, Lammer EJ, Rosenberg L, Mitchell AA (1991) Maternal alcohol use in relation to selected birth defects. Am J Epidemiol 134:691-698.

232. White E (1996) Life, death, and the pursuit of apoptosis. Genes Dev 10:1-15.

233. Winder SJ, Ayscough KR (2005) Actin-binding proteins. J Cell Sci 118:651.

234. Wynter JM, Walsh DA, Webster WS, McEwen SE, Lipson AH (1983) Teratogenesis after acute alcohol exposure in cultured rat embryos. Teratog Carcinog Mutagen 3:421-428.

235. Yamada Y, Nagase T, Nagase M, Koshima I (2005) Gene expression changes of sonic hedgehog signaling cascade in a mouse embryonic model of fetal alcohol syndrome. J Craniofac Surg 16:1055-61; discussion 1062-3.

236. Yelin R, Kot H, Yelin D, Fainsod A (2007) Early molecular effects of ethanol during vertebrate embryogenesis. Differentiation 75:393-403.

237. Yelin R, Schyr RB, Kot H, Zins S, Frumkin A, Pillemer G, Fainsod A (2005) Ethanol exposure affects gene expression in the embryonic organizer and reduces retinoic acid levels. Dev Biol 279:193-204.

238. Yoshinaga T, Hashimoto E, Ukai W, Toki S, Saito S, Saito T (2007) Neural stem cell transplantation in a model of fetal alcohol effects. J Neural Transm Suppl 331-337.

239. Ziegler U, Groscurth P (2004) Morphological features of cell death. News in physiological sciences: an international journal of physiology produced jointly by the International Union of Physiological Sciences and the American Physiological Society 19:124.